Stony Brook University

Mechanism of type III secretion system-triggered killing of *Yersinia* in macrophages

A Dissertation Presented

by

Xiaoying Wang

to

The Graduate School

in Partial Fulfillment of the

Requirements

for the Degree of

Doctor of Philosophy

in

Molecular and Cellular Biology

Stony Brook University

May 2015

Stony Brook University

The Graduate School

Xiaoying Wang

We, the dissertation committee for the above candidate for the

Doctor of Philosophy degree, hereby recommend

acceptance of this dissertation.

James B. Bliska – Dissertation Advisor
Professor, Molecular Genetics and Microbiology

Wali Karzai - Chairperson of Defense
Professor, Biochemistry and Cell Biology

Adrianus van der Velden
Assistant Professor, Molecular Genetics and Microbiology

James Konopka
Professor, Molecular Genetics and Microbiology

Gloria Viboud
Associate Professor, Clinical Laboratory Sciences

This dissertation is accepted by the Graduate School

Charles Taber
Dean of the Graduate School

Abstract of the Dissertation

Mechanism of type III secretion system-triggered killing of *Yersinia* in macrophages

by

Xiaoying Wang

Doctor of Philosophy

in

Molecular and Cellular Biology

Stony Brook University

2015

The mammalian immune system has the ability to discriminate between pathogens and innocuous microbes by detecting conserved molecular patterns. In addition to conserved microbial patterns, the mammalian immune system may recognize distinct pathogen-induced processes, the mechanism of which is poorly understood. Pathogenic *Yersinia* species utilize a type III secretion system (T3SS) to translocate various bacterial effectors into target cells, which aim to modify multiple host signaling pathways. Interestingly, previous studies have shown that the T3SS in *Yersinia pseudotuberculosis* leads to decreased survival of this bacterium in primary murine macrophages, the mechanism of which is unknown. Here, we use colony forming unit assays and fluorescence microscopy to investigate how the T3SS triggers killing of *Yersinia* in naïve murine macrophages.

To identify specific effectors that limit *Yersinia* intracellular survival, the intra-macrophage survival of wild-type strain and several *Yersinia* outer protein (*yop*) deletion mutants was compared. Additionally, intra-macrophage survival of *Yersinia* producing YopE or YopE

variants was tested to further investigate the role of YopE GAP activity in this process. Furthermore, experiments were performed to better characterize the mechanism of YopE-induced killing of *Yersinia* inside macrophages.

Our results show that YopE and YopH limit survival of *Yersinia* inside macrophages, while YopT counteracts the YopE-triggered killing effect. YopE-induced killing of *Yersinia* is an independent pathway from Synaptotagmin VII (SytVII) -mediated phagolysosome fusion. Importantly, data presented here suggest that the GAP activity of YopE towards Rho GTPases is essential for restricting *Yersinia* survival inside macrophages. *Clostridium difficile* Toxin B is able to mimic the effect of YopE and decrease *Yersinia* survival inside macrophages. Interestingly, macrophages limit *Yersinia* survival in response to Rac1 inhibition, but not Rho inhibition. In addition, our work indicates that LPS-TLR signaling is dispensable for YopE-stimulated intracellular killing. Remarkably, translocated YopE stimulates higher levels of nitric oxide (NO) from infected macrophages. However, NO production does not seem to mediate YopE-triggered killing. Moreover, signaling pathways that require capase-1/11, NOD1 or autophagy are not involved in the YopE-elicited killing response.

In summary, I have shown that primary macrophages sense manipulation of Rho GTPases by *Yersinia* YopE and actively counteract pathogenic infection by restricting intracellular bacterial survival. Our results uncover a new mode of innate immune recognition in response to pathogenic infection.

Table of Contents

List of Figures

List of Tables

List of Abbreviations

ASC   apoptosis-associated speck-like protein containing a CARD

BMDMs   bone marrow-derived macrophages

CFU   colony forming unit

CNF1   cytotoxic necrotizing factor 1

CTB   cholera toxin B

DAP   diaminopimelic acid

ETIR   effector-triggered immune response

FADD   Fas-associated death domain

FAK   focal adhesion kinase

Fyb   Fyn binding protein

GAPs   GTPase activating proteins

GDI   guanine dissociation inhibitor

GEFs   guanine exchange factors

IFNs   type I interferons

IKKβ   inhibitor of kappa B kinase β

IL-1β   interleukin-1 β

iNOS   inducible nitric oxide synthase

IPTG   Isopropyl-β-D-thiogalactopyranoside

LPS   lipopolysaccharide

LRR   leucine-rich repeat

MAMPs   microorganism-associated molecular patterns

MAPKs	mitogen-activated protein kinases
MDP	muramyl dipeptide
MLD	membrane localization domain
MLNs	mesenteric lymph nodes
MyD88	myeloid differentiation primary-response protein 88
NF-κB	transcription factor nuclear factor-κB
NLRC	NLR family CARD domain containing-protein
NLRP	NOD, Leucine rich repeat and pyrin domain containing protein
NLR	Nucleotide-binding oligomerization domain leucine-rich repeat receptor
NO	Nitric oxide
NO_2^-	nitrite
NOD	Nucleotide-binding oligomerization domain-containing protein
p130Cas	p130Crk-associated substrate
PAMP	pathogen associated molecular patterns
PFA	paraformaldehyde
PMNs	polymorphnuclear neutrophils
PPs	Peyer's patches
PRK2	protein kinase C-like 2
PRRs	pattern recognition receptors
RIPK1	receptor-interacting serine/threonine kinase 1
RLRs	RIG-like receptors
RNS	reactive nitrogen species
ROS	reactive oxygen species
RSK1	ribosomal protein S6 kinase

SytVII	Synaptotagmin VII
T3SS	Type III secretion system
T4SS	Type IV secretion system
T6SS	Type VI secretion system
TAK1	transforming growth factor β-activated kinase 1
TLRs	Toll-like receptors
TNF	Tumor necrosis factor
TRIF	TIR-domain-containing adaptor inducing IFN-β
YCVs	*Yersinia* containing vesicles
Yops	*Yersinia* outer proteins

Acknowledgments

First and foremost, I would like to express my sincerest gratitude to my advisor Dr. James Bliska for his constant support and guidance through my dissertation research. Without his critical advice, continuous patience and encouragement, this thesis would not have been possible. His enthusiasm, calmness and thoroughness as a scientist showed me a great role model to learn from.

I thank all Bliska lab members who have been great colleagues and made the lab an enjoyable environment to work in. I thank Yue Zhang for being patient all the time, answering all my questions. I thank Maya Ivanov, who has been a great friend, listener and gym partner, giving me helpful suggestions on my lab work and my personal life. I thank Hana Fukuto, Lawton Chung, and Taylor Schoberle for being great accompanies in the lab, and for their helpful suggestions on experimental techniques and stimulating discussions on the project. I am grateful to Galina Ivanov for her technical assistance in preparing bone marrow derived macrophages. I thank previous lab member Joe McPhee for guiding me in my rotation and helped me setting up when I first joined the lab.

I would like to thank my committee members, Wali Karzai, Adrianus van der Velden, James Konopka and Gloria Viboud for agreeing to serve on my committee and spend valuable time on my thesis dissertation. I am incredibly thankful for their critical comments, helpful advice and inspiring discussions during committee meetings.

There are many friends that I want to acknowledge. I thank Dou, Kai, Fang and Veronica for helping me settling down at Stony Brook from the very beginning. I thank Boris, Nancy, Sal, Ying, Qiwen, Yifeng, Jian, Zhichao, Zhu, and Qiang, who have made my graduate school experience and my time at Stony Brook fun and memorable.

Finally, I would like to thank my family, especially my parents, who have always been there with constant support and endless love. I want to thank my wonderful husband Cunyou, who has helped me to get where I am today. I am deeply grateful for his unending love, encouragement, patience and support.

Chapter 1: Introduction

1.1 Recognition of pathogens by the mammalian immune system

Innate immunity and professional phagocytes. Innate immunity provides an early and critical protection against pathogenic infections. Professional phagocytes, such as neutrophils, monocytes, macrophages and dendritic cells, are key cellular components of the innate immune system. These specialized hematopoietic cells are able to seek, engulf and destroy invading microorganisms rapidly as the first line of defense against pathogenic attack. Once the pathogen is internalized, the phagosome undergoes acidification and fusion with lysosomes to obtain degradative proteases and anti-microbial peptides [1,2]. Highly toxic reactive oxygen and nitrogen species are also generated during activation of a "respiratory burst" [1,2]. These bactericidal weapons all contribute to the destruction of the invading microorganism. In addition, macrophages and dendritic cells can secrete pro-inflammatory cytokines, process microbial material and serve as antigen-presenting cells to direct the development of an adaptive immune response [1,2].

MAMPs and PRRs. How do immune cells initially sense the invading microorganisms? In the dominant paradigm of innate immunity, host cells detect pathogens by recognizing "microorganism-associated molecular patterns" (MAMPs) via germline-encoded pattern recognition receptors (PRRs) [3]. The wide range of PRRs in mammalian cells recognizes various microbial molecules, ranging from proteins, lipids, and carbohydrates to nucleic acids.

Over the past decade, two major classes of PRRs have been described: trans-membrane receptors, such as Toll-like receptors (TLRs), scavenger receptors and C-type lectin receptors,

and cytosolic soluble receptors, such as nucleotide-binding oligomerization domain leucine rich repeat receptors (NLRs) and retinoic acid-inducible gene 1 (RIG) like receptors (RLRs).

As the first set of sensors identified, TLRs are the best-characterized PRRs that function on the cell surface or within endosomal compartments [4,5]. TLR4 senses lipopolysaccharide (LPS), an essential component in the outer membrane of Gram-negative bacteria; TLR5 recognizes flagellin, a globular protein that forms the filament in bacterial flagellum; TLR2, sometimes in cooperation with other TLRs, detects a variety of microbial components including lipoproteins, peptidoglycans, lipoarabinomannan, and lipoteichoic acid; TLR9 recognizes bacterial DNAs containing unique CpG motifs. Ligand engagement to TLRs facilitates dimerization of TLRs and activation of downstream signaling pathways through different adaptor proteins, such as myeloid differentiation primary-response protein 88 (MyD88) and TIR-domain-containing adaptor inducing IFN-β (TRIF). The MyD88 dependent pathway mediates activation of mitogen-activated protein kinases (MAPKs) and transcription factor nuclear factor-κB (NF-κB), while the TRIF-dependent pathway mainly controls type I interferons (IFNs) production [4,5].

Unlike TLRs, members of the NLR family are intracellular soluble receptors. Nucleotide-binding oligomerization domain-containing protein 1 (NOD1) and NOD2, as the first members of the NLR family identified, respond to intracellular diaminopimelic acid (DAP) and muramyl dipeptide (MDP) respectively, which are fragments of peptidoglycans found in the bacterial cell wall [6]. Following ligation to the ligands, NOD1 and NOD2 stimulate both NF-κB activation and production of IFNs [6]. Other members of the NLR family, such as NLRP1 (NOD, Leucine rich Repeat and Pyrin domain containing Protein 1), NLRP3, NLRP6 and NLRC4 (NLR family CARD domain containing-protein 4), mediate the assembly of inflammasomes and the activation

2

of inflammatory caspases in response to numerous infectious and distinct stimuli [7,8]. For example, NLRP3 has been proposed to respond to the potassium efflux induced by bacterial toxins, reactive oxygen species (ROS) generated from damaged mitochondria and phagolysosome membrane destabilization [9]. NLRC4 induces inflammasome activation in response to cytosolic bacterial flagellin and T3SS injectisome component PrgJ [9]. After stimulation, the NLRs undergo oligomerization, which facilitates recruitment of pro-caspase-1 through their CARD domain or via the CARD of the adaptor protein ASC (apoptosis-associated speck-like protein containing a CARD) [9]. Once recruited to the inflammasome complex, pro-caspase-1 undergoes autocatalytic cleavage to form active caspase-1. Active caspase-1 further promotes processing and secretion of cytokines such as interleukin-1 β (IL-1β) and IL-18, and a lytic form of cell death called pyroptosis [7,8].

Overall, PRRs initiate signaling pathways to promote inflammatory responses, which recruit and stimulate circulating immune cells, and help shape the development of adaptive immune response.

Patterns of pathogenesis and ETIR. PRRs are indispensable components of the innate immune system, which sense invading microorganisms by recognizing MAMPs. However, MAMPs, such as flagellin or lipopolysaccharide, are conserved microbial structures found in both pathogenic and nonpathogenic bacteria. How then do host cells distinguish pathogens from innocuous microbes? Alternate theories propose that, in addition to MAMPs, host cells also respond to distinct pathogen-induced signals, termed "patterns of pathogenesis" [10]. Such signals are commonly associated with pathogenic infections and contribute to the development of diseases [10-12]. Several mechanisms of how host cells detect patterns of pathogenesis have been proposed, such as by sensing bacterial replication, pore formation/phagosome disruption on host

membranes, delivery of ligands/enzymes into host cytosol and disruption of host actin cytoskeleton [10].

One common pattern shared by many pathogens is their ability to replicate in their hosts upon invasion. Vance, Isberg and Portnoy proposed that the immune system detects molecules associated with bacterial growth, and can respond differently to alive or dead bacteria [10]. Signature molecules of microbial life, named "MAMP per vita", may include peptidoglycan produced by growing bacteria, quorum-sensing regulators or bacterial pyrophosphates [10]. Indeed, Sander and colleagues identified bacterial mRNA as one such MAMP per vita, which is present in viable bacteria but not in dead bacteria [13]. Detection of bacterial mRNA induces protective immunity, leading to production of IFNβ in a TRIF dependent manner, activation of NLRP3 inflammasome and caspase-1, ensuing IL-1β production and pyroptosis [13].

Another distinguished feature of many bacterial pathogens is their ability to produce and secrete virulence effectors, many of which enter the host cell cytosol via different mechanisms. Once delivered, those virulence effectors often act to modify specific cellular targets or alter certain cellular processes. Although virulence effectors are mainly studied in how they mediate immune evasion, recent studies have demonstrated that host cells recognize the effects of bacterial effectors, such as inhibition of host protein synthesis, activation of host Rho GTPases or pore formation on host membrane, resulting in a protective immune defense against the pathogens [14-19]. For example, inhibition of host protein synthesis by *Legionella pneumophila* effectors (Lgt1, Lgt2, Lgt3, SidI and SidL) has been shown to activate the MAPKs signaling pathway and augment the NF-κB signaling pathway, eliciting a protective response against *L. pneumophila* on the transcriptional level [15]. Boyer et *al.* demonstrated that *Escherichia coli* (*E.coli*) effector cytotoxic necrotizing factor 1 (CNF1) stimulated the IMD kinase innate immune pathway via

activation of Rac2, generating a protective response to bacterial challenge in flies [14]. Thus, host cells sense the activities of virulence effectors indirectly by monitoring the status of vulnerable cellular targets and the state of cellular homeostasis. The protective immune response that is triggered by the detection of microbial effectors is defined as an "effector-triggered immune response" (ETIR). Recognition of virulence effectors allows host cells to evaluate the virulence potential of an invading microorganism and fight against the attack to the appropriate level [10-12]. This idea of ETIR was originally established and demonstrated in the plant immunity field as the "guard hypothesis" [20]; the molecular mechanisms of ETIR in metazoans are just beginning to emerge [14-19]. In general, very little is known about the recognition mechanisms of "patterns of pathogenesis" or the surveillance signaling pathways of ETIR in metazoans. More studies are needed to explore this area to better understand the basic mechanisms of innate immunity.

1.2 *Yersinia* **pathogenesis and type III secretion system**

Classification of the *Yersinia* species. *Yersiniae* are Gram-negative rod-shaped bacteria that belong to the family of *Enterobacteriaceae*. The genus of *Yersinia* consists 11 species, three of which are pathogenic for humans and animals: *Y. pestis, Y. pseudotuberculosis and Y.enterocolitica. Y. pestis* is the causative agent of plague, an acute and deadly infectious disease in humans, which is typically acquired by humans from fleabites or aerosols [21,22]. *Y. pestis* was originally classified into three subgroups or biovars: Antiqua, Mediaevalis and Orientalis, each of which was historically associated with a major plague epidemic. *Y. pseudotuberculosis* and *Y. enterocolitica* are enteropathogens associated with self-limiting gastroenteritis in humans, which are transmitted by the fecal-oral route [21]. Twenty-one different serogroups of *Y. pseudotuberculosis* have been identified based on the O-antigens of LPS [23]; six biogroups of

Y.enterocolitica (1A, 1B, 2, 3, 4 and 5) have been defined according to their phenotypic features [21]. *Y. pestis* and *Y. pseudotuberculosis* are closely related on the genomic level, while *Y.enterocolitica* evolved independently as a distinct lineage [21]. Genetic studies indicated that *Y. pestis* evolved from *Y. pseudotuberculosis* recently-around 1,500-20,000 years ago by a process combining lateral gene transfer, genome decay and rearrangement [21]. This study exclusively focused on the pathogenesis of *Y. pseudotuberculosis*.

***Y. pseudotuberculosis* pathogenesis.** *Y. pseudotuberculosis* is commonly transmitted to human by consumption of contaminated food or water. After ingestion, the bacteria travel through the stomach and pass into the small intestine. From there, the bacteria are internalized by the M cells in Peyer's patches (PPs), which allows their translocation across the epithelial barrier [24]. The *Yersinia* invasin proteins bind to the β1 integrins of M cells with high affinity and specificity, facilitating bacterial attachment and uptake by M cells [25]. Studies have shown that phagocytes under the follicle-associated epithelium are able to internalize the bacteria at the early stage of infection [26]. *In vitro* studies have also demonstrated that *Y. pseudotuberculosis* can survive and even replicate inside naïve murine macrophages [26]. It is therefore proposed that migrating phagocytes further transfer the bacteria into the mesenteric lymph nodes (MLNs) [26]. Once reaching the PPs and MLNs, the bacteria multiply externally to the host cells within granuloma-like lesions. In immunocompetent humans, *Y. pseudotuberculosis* infection is usually limited to the small intestine, the PPs and the MLNs, causing self-limiting gastroenteritis such as mesenteric adenitis and terminal ileitis [27]. Under rare events, like in immunocompromised patients, the infection can also become systemic and lethal. In rodents, *Y. pseudotuberculosis* commonly enters the blood stream from the intestinal tract and spreads to lymphatic organs such as spleen and liver [27].

The *Yersinia* type III secretion system. The type III secretion system (T3SS) is a complex

protein export pathway, which has a needle-like appendage extending from a basal body

equipped with an ATPase protein pump [28,29] (Figure 1.1). The needle-like appendage

protrudes outside the bacterium, while the basal body spans the bacterial membranes and the

peptidoglycan layer. The T3SS, also called an "injectisome", shares significant homology with

the bacterial flagellum as revealed by genetic studies [30]. Numerous Gram-negative bacterial

pathogens use the T3SS to deliver bacterial proteins into host cell cytosol or into host cell

membrane [29,31,32]. It is a conserved virulence mechanism found in many human pathogens,

such as *Salmonella*, *Pseudomonas*, *Shigella*, enteropathogenic *Escherichia coli* and *Yersinia*

species [29]. Generally, animal pathogens equipped with the T3SS inject between 6 and 20

bacterial proteins into their target cells [28]. Those bacterial proteins are powerful effectors that

display a wide range of biochemical activities and modulate crucial host signaling, like

promotion or inhibition of bacteria uptake, regulation of pro-inflammatory responses, induction

or inhibition of cell death pathways, or modulation of intracellular trafficking [33,34].

For all three species of pathogenic *Yersinia*, their virulence ability requires a virulence

plasmid encoded T3SS and a suite of virulence factors known as *Yersinia* outer proteins (Yops).

The 70kb virulence plasmid is named as pCD1 in *Y. pestis* or pYV in *Y. pseudotuberculosis* and

Y. enterocolitica. *In vitro*, expression of *Yersinia* T3SS genes and secretion of Yops are primarily

regulated by temperature and calcium concentration, a phenomenon known as the low calcium

response [35,36]. At 26 ℃, genes of the *Yersinia* T3SS are weakly expressed; upon temperature

shift from 26 ℃ to 37 ℃, T3SS and Yop genes are upregulated and the injectisome is assembled.

At 37 ℃, millimolar level of calcium keeps production of Yops at a low level and inhibits

secretion of these proteins into the culture medium [35,36]. On the other hand, at 37 ℃ *in vitro*,

7

chelating calcium to a micromolar level stimulates massive Yops production and secretion into the culture medium [35,36].

In vivo, physical contact with a host cell activates *Yersinia* T3SS injectisomes and initiates secretion of numerous proteins, including the LcrV protein and Yops. LcrV and translocators YopB and YopD are essential for the formation of T3SS channel in the host cell membrane. LcrV localizes to the distal end of the injectisome, where it polymerizes into a pentameric tip complex [28,37] (Figure 1.1). Translocators YopB and YopD are pore-forming proteins containing hydrophobic transmembrane domains. It is believed that, with the LcrV tip complex serving as a scaffold platform, YopB and YopD insert into the plasma membrane and form a translocation channel referred to as a "translocon" [38]. A "one-step model" suggests that LcrV maintains direct contact with the YopB/D translocon forming a translocation pore complex, which completes a sealed conduit connecting the injectisome to the host cell [38] (Figure 1.1). Through the translocation pore complex, effector Yops are delivered from the bacterium to the host cell cytosol. In *Y. pestis* and *Y. pseudotuberculosis*, the effector Yops are YopE, YopH, YopT, YopK, YopM, YpkA and YopJ (in *Y.enterocolitica*, the last two are designated as YopO and YopP, respectively) [27]. Six effectors, YopE, YopH, YopT, YopM, YpkA and YopJ, directly target host proteins to modulate signaling pathways [27] (Figure 1.2), while YopK interacts with translocators YopB and YopD to regulate translocation rate and fidelity [39,40]. Pathogenic *Yersinia* species have been extensively studied in the context of T3SS function, as a model to explore the crosstalk between bacterial pathogen and host cell [27]. For example, using the TEM system, *Yersinia* has been shown to target polymorphonuclear neutrophils (PMNs), macrophages, and dendritic cells for Yops delivery *in vivo* [41-44], which is

8

broadly applicable to the studies of pathogens using T3SS, Type IV secretion system (T4SS) or Type VI secretion system (T6SS).

1.3 Inhibition of host immune responses by *Yersinia* T3SS effectors

Inhibition of phagocytosis by *Yersinia* T3SS effectors. Yop effectors act to modulate multiple host signaling pathways to counteract innate immune response and benefit bacterial pathogenesis [27,45]. In the later stage of infection, *Yersinia* predominantly replicates in an extracellular form; four Yop effectors regulate actin dynamics to block phagocytosis in a concerted way. YopE, YopH, YopT and YpkA act to target Rho GTPases and exert negative effects on cytoskeleton dynamics via distinct mechanisms (Figure 1.2). YopE mimics the eukaryotic GTPase activating protein (GAP). It binds to Rho GTPases, introduces "an arginine finger" into the GTPases catalytic site and promotes efficient GTP hydrolysis [46]. The resulting conformational change reduces the binding affinity of Rho GTPases to the downstream effectors, thus switching the Rho GTPases into the inactive form. YopH is a powerful protein tyrosine phosphatase, which targets several cytoskeleton proteins including focal adhesion kinase (FAK), the FAK-homolog Pyk, Lyn, P85 (the regulatory subunit of the PI3Kinase), Fyn binding protein (Fyb), p130Crk-associated substrate (p130Cas) and paxillin [27,34]. Dephosphorylation of kinases and adaptor proteins in the focal adhesion complex by YopH interrupts activating signals for guanine exchange factors (GEFs), and therefore inhibits activation of Rho GTPases. YopT is a cysteine protease, which proteolytically removes the C-terminal isoprenoid moiety of Rho GTPases. It releases Rho GTPases from their membrane anchors leading to the inactivation of Rho GTPases [47]. YpkA binds to GDP- and GTP-bound Rho GTPases with a C-terminal guanine dissociation inhibitor (GDI) domain [27]. It has been shown that YpkA sequesters and prevents activation of GDI-free Rac1 at the plasma membrane [48]. By disturbing Rho GTPase activity, YopE, YopH,

9

YopT and YpkA modulate actin polymerization, regulate cytoskeleton dynamics and contribute to the anti-phagocytic activity of the *Yersinia* T3SS. These Yops also counteract downstream responses associated with phagocytosis. For example, YopH rapidly inhibits Ca^{2+} signaling downstream of invasin-β1 integrin signaling in *Y. pseudotuberculosis* infected neutrophils [49], and therefore may prevent oxidase activation and cell degranulation that requires Ca^{2+} signaling [50]. Inhibition of phagocytosis may be crucial for *Yersinia* to resist killing by neutrophils or activated macrophages [27].

LcrV counteracts production of proinflammatory cytokines. In addition to inhibition of phagocytosis, the *Yersinia* T3SS also counteracts the production of pro-inflammatory cytokines. Detection of bacterial molecules causes prompt upregulation of proinflammatory cytokines through the MAMP-PRR signaling pathways, which initiate innate immune responses [3]. Once expressed, the proinflammatory cytokines function in a variety way to protect against infection, such as induction of fever (IL-1 and TNF-α), recruitment and activation of professional phagocytes (IL-8, IL-1 and IFN-γ), promotion of leukocyte adherence and migration (IL-1 and TNF-α), and upregulation of reactive oxygen intermediates expression (IFN-γ and TNF-α). The inflammatory response is eventually inhibited by anti-inflammatory cytokines, such as IL-10, to block overwhelming inflammation and to ensure homeostasis in host cells. The *Yersinia* T3SS works through multiple signaling pathways to counteract the production of proinflammatory cytokines, the mechanism of which is multifactorial and complicated. One unique and potent protein in this process is LcrV (also known as V-antigen), a well-characterized protective antigen [51]. Mice infected with pCD⁻ but not pCD⁺ *Y. pestis* generated systemic inflammatory response with dramatic upregulation of IFN-γ and TNF-α in the spleen [52]. Passive immunization with anti-LcrV restored the full inflammatory response and rescued mice infected with pCD⁺ *Y. pestis*

[52]. LcrV exhibits a direct immunosuppressive activity by activation of TLR2 signaling and upregulation of IL-10 production [52,53]. IL-10 performs anti-inflammatory activities and acts to suppress the production of IFN-γ and TNF-α [52,53]. The anti-inflammatory activity of LcrV supports growth of pCD$^+$ *Y. pestis* in focal necrotic lesions that fail to attract inflammatory cells [52].

YopJ induces macrophage and dendritic cell death and caspase-1 activation. Depending on their activation state and the specific cell type involved, *Yersinia*-infected macrophages and dendritic cells can exhibit properties of apoptosis, pyroptosis or necrosis [54-59]. The effector YopJ plays a very important role in the process of inducing cell death in naive macrophages and dendritic cells upon *Yersinia* infection. YopJ has acetyl-transferase activity, which binds to and acetylates Ser and Thr residues in the activation sites of several kinases, including the MAP kinase kinases, the inhibitor of kappa B kinase beta (IKKβ) and transforming growth factor β-activated kinase-1 (TAK1) [60-62] (Figure 1.2). Acetylation of those kinases inhibits their phosphorylation and therefore prevents their activation. In *Yersinia*-infected naïve macrophages, TLR4 recognition of *Yersinia* LPS initiates MAPK and NF-κB signaling pathways as well as a TRIF-dependent apoptotic pathway. With its acetyl-transferase activity, YopJ efficiently inhibits MAPK and NF-κB signaling pathways, allowing *Yersinia* to suppress the production of proinflammatory cytokines and pro-survival proteins [63]. As a result of the reduced expression of pro-survival proteins, the TRIF-dependent apoptotic signaling predominates. TRIF-dependent signaling induces cleavage of multiple caspases, including the apoptotic initiator caspase-8 and downstream executioner caspase-9, -7, and -3, leading to apoptosis of *Yersinia* infected naïve macrophages [56-59].

Interestingly, YopJ-induced apoptosis in naïve macrophages infected with *Y. pestis* is accompanied by caspase-1 activation and release of proinflammatory IL-1β and IL-18 [40,64,65]. The extent of caspase-1 activation correlates with the inhibitory ability of YopJ [40,64]. YopJ-induced caspase-1 processing can occur in the absence of inflammasome proteins such as NLRP3, NLRC4 or ASC [40,55], whereas YopJ-dependent processing and release of IL-1β and IL-18 does require NLRP3 and ASC [64].

Recent studies demonstrated that receptor-interacting serine/threonine kinase 1 (RIPK1), caspase-8 and Fas-associated death domain (FADD) are indispensable mediators for YopJ-induced cell death and caspase-1 activation in naïve macrophages [66,67]. TLR4-TRIF signaling stimulates RIPK1/FADD, which then triggers caspase-8 activation and ensuing caspase-1 activation and cell death [66,67].

Whether YopJ-dependent cell death benefits bacterial virulence or host defense *in vivo* remains controversial. Several studies showed that YopJ promotes bacterial dissemination, contributing to systemic disease and barrier dysfunction [59]. On the other hand, *Y. pseudotuberculosis* ectopically expressing a hypercytotoxic YopP (from *Y. enterocolitica*) showed reduced virulence in oral mouse infection [68]. Inducing cell death via apoptosis could potentially favor *Yersinia* persistence by eliminating immune cells in an immunologically silent way [59,69]. However, the accompanied caspase-1 activation, pyroptosis and release of IL-1β and IL-18 may promote proinflammatory responses to favor host resistance against *Yersinia* infection. A number of studies suggest that host cell death in response to *Yersinia* infection is important for anti-*Yersinia* immunity [66-68,70]. Thus, fine tuned secretion and cytotoxicity of YopJ may be important for optimal virulence of *Yersinia*.

YopK regulates translocation rate and prevents inflammasome activation. In macrophages infected with effectorless mutants, but not wild-type *Yersinia*, recognition of T3SS translocon has been shown to stimulate inflammasome activation (see the next section) [40,71]. The effector YopK has been demonstrated to inhibit caspase-1 activation, release of IL-1β and pyroptosis, which occurs in response to T3SS recognition (Figure 1.4) [40].

YopK is an essential effector for *Yersinia* virulence, as a *yopK* mutant is severely attenuated compared to wild-type in mouse infection [72]. YopK has no known enzymatic activity and shares no primary sequence homology with other known proteins. Early studies found that *yopK* mutant strains displayed a hypertranslocation phenotype, whereas overexpression of YopK inhibits translocation of other Yops [72]. YopK regulates T3SS translocation rate and performs this regulatory function within target cells [39]. The specific mechanism by which YopK regulates T3SS translocation is not entirely known. Hemolytic assays using erythrocytes suggested that YopK might affect pore size or conformation to affect translocation [72]. Also, YopK has been shown to be directly associated with translocon proteins YopB and YopD, which may in turn influence translocation [39].

Remarkably, YopK prevents inflammasome activation in response to *Yersinia* T3SS recognition both *in vitro* and *in vivo* [40]. Inhibition of inflammasome activation by YopK promotes *Yersinia* multiplication, dissemination and persistence during infection *in vivo* [40]. Whether YopK counteracts inflammasome activation by blocking translocon-induced perturbation in the plasma membrane of infected cells or by limiting translocation of an unknown substrate remains to be investigated.

YopM interrupts inflammasome assembly and caspase-1 activation in activated macrophages. The effector YopM contains variable numbers (~12 to 21) of leucine-rich repeats (LRRs) among different *Yersinia* strains. The LRR region of YopM displays an unusual horse shoe-like structure, which is believed to serve as a binding platform for host cell proteins [73]. YopM forms a complex with two protein kinases RSK1 and PRK2, which leads to activation of both kinases in host cell cytosol (Figure 1.2) [74,75]. The biological significance of YopM/RSK1 or YopM/PRK2 complex has not been established. In mice infected with *Y. pestis,* YopM has been shown to be a critical virulence factor that is associated with suppression of innate immunity [27,76]. In *Y. pseudotuberculosis* infected mice, YopM has been linked to systemic stimulation of anti-inflammatory IL-10 [77].

Notably, a recent study reported that a YopM isoform in *Y. pseudotuberculosis* strain YPIII (YopM[YPIII]) binds to and antagonizes activation of caspase-1 in LPS-activated macrophages (Figure 1.4) [78]. Purified YopM[YPIII] binds to cleaved, active caspase-1 and directly blocks caspase-1 activity *in vitro*, without being cleaved itself. An YLTD motif in the 10th LRR of YopM[YPIII] is required for binding to and inhibition of caspase-1. This YLTD motif is similar to the caspase-1 substrate YVAD, and it acts as a pseudosubstrate to sequester caspase-1 and abrogates caspase-1 binding to the preinflammasome complex [78]. It has been shown that YopM[YPIII] prevents caspase-1 binding to the preinflammasome, activation of caspase-1, processing and release of IL-1β, lysosome exocytosis and pyroptosis in LPS-activated macrophages infected with *Y. pseudotuberculosis* (Figure 1.4). Presence of YopM[YPIII] delays but not completely blocks T3SS translocon-induced caspase-1 activation in *Y. pseudotuberculosis* infected LPS-activated macrophages [78]. Caspase-1 activation contributes to the anti-*Yersinia*

immunity *in vivo*, and consequently inhibition of caspase-1 by YopM is critical for *Yersinia* virulence [78].

Very recently, additional YopM isoforms have been studied for their ability to inhibit caspase-1 in *Yersinia*-infected macrophages. A *Y. pestis* isoform (YopM^{KIM}) that contains the YLTD motif, and a *Y. pseudotuberculosis* isoform (YopM^{32777}) that does not, were both able to inhibit activation of caspase-1 in *Yersinia*-infected macrophages [79]. Although both isoforms were able to inhibit activation of caspase-1 in *Yersinia*-infected macrophages, only YopM^{KIM} bound to caspase-1 [79]. Additionally, YopM^{KIM} binds to the scaffolding protein IQGAP1, which is required for activation of caspase-1 in *Yersinia*-infected macrophages [79]. Together, these data show that distinct isoforms of YopM can inhibit activation of caspase-1, and that the variable LRR domains of these proteins target different host proteins to perform this function.

1.4 Activation of host immune responses by *Yersinia* T3SS

Translocon insertion stimulates a pore formation pathway and pro-inflammatory responses in *Yersinia* infected cells. The *Yersinia* T3SS and Yop effectors have been extensively studied in how they counteract the innate immunity and benefit bacterial pathogenesis. However, emerging evidence suggests that host cells may have evolved mechanisms to recognize these bacterial signals to activate immune response [19]. In epithelial cells, infection with a *Y. pseudotuberculosis* multi-*yop* mutant strain lead to pore formation and subsequent cell lysis, which was inhibited by catalytically active YopE or YopT in wild-type strain infected cells [27,80]. The pore formation phenotype is dependent on YopB and requires actin polymerization [27]. Furthermore, a YopB-dependent proinflammatory response was observed in *Y. pseudotuberculosis* infected epithelial cells, which resulted in activation of the

15

small GTPase Ras, the MAP kinase ERK and JNK, the NF-κB signaling pathway and production of IL-8 [27,81]. Catalytically active YopE, YopH, YopT and YopJ counteracted this proinflammatory response in wild-type strain infected cells [19]. Thus, translocon insertion by *Yersinia* T3SS induces a pore formation pathway and a gene expression pathway in epithelial cells, both of which are then inhibited by several effector Yops once they are delivered (Figure 1.3 A) [19].

One intriguing question to ask here is why would *Yersinia* induce pore formation and gene expression pathways that could possibly alarm the host cells? YopB-dependent signaling is required for efficient Yop translocation, which could be triggered by *Yersinia* intentionally [19]. It was found that actin polymerization inhibitor or Rho specific inhibitor decreased Yop translocation in *Yersinia* infected epithelial cells [82]. Thus translocon insertion triggers Rho activation, stimulates actin polymerization and promotes Yop translocation [82]. Once Yops are translocated, their activities downregulate T3SS translocation as a negative feedback to avoid further cell damage.

Unlike in epithelial cells, TLRs are important mediators generating signaling responses by sensing MAMPs in *Yersinia* infected macrophages [83]. Additionally, there are TLR-independent signaling events stimulated by *Yersinia* infection [84]. Recognition of the *Yersinia* T3SS triggers activation of NF-κB- and TNF-regulated genes in macrophages lacking TLR signaling (*MyD88*$^{-/-}$/*Trif*$^{-/-}$ macrophages) [84]. This transcriptional response is not dependent on NOD1 or NOD2, but requires bacterial expression of YopB and YopD. Several effectors modulated this signaling response: YopJ dampened the response and partially suppressed TNF-α production, while YopT and YopE amplified the response causing increased production of TNF-

α, which required their enzymatic activity [84]. It was proposed that the infected macrophages sensed pore formation induced by translocon insertion or recognized an unknown cytosolic MAMP delivered by *Yersinia* T3SS (Figure 1.3 B) [84]. To investigate whether T3SS-induced pore formation was sufficient to trigger TLR-independent signaling in macrophages, Kwuan et al. used an effectorless *Y. pseudotuberculosis* strain that expressed a YopD allele missing its transmembrane domain (YopD$_{\Delta TM}$) [71]. The YopD$_{\Delta TM}$ mutant, defective in translocation but capable of forming pores in macrophages, did not elicit TNF-α expression in *MyD88$^{-/-}$/Trif$^{-/-}$* macrophages. These data support the model that YopBD-mediated translocation of an unknown MAMP leads to the transcriptional response in macrophages. However, as the YopD$_{\Delta TM}$ mutant formed smaller pores with delayed kinetics compared to wild-type strain, an alternative possibility is that wild-type YopBD translocon is specifically recognized by macrophages [71].

Translocon insertion stimulates inflammasome activation in *Yersinia* infected cells. In addition to the host response described above, translocon insertion by the *Yersinia* T3SS triggers inflammasome mediated pathways in macrophages (Figure 1.4). Infection with effectorless *Y. pseudotuberculosis* stimulates rapid caspase-1 activation in both naïve and LPS-primed activated macrophages, which requires YopBD translocon insertion and is mediated by the ASC adaptor [40]. Macrophages deficient in NLRP3 showed dramatically decreased caspase-1 activation, suggesting a key role for NLRP3 in this process. NLRC4 also contributed to inflammasome activation triggered by *Yersinia* T3SS, which was only detectable in macrophages lacking NLRP3 (Figure 1.4) [40]. Translocon insertion induced caspase-1 activation leads to proinflammatory host cell death (pyroptosis) and secretion of proinflammatory IL-1β, which may contribute to anti-*Yersinia* immunity [40,71]. Membrane damage induced by translocon

insertion or delivery of an unknown substrate by T3SS could potentially promote inflammasome pathways in *Yersinia*-infected macrophages.

In addition to caspase-1 dependent canonical inflammasome activation, a caspase-11 dependent noncanonical pathway has been described in macrophages infected with Gram-negative pathogens, such as *E. coli* and *Vibrio cholerae*, or treated with particular toxins, like cholera toxin B (CTB) [85,86]. The noncanonical inflammasome activation requires LPS-stimulated TLR4 signaling via TRIF and TRIF-dependent type I IFN signaling. Capase-11 activation contributes to an NLRP3-independent, caspase-1-independent pathway that leads to host cell death and release of IL-1α. Caspase-11 also facilitates NLRP3-dependent, caspase-1 dependent canonical inflammasome pathway. Interestingly, in macrophages infected with an effectorless *Y. pseudotuberculosis* strain, translocon insertion stimulates host response involving both canonical and noncanonical inflammasome pathways [87]. The noncanonical inflammasome activation induced by *Yersinia* T3SS does not require priming with TLR4-IFN signaling and results in rapid macrophage cell death and robust release of IL-α [87]. The detailed mechanism of canonical and noncanonical inflammasome activation in response to *Yersinia* T3SS translocon insertion remains to be determined.

Translocon insertion impacts *Yersinia* survival in macrophages. *Yersinia* grows primarily in an extracellular form *in vivo*; however, these bacteria can survive and grow inside phagocytic cells, which may be important at the early stages of infection (see the next section below). The ability of *Yersinia* to survive in murine macrophages *in vitro* is influenced by the state of host cell activation and T3SS expression in the bacteria. Remarkably, unlike other bacterial pathogens where T3SS function is necessary for intracellular growth, the *Yersinia* T3SS can inhibit survival of *Y. pseudotuberculosis* in macrophages [88,89]. Roy et al. obtained evidence

18

that during internalization of *Salmonella Typhimurium* or *Y. pseudotuberculosis,* the T3SSs of these pathogens stimulated phagolysosome fusion in macrophages [88]. Phagosome-lysosome fusion required Synaptotagmin VII (SytVII), a protein that localizes to lysosomes, and regulates vesicle fusion in a Ca^{2+}-dependent manner. A *Y. pseudotuberculosis* YopE⁻ YopH⁻ YopT⁻ mutant (*yopEHT*) survived better in *SytVII^{-/-}* macrophages than in wild-type macrophages, while a T3SS-null mutant survived equally in both types of cells [88]. Additionally, the *yopEHT* mutant, but not the T3SS⁻ mutant, caused lysosomal exocytosis in fibroblasts and pore formation in macrophages [88]. From these data it was suggested that after phagocytosis, translocon insertion by the *yopEHT* mutant resulted in pore formation and Ca^{2+} influx into cytosol, stimulating SytVII-mediated phagosome-lysosome fusion and subsequent bacterial killing. Interestingly, recent data show that a T3SS in *Salmonella* (T3SS-1) and the *Y. pseudotuberculosis* T3SS stimulate Ca^{2+}-dependent lysosome exocytosis in infected macrophages via a process that requires caspase-1 [90]. One can envision that Ca^{2+}-and caspase-1-dependent lysosome exocytosis is a general and conserved response to membrane perturbation by translocon insertion, leading to increased killing of intracellular bacteria and release of antimicrobial host factors.

On the other hand, the T3SS in *Y. enterocolitica* has been shown to inhibit β1-integrin mediated bacterial internalization, protecting the bacteria from an autophagy-dependent killing pathway inside macrophages [91]. Autophagy may play a species specific role in survival of *Yersinia* in macrophages, because Moreau et al. demonstrated that autophagosomes supported *Y. pseudotuberculosis* replication in macrophages, while inhibition of autophagy resulted in bacterial killing [92]. It is important to note that in the experiments of Moreau et al., the expression of T3SS was not induced before infection. Therefore, the effect of the T3SS on

bacterial survival in macrophages or modulation of autophagy was not explored. A better understanding of how the T3SS influences autophagy and survival of different *Yersinia* species in macrophages will require more investigation.

1.5 Rationale and Hypothesis

Evidence for intracellular survival of *Yersinia* in macrophages. *Yersinia* is generally considered as an extracellular pathogen, as the bacteria grow primarily in an extracellular form at later stage of infection *in vivo*. Several Yops cooperate to antagonize the phagocytosis of *Yersinia* by phagocytes. However, even under optimal Yop inducing conditions *in vitro*, approximately 50 % of the bacteria that come into contact with macrophages are internalized [93-95]. Therefore, Yops decrease but do not completely block uptake of *Yersinia* by macrophages. *Y. pestis* has long been known as a facultative intracellular pathogen; *Y. pseudotuberculosis* and *Y. enterocolitica* also have the ability to survive and multiply in macrophages [26].

Several studies provided *in vivo* evidences showing that *Yersinia* was able to survive inside macrophages. Finegold et al. infected Rhesus monkeys with aerosolized *Y. pestis* and showed structurally intact bacteria in phagosomes of alveolar macrophages from the lung sections by electron microscopy [96]. Fujimura et al. observed bacteria inside follicle-associated macrophages of the Peyer's patches, which were recovered from rabbits infected with *Y. pseudotuberculosis* via ileal loops for 2 or 4 h [97]. Similarly, intact bacteria were found inside monocytic cells of the PPs from *Y. enterocolitica*-infected rabbits after 3 to 6 h of infection [98]. When animals infected for longer than 12 h were analyzed, *Yersinia* were typically found as

aggregates of extracellular organisms in the infected tissues, indicating that intra-macrophage survival may be of greatest importance at early stages of infection [26].

In vitro studies using cultured macrophages have also demonstrated that *Y. pestis, Y. pseudotuberculosis* and *Y. enterocolitica* share the ability to survive and replicate inside macrophages under certain conditions [26,99-101]. The ability of *Yersinia* to survive in macrophages does not require the virulence plasmid encoded T3SS; a second distinct T3SS encoded on the chromosomes is also dispensable [101]. It is important to point out that those studies generally utilized bacteria grown at 26 °C, thus the expression of T3SS Yops was not pre-induced before infection. Therefore, the potential effect of T3SS on *Yersinia* intra-macrophage survival was not explored in those studies.

Several studies showed that PhoP, the response regulator of the two-component PhoP/PhoQ sensory transduction system, is required for survival and replication of *Y. pestis* and *Y. pseudotuberculosis* in macrophages [102-104]. PhoP promotes bacterial adaption to the hostile environment in phagosomes by regulating two major groups of genes: genes needed for survival under low magnesium conditions and genes required for modification of the outer membrane [104]. *Y. pestis* and *Y. pseudotuberculosis phoP* mutants are less virulent in comparison to their corresponding wild-type strains in mouse infection models (75-fold and 100-fold less virulent individually as determined by an LD_{50} assay) [102,103], suggesting that PhoP plays a critical role for *Yersinia* virulence. These data also indicate that the ability to survive and replicate in macrophages is critical for *Yersinia* pathogenesis.

Roles of intracellular survival in *Yersinia* pathogenesis. The ability to survive and proliferate in macrophages may promote *Yersinia* pathogenesis from several aspects. Macrophages could

serve as permissive sites for bacterial replication at early stages of infection, which protect the bacteria from killing by neutrophils recruited to the site of infection [26]. The ability to survive in macrophages helps the bacteria to avoid destruction upon entering the host, giving the bacteria time to become conditioned for growth at 37 ℃ and get equipped with T3SS. This might be of great significance for *Y. pestis* pathogenesis, since the organisms would be at ambient temperature in the flea just before infection. In addition, macrophages may serve as transport vehicles facilitating dissemination of *Yersinia* in the host during the infection [26]. Very little is known about how *Yersinia* transfers from the initial infection site to deeper lymph tissues. It is believed that the intracellular bacteria are transported into deeper tissues while the macrophages are migrating, which promotes bacterial spreading in the host. Moreover, macrophages serve as antigen-presenting cells to direct the development of adaptive immune response. The ability of *Yersinia* to survive in macrophages reduces bacterial antigen processing, which delays activation of an early immune response [26].

***Yersinia* T3SS negatively affects bacterial survival inside macrophages.** Interestingly, T3SS-dependent killing of wild-type *Y. pseudotuberculosis* in macrophages was observed under experimental conditions in which T3SS expression was pre-induced [89]. Macrophages restricted intracellular survival of wild-type strain, but not a *yopB⁻* mutant (deficient in Yops translocation) or a pYV⁻ mutant (missing the entire T3SS) [89]. These results suggested that some T3SS-dependent factor encoded in wild-type strain limits *Yersinia* survival in macrophages, the mechanism of which remains unclear.

Thus, the aims of this study are to identify the specific T3SS-dependent factor that restrict *Yersinia* intra-macrophage survival and investigate the specific mechanism of the process. *Yersinia* T3SS effectors, with their activities to counteract and activate immune

response, are potential candidates that hinder bacterial intracellular survival. We hypothesize that the activities of T3SS effectors might be sensed as patterns of pathogenesis, promoting killing of intracellular bacteria by host cell as a protective ETIR. Giving the fact that *Yersinia* survives and proliferates in macrophages both *in vivo* and in *vitro* and the potential roles of intra-macrophage survival in *Yersinia* pathogenesis, the study of how T3SS and Yop effectors impact bacterial intracellular survival is important for a better overall understanding of *Yersinia* pathogenesis. Through the study of T3SS-dependent intracellular killing process and ETIR, I hope to contribute to a broader understanding the mechanisms of innate immunity and provide further insights into bacterial pathogenesis.

1.6 Figures
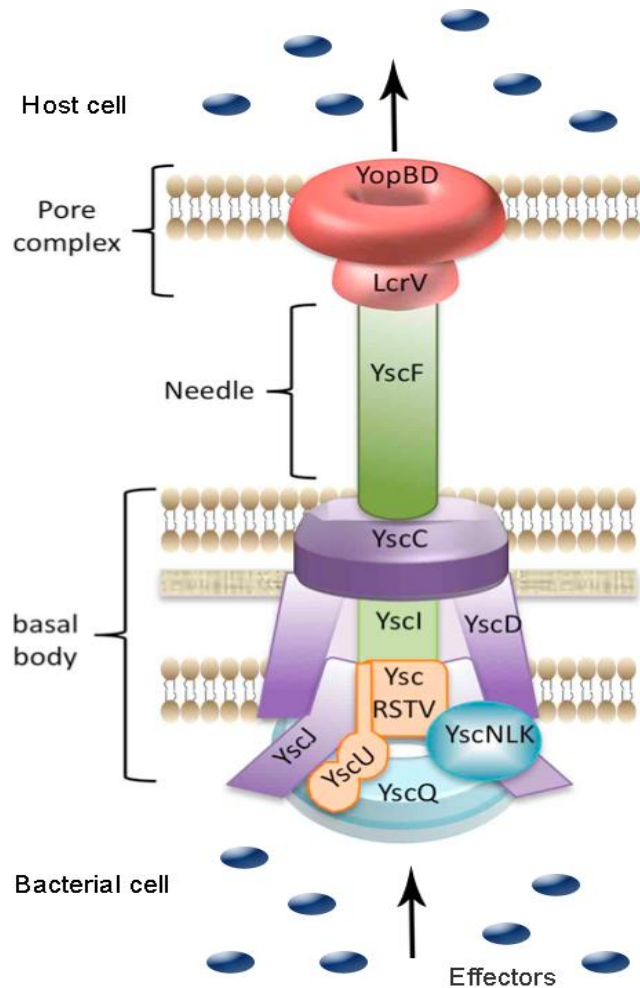
Figure 1.1: Model of the *Yersinia* Type III secretion injectisome.

Shown is a cartoon model representing the structural components of the *Yersinia* injectisome. The injectisome is composed of a basal body extending from the bacterial cell, a needle-like appendage, and a pore complex on the tip. The basal body consists of scaffold proteins (YscC, YscD and YscJ in purple), export apparatus proteins (YscR, YscS, YscT, YscU and YscV in orange), and cytoplasmic components (YscQ, YscN, YscL and YscK in light blue). YscN, YscL and YscK form the ATPase complex on the cytosolic face of the basal body. The need protein YscF and the rod protein YscI are shown in green. LcrV and YopB/YopD forms the pore complex (in red) on the distal end of the injectisome. Yop effectors are shown in dark blue. Adapted from Dewoody, 2013 [39].
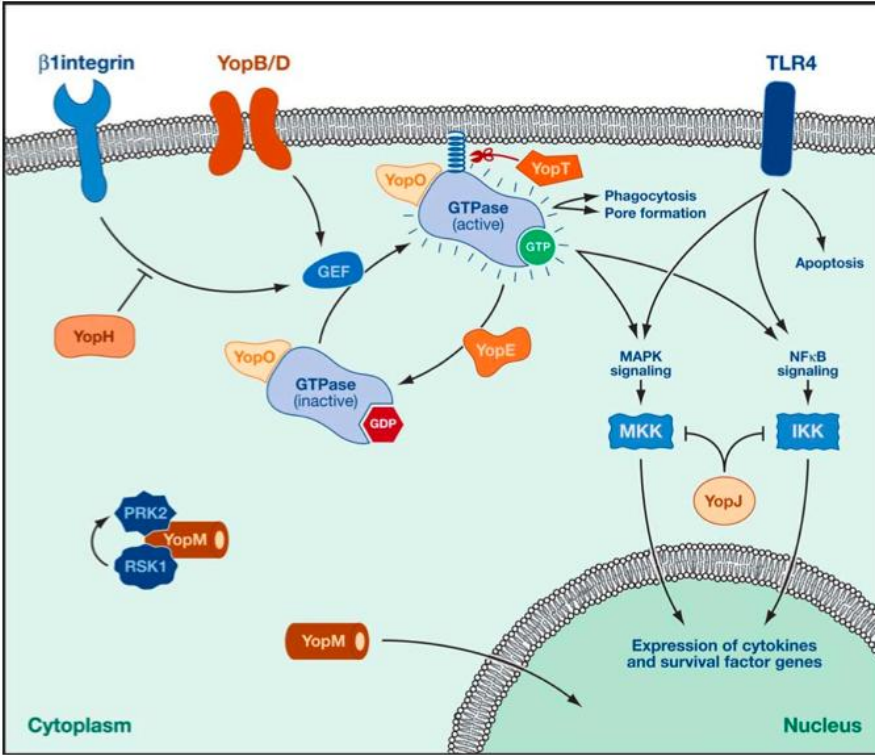
Figure 1.2: Modulation of host signaling pathways by Yops.

Upon delivery into host cell cytosol, Yop effectors perform a variety of activities to disturb host cellular processes, as shown above. Activation of β1-integrin signaling leads to phagocytosis, which is counteracted by YopE, YopH, YopT and YopO. Stimulation of TLR4 signaling promotes activation of MAPK and NF-κB pathways, both of which are inhibited by YopJ. YopM can be translocated into the nucleus or forming a complex with protein kinase C-like 2 (PRK2) and ribosomal protein S6 kinase (RSK1). Adapted from Viboud and Bliska, 2005 [27].
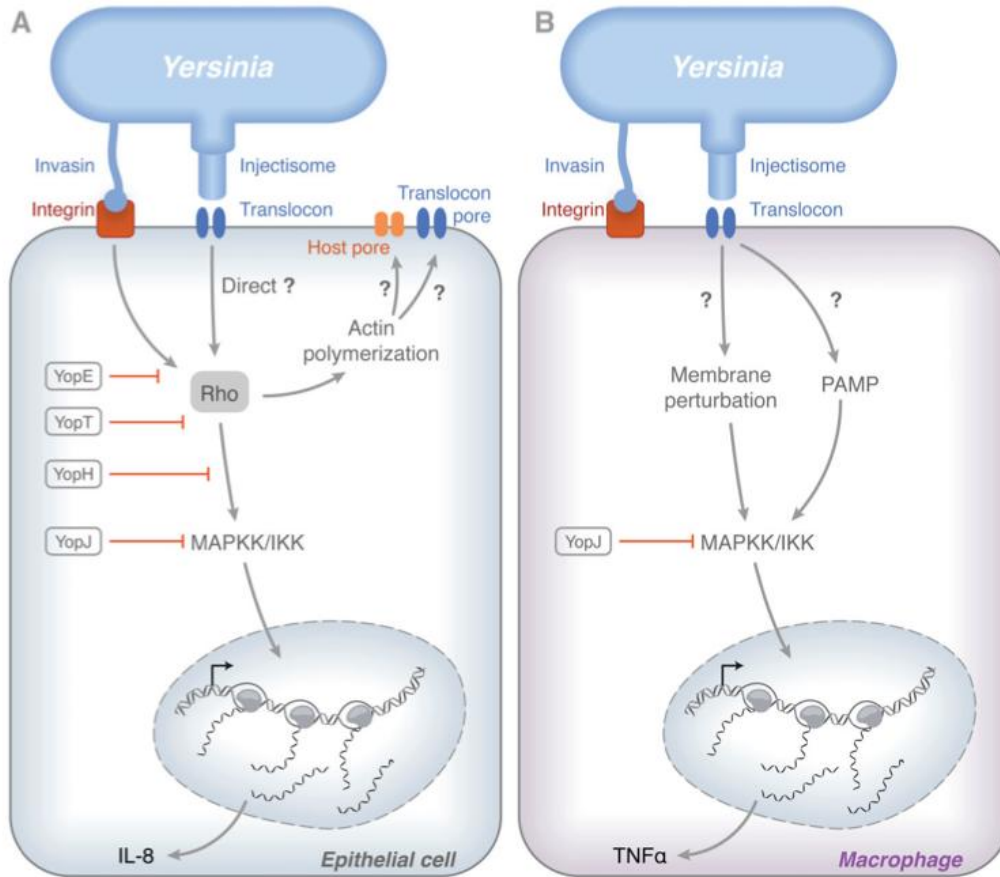
Figure 1.3: Model showing how translocon insertion stimulates pore formation pathway and pro-inflammatory responses in *Yersinia* infected epithelial cells or macrophages.

(A) In epithelial cells, translocon insertion induces Rho activation, leading to pore formation on the host plasma membrane, which requires actin polymerization. Rho activation also promotes gene expression pathways. YopE and YopT directly inhibit Rho. YopH and YopJ also counteract the pro-inflammatory response. (B) In macrophages, translocon insertion triggers host gene expression and production of TNF-α. Host cells may sense membrane perturbation directly or recognize an unknown translocated MAMP (or called PAMP). YopJ dampens the response and partially suppresses TNF-α production. Adapted from Bliska, 2013 [19].
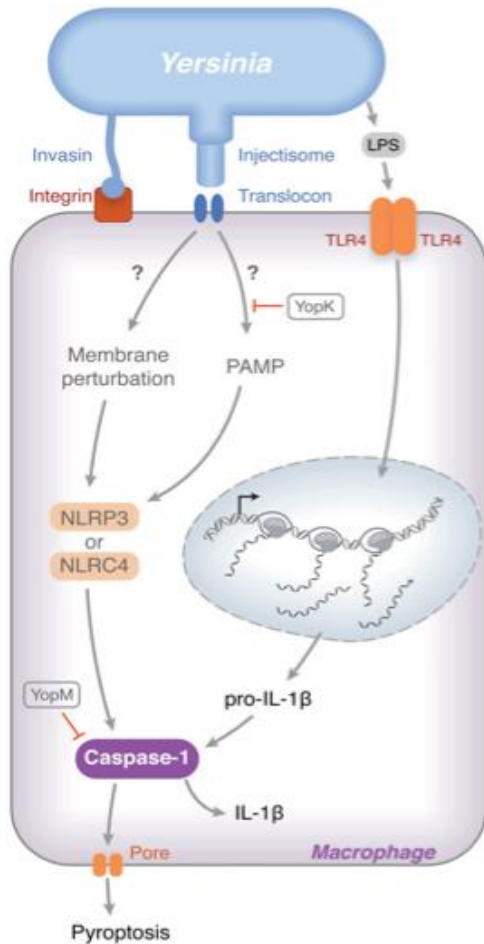
Figure 1.4: Model depicting how translocon insertion stimulates inflammasome activation in *Yersinia* infected macrophages.

LPS-TLR4 signaling promotes production of pro IL-1β and other inflammasome components (not shown). Translocon insertion triggers caspase-1 activation through NLRP3 or NLRC4, leading to pyroptosis and IL-1β secretion. In this process, host cells may respond to membrane perturbation or an unknown PAMP delivered by the T3SS. YopK regulates translocation rate and prevents inflammasome activation in naïve or LPS-primed macrophages. YopM interrupts inflammasome assembly and caspase-1 activation in LPS-primed macrophages. Adapted from Bliska, 2013 [19].

Chapter 2: Identification of T3SS dependent effector that decreases *Yersinia* survival inside macrophages.

2.1 Summary

Y. pseudotuberculosis has the ability to survive and even multiply inside murine macrophages [26]. Interestingly, T3SS expression negatively impacts survival of the bacteria in macrophages *in vitro* [88,89], the mechanism of which requires more studies. The aim of this chapter is to identify specific T3SS dependent effector that inhibits *Yersinia* intra-macrophage survival. The survival of IP2666 (wild-type) and several *yop* deletion mutants were studied by gentamicin protected CFU assay and fluorescence microscopy. Our results show that YopE and YopH limit survival of *Yersinia* inside macrophages, while YopT counteracts the effect of YopE and promotes bacterial intra-macrophage survival. Additionally, comparison of wild-type and *SytVII* $^{/-}$ macrophages revealed that SytVII-mediated phagolysosome fusion does not contribute to YopE-dependent reduced survival of *Yersinia* in macrophages. Furthermore, control experiments show that the reduced intracellular survival of wild-type strain is not due to increased gentamicin internalization or YopJ-induced macrophage cell death.

2.2 Introduction

Yersinia has the ability to survive inside macrophages as supported by both *in vivo* and *in vitro* evidences [26,96-101]. This intracellular survival ability of *Yersinia* may be important for its early stage of colonization, as macrophages might serve as permissive sites for bacterial replication or even as transport vehicles from the initial infection site into deeper lymph tissues [101]. Interestingly, T3SS function inhibits survival of *Y. pseudotuberculosis* in macrophages *in*

28

vitro. Under experimental conditions in which T3SS expression is pre-induced, reduced survival of the wild-type strain was observed in comparison to a yopB− mutant (deficient in Yops translocation) or a pYV− mutant (missing the entire T3SS) [89], the mechanism of which is enigmatic. It has been shown that upon infection, the T3SS of *Y. pseudotuberculosis* triggers phagolysosome fusion in macrophages, which is mediated by the Ca2+ sensor SytVII, leading to increased killing of intracellular bacteria [88]. Yet, more studies are needed to determine if Ca2+-SytVII dependent intracellular killing mediates this process and the potential role of Yop effectors in determining the fate of intracellular bacteria in macrophages.

2.3 Materials and Methods

Bacterial strains and plasmids. The *Y. pseudotuberculosis* strains used in this study are listed in Table 2.1. These bacteria were grown on LB agar plates or in LB broth at 28 ℃ supplemented with 100 μg/ml ampicillin, 25 μg/ml kanamycin or 30 μg/ml chloramphenicol as needed. The plasmids pMMB67HE [105], pYopT [80], pPTYopT [81], pYopTC139S [84] and p67GFP3.1 [101] have been previously described.

Cell culture. Bone marrow-derived macrophages (BMDMs) were isolated and cultured from femurs of C57BL/6 wild-type mice (Jackson Laboratory) or *SytVII$^{-/-}$* C57BL/6 mice (a generous gift from Dr. Norma Andrews, University of Maryland) as previously described [106]. 24h before infection, macrophages were seeded into 24-well tissue culture plate at a density of 1.5×10^5 cells per well in Dulbecco's modified Eagle medium supplemented with 10% fetal bovine serum (Hyclone), 15% L-cell conditioned medium, 1 mM sodium pyruvate and 2 mM glutamate.

Infection conditions. *Y. pseudotuberculosis* strains were grown at 28 ℃ in LB broth with aeration overnight. The next day, overnight cultures were diluted 1:40 into fresh LB broth containing 2.5 mM $CaCl_2$ and sub-cultured at 37 ℃ for 2 h to induce *yop* gene expression. Bacteria were washed once and resuspended in HBSS to obtain optical density at OD 600nm. Next, bacteria were diluted into cell culture medium to infect macrophages at an MOI of 10, unless specified. After centrifugation for 5 min at 700 rpm to facilitate bacterial contact with macrophages, another 15 min incubation was performed at 37 ℃, giving the total infection time of 20 min. The end of 20 min incubation is considered as 0 h post infection. To eliminate extracellular bacteria, unless specified, the cells were then incubated in medium containing 8 μg/ml gentamicin for 1 h, and then maintained in fresh medium containing 4.5 μg/ml gentamicin until the end of incubation.

CFU assay. BMDMs were prepared and infected as described above. At the time points indicated in the figures, the infected BMDMs were washed twice with HBSS, lysed and scraped with 500 μl 0.1% Triton X-100 in HBSS to release intracellular bacteria. After collecting the lysates, 500 μl HBSS was used to rinse the wells and collect any residual bacteria. The lysates and the wash were combined, serially diluted and spread on LB plates, and then incubated at 28 ℃ for 2 days to enumerate output CFU.

Fluorescence microscopy. BMDMs were prepared and infected as described above, except that they were seeded into wells with glass coverslips, which had been washed with acetone and heated at 180 ℃ for 4 h to remove LPS. At indicated time points, infected BMDMs were washed three times with PBS and fixed with 2.5% PFA for 10 min. When needed, 0.5 mM Isopropyl-β-D-thiogalactopyranoside (IPTG) was added at 1 h before fixation to induce de novo GFP expression. After washing with PBS, the coverslips were inverted onto 6 μl Prolong Gold anti-

fade reagent (Invitrogen) on a microscope slide. The slides were examined by fluorescence microscopy using a Zeiss Axioplan2 microscope with a $32\times$ objective. Three randomly selected fields of each slide were examined. In each field, about 50 BMDMs were examined from merged images of phase contrast and fluorescence, which were captured with a Spot camera (Diagnotic Instruments, Inc) and processed with Adobe Photoshop.

Mouse genotyping. Chromosome DNA was isolated from C57BL/6 wild-type or *SytVII*$^{-/-}$ mouse tails and used as templates for PCR amplification. Briefly, tail tips were digested in 500 μl lysis buffer (0.1 M NaCl, 0.05 M Tris-HCL pH7.7, 1% SDS and 2.5 mM EDTA) with 40 μg/ml freshly added proteinase K (Sigma), and incubated at 55 ℃ overnight. The resulting supernatant were collected and mixed with 500 µl isopropanol to precipitate chromosomal DNA. After centrifugation (14000 rpm, 10 min, RT), the pellets were washed twice with 70% ethanol, air-dried for 5 min, and dissolved in 100 µl TE buffer. Genotyping PCR were performed with the following primers: P1 (5'-CATCCTCCACTGGCCATGAATG-3'), P2 (5'-GCTTCACCTTGGTCTCCAG-3'), P3 (5'-CTTGGGTGGAGAGGCTATTC-3') and P4 (5'-AGGTGAGATGACAGGAGATC-3'). PCR products were analyzed by agarose gel electrophoresis.

Immunoblotting. The primary antibodies used in this study were a cocktail of two monoclonal mouse anti-YopE antibodies designated 202 and 149 (unpublished data), the monoclonal mouse anti-YopH antibody designated 3D10 (a gift from Dr. Richard Siegel, NIH) diluted 1:1000, a polyclonal rabbit anti-YopT antibody diluted 1:500 [81], and a polyclonal rabbit anti-β-actin antibody (Cell signaling) diluted in 1:1000. The secondary antibodies used were a goat anti-mouse antibody conjugated to IRD800 (Rockland) diluted 1:5000 and a donkey anti-rabbit antibody conjugated to IRD800 (Rockland) diluted 1:5000.

The protein samples were separated by sodium dodecyl sulfate-polyacrylamide (SDS) gel electrophoresis, transferred to nitrocellulose membranes, and subjected to immunoblotting with specific primary and secondary antibodies. The membranes were then scanned and analyzed with the Odyssey system (Li-Cor Biosciences).

Secretion assay. *Y. pseudotuberculosis* stains were grown at 28 ℃ in LB broth with aeration overnight. The next day, overnight cultures were diluted 1:40 into fresh LB broth supplemented with 20 mM NaOX and 20 mM $MgCl_2$ and sub-cultured at 28 ℃ for 2 h. After 2 h, bacterial cultures were shifted to 37 ℃ and shaken for 4 h to maximally induce Yop secretion. Next, supernatants of bacterial cultures were collected and precipitated with TCA at 4 ℃ overnight. The precipitates were then subjected to SDS gel electrophoresis, which was followed by staining with GelCode Blue Stain Reagent or immunoblotting to analyze secreted Yops, as described above.

Detergent extraction assay. Detergent extraction assays were performed as previously described [107]. BMDMs were infected as described above, except that they were seeded in 6 well plates at a density of 8×10^5 cells/well and infected at an MOI of 30 for 2 h. The infected cells were washed twice with ice-cold HBSS and lysed with 50 μl 1% Triton X-100 in HBSS containing EDTA-free protease inhibitor cocktail (ROCHE). After 10 min on ice, the cells were scraped from the plate to collect the lysates. The soluble and insoluble fractions of the lysates were separated by centrifugation (14000 rpm, 10 min, 4 ℃) and subsequently analyzed using immunoblotting as described above.

2.4 Results

YopE and YopH restrict intra-macrophage survival of *Y. pseudotuberculosis*. To examine

whether specific Yop effectors contribute to the reduced survival of *Y. pseudotuberculosis*, the

survival of the wild-type (IP2666) and several *yop* mutant strains were studied. Initially, IP2666

(wild-type), IP17 (*yopEH⁻*), IP27 (*yopEHJ*) and IP37 (*yopEHJMKYpkA⁻*) (Table 2.1) were

compared for the ability to survive inside BMDMs. For this purpose, naïve BMDMs were

infected with indicated strains and then treated with gentamicin to eliminate extracellular

bacteria. At indicated time points, infected BMDMs were lysed and spread on LB plates to count

viable intracellular bacteria. With CFU at 1h post infection considered as the initial intracellular

bacteria count, the ratio of CFU between 23h and 1h post infection was calculated for each

indicated strain. At 1h post infection, IP2666 displayed slightly lower CFU in comparison to

IP17, IP27 and IP37 (Figure 2.1A). This is because IP2666 expresses Yops with anti-phagocytic

function (YopE and YopH), while the other strains are *yopEH⁻* mutants. At 23h post infection,

the CFU level of IP17 was significantly higher than IP2666, but similar to IP27 and IP37 (Figure

2.1B). As for the ratio of CFU at 23h/1h, IP17 displayed significantly increased level in

comparison to IP2666, but comparable to IP27 and IP37 (Figure 2.2A). To investigate if the

initial internalization level determines the intracellular survival phenotypes we observed,

BMDMs were infected with IP2666 or IP17 at different MOIs (Figure 2.3). Even with higher

CFU at 1h post infection, IP2666 (MOI=10) still showed decreased survival in comparison to

IP17 (MOI=5 or 2.5) at 23h post infection (Figure 2.3). Thus, IP2666 exhibits reduced

intracellular survival in comparison to IPI7, which displayed an intracellular growth phenotype,

indicating that deletion of *yopE* and *yopH* promotes *Y. pseudotuberculosis* survival in

macrophages.

To further elucidate the effects of YopE and YopH on *Yersinia* intracellular survival, IP2666 (wild-type), IP6 (*yopE⁻*), IP15 (*yopH⁻*) and IP17 (*yopEH⁻*) (Table 2.1) were compared by CFU assay (Figure 2.2B). IP6 exhibited an intracellular growth phenotype comparable to IP17, while IP15 showed an intermediate phenotype (Figure 2.2B). The results were further confirmed by fluorescence microscopy, in which IP2666, IP6 and IP17 encoding GFP were used to infect BMDMs for different lengths of time. One hour before fixation of the samples, IPTG was added to induce de novo expression of GFP from viable intracellular bacteria (Figure 2.4). At 23h post infection, IP6 and IP17 showed greatly improved survival in comparison to IP2666 (Figure 2.4). These results indicate that YopE contributes to the reduced survival of *Yersinia* in macrophages, while YopH cooperates with YopE in this process.

Reduced intra-macrophage survival of *Y. pseudotuberculosis* does not require SytVII. To determine if SytVII is essential for restricting intracellular survival of *Yersinia*, *SytVII⁻/⁻* BMDMs were compared to wild-type BMDMs for their ability to constrain intracellular survival of IP2666, IP17 or IP40 (*yopB* mutant, Table 2.1). The *SytVII⁻/⁻* genotype was confirmed by PCR using mouse-tail genomic DNA, in comparison to wild-type mice (Figure 2.5A). No significant difference was observed for IP2666 survival inside wild-type or *SytVII⁻/⁻* BMDMs as determined by CFU assay (Figure 2.5B), suggesting that SytVII-mediated phagolysosome fusion does not contribute to the YopE-dependent reduced survival of *Yersinia* in macrophages.

Reduced intra-macrophage survival of *Y. pseudotuberculosis* is not due to increased gentamicin uptake or YopJ induced macrophage cell death. As control experiments, we examined the possibility that IP2666 infection induces gentamicin internalization, which results in elevated bacterial killing by gentamicin. If this hypothesis is true, with increasing amount of gentamicin, intracellular IP2666 would be more susceptible than IP17, due to more gentamicin

uptake. To test this hypothesis, the survival of IP2666 and IP17 in macrophages was compared in the presence of increasing amount of gentamicin. IP2666 and IP17 responded similarly to increasing amounts of gentamicin (Figure 2.6), suggesting that decreased intracellular survival of IP2666 is not due to increased gentamicin uptake.

In addition, we investigated the possibility that IP2666 infection induces higher level of macrophage cell death, which could expose intracellular bacteria to gentamicin and therefore decrease bacterial survival. Since YopJ is the essential effector causing cell death in naive macrophages upon *Yersinia* infection, the intra-macrophage survival of IP2666, IP6 (*yopE⁻*), IP26 (*yopJ*) and IP31 (*yopEJ*) (Table 2.1) were analyzed by CFU assay (Figure 2.7). IP26 had a similar phenotype as IP2666, displaying reduced intracellular survival in comparison to IP6 or IP31, indicating that YopJ does not affect *Yersinia* intracellular survival (Figure 2.7). Moreover, under our experimental conditions, *Yersinia* infection does not stimulate significant macrophage cell death (below 2% LDH release from IP2666 or IP6 infected macrophages at 23h post infection, data not shown). Accordingly, the decreased intracellular survival of the wild-type strain is not caused by *Yersinia*-induced macrophage cell death.

Overexpression of YopT counteracts the effect of YopE and promotes survival of *Y. pseudotuberculosis* in macrophages. In addition to YopE and YopH, YopT is another important effector that directly targets Rho GTPases in *Yersinia* infected macrophages. Given that YopE and YopH restrict survival of *Yersinia* inside macrophage, the potential influence of YopT in this process was also studied. IP2666 is a naturally-occurring *yopT* mutant, as the *yopT* gene contains a deletion in pYV in this strain [81]. Plasmid vectors that overproduce YopT or catalytically-inactive YopTC139S were introduced into IP2666 (named as IP2666+pYopT and IP2666+pYopTC139S respectively, Table 2.1). In parallel, strains containing an empty plasmid

or a plasmid expressing native levels of YopT (IP2666+YopT) were also created as controls (Table 2.1). Analysis of bacterial samples prepared from secretion assays using SDS-PAGE and immunoblotting showed that YopT and YopTC139S were overproduced at equal levels, while the native level of YopT was undetectable (Figure 2.8A, compare lanes 2, 3 and 4). Remarkably, when those strains were used to infect macrophages, overexpression of YopT in IP2666 dramatically improved *Yersinia* intra-macrophage survival, giving the opposite effect of YopE (Figure 2.8B and Figure 2.9A). Overexpressed YopTC139S moderately increased IP2666 survival in macrophages (Figure 2.8B and Figure 2.9A), suggesting that YopT catalytic activity is critical for counteracting YopE-triggered bactericidal effect. When native level of YopT was produced, *Yersinia* survival in macrophages was slightly increased (Figure 2.8B and Figure 2.9A).

To compare the amounts of YopE that were translocated by the different strains, detergent extraction assay and immunoblotting were performed to analyze lysates of infected macrophages. Overexpression of YopT or YopTC139S in IP2666 reduced YopE translocation to 8% or 25% of wild-type level respectively, while native level of YopT in IP2666 slightly decreased YopE translocation (75% of wild-type level) (Figure 2.10).

To further examine the mechanism by which YopT promotes survival of *Yersinia* in macrophages, plasmids that overexpress active or inactive YopT (YopTC139S or YopTH258A) were introduced into IP6 or IP37 (Table 2.1). Overexpression of YopT or YopTC139S in IP6 equally improved *Yersinia* survival (Figure 2.9B), while overexpression of active or inactive YopT proteins in IP37 had no effect on *Yersinia* survival inside macrophages (Figure 2.9C).

Taken together, these results suggest that YopT has the ability to counteract the negative effect of YopE on *Yersinia* intracellular survival, which is partially dependent on YopT enzymatic

36

activity. YopT catalytic activity may counteract the YopE effect by competing with YopE for a Rho GTPase target or by reducing YopE translocation.

2.5 Discussion

Zhang *et al.* reported that the presence of a functional T3SS negatively impacts *Y. pseudotuberculosis* survival following phagocytosis by macrophages; macrophages restrict intracellular survival of wild-type but not *yopB⁻* or pYV⁻ *Yersinia* strains [89]. In this chapter, studies were taken to identify T3SS-dependent factors that impact *Yersinia* survival inside macrophages. Our results reveal that YopE and YopH are essential factors that reduce *Yersinia* intra-macrophage survival (Figure 2.2). Three known Yops directly disrupts host Rho GTPases function: YopE, YopT and YpkA; while YopH inhibits signals that activate Rho GTPases. We hypothesize that the activities of YopE and YopH are recognized by macrophages as "patterns of pathogenesis", generating bacterial killing effect as a protective response. Unlike YopE and YopH, YpkA has very mild effect on *Yersinia* intracellular survival (data not shown), perhaps due to its low expression level in comparison to other Yops. Interestingly, overexpression of YopT counteracts the effect of YopE and increases *Yersinia* intracellular survival (Figure 2.8). This effect of YopT partially requires its protease activity (Figure 2.8). *In vivo* studies have shown that YopE is preferably effective on Rac1, while YopT is mainly active on RhoA. However, it has been observed that overexpressed YopT also targets Rac1 in *Yersinia*-infected epithelial cells [108]. In this case, YopT competes with YopE for the same pool of membrane-associated Rac1, promotes translocation of cleaved Rac1 into the nucleus, and hence interferes with the ability of YopE to inhibit Rac1 [108]. We speculate that an important biological function of YopT is to counteract recognition of YopE by the innate immune system, possibly by preventing YopE access to Rho GTPase targets or by decreasing YopE translocation level. The

37

crosstalk between YopE and YopT could ensure well-balanced manipulation of host cell Rho GTPases, benefiting bacterial pathogenesis without over-stimulating innate immune responses. Future studies will be needed to determine if YopE catalytic activity towards Rho GTPases is critical for the reduced survival of *Yersinia* in macrophages.

Roy *at el.* observed that upon infection, the T3SS of *Y. pseudotuberculosis* stimulated phagolysosome fusion and bacterial killing in macrophages, a process that was mediated by the Ca^{2+} sensor SytVII. Our data suggest that YopE-dependent reduced survival of *Yersinia* does not require SytVII (Figure 2.5), indicating that there are at least two independent pathways by which macrophages sense and restrict *Yersinia* intracellular survival. The YopE-dependent pathway might recognize manipulation of Rho GTPases, while the SytVII-dependent pathway seems to sense translocon insertion in the plasma membrane. Although SytVII-mediated bacterial killing pathway was not observed in our experimental conditions, it would be interesting to determine if Yop effectors influence SytVII-dependent phagolysosome fusion to impact *Yersinia* infection.

2.6 **Figures and Tables**

Table 2.1: *Yersinia pseudotuberculosis* **strains used in this study.**

Strain name	Relevant Characteristics	Reference
IP2666	Wild-type, pYV$^+$, naturally *yopT* $^-$	[109]
IP6	*yopE* $^-$	[110]
IP15	*yopH* $^-$	[111]
IP17	*yopEH* $^-$	[111]
IP26	*yopJ* $^-$	[65]
IP27	*yopEHJ* $^-$	[112]
IP31	*yopEJ* $^-$	[65]
IP37	*yopEHJMKypkA*$^-$	[65]
IP40	*yopB* $^-$	[113]
IP2666+empty vector	IP2666 (pMMB67HE)	This study
IP6+empty vector	IP6 (pMMB67HE), *tac* promoter	[110]
IP37+empty vector	IP37 (pMMB67HE)	This study
IP6+pYopE	IP6 (pYopE), *yopE* controlled by *tac* promoter	[110]

IP6+pYopER144A	IP6 (pYopER144A)	[110]
IP6+YopE	IP6 (pPEYopE), *yopE* controlled by native promoter	[81]
IP6+YopE3N	IP6 (pPEYopE L55N I59N L63N)	This study
IP6+YopER62K	IP6 (pPEYopER62K)	This study
IP6+YopEL109A	IP6 (pPEYopEL109A)	This study
IP6+YopE-SptP	IP6 (pPEYopE$_{1-100}$ SptP$_{166-293}$)	This study
IP2666+YopT	IP2666 (pPTYopT), *yopT* controlled by native promoter	[81]
IP6+YopT	IP6 (pPTYopT)	[81]
IP2666+pYopT	IP2666 (pYopT), *yopT* controlled by *yopH* promoter	[81]
IP2666+pYopTC139S	IP2666 (pYopTC139S)	This study
IP6+pYopT	IP6 (pYopT)	This study
IP6+pYopTC139S	IP6 (pYopTC139S)	This study
IP37+pYopT	IP37 (pYopT)	This study
IP37+pYopTC139S	IP37 (pYopTC139S)	This study

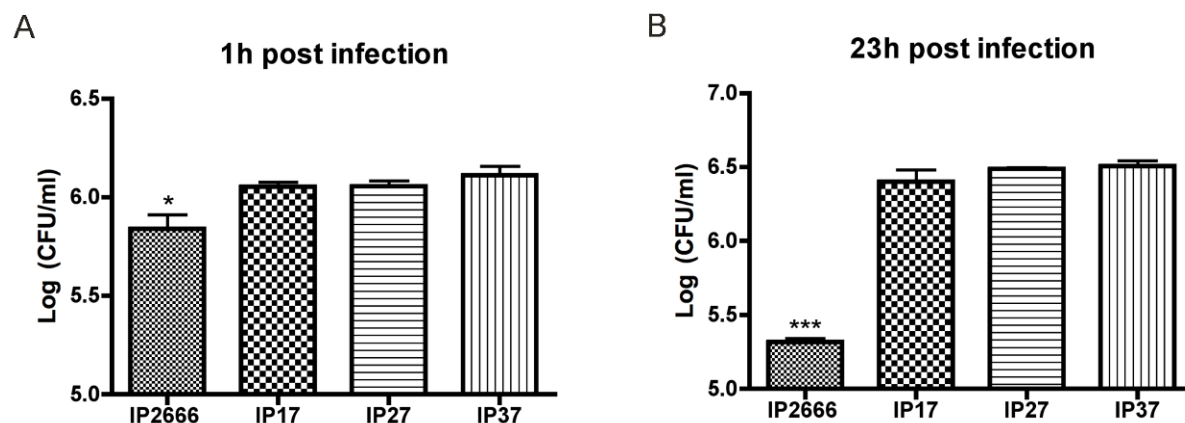|		
IP37+pYopTH258A	IP37 (pYopTH258A)	This study
yadA[-]	IP2666 *ΔyadA*	[41]
inv[-]	IP2666 *Δinv*	[41]
yadA[-]*inv*[-]	IP2666 *ΔyadAΔinv*	[41]

Figure 2.1: Survival of *Y. pseudotuberculosis* inside macrophages as determined by CFU assay.

BMDMs were infected with the indicated strains at an MOI of 10 for 20 min, followed by gentamicin treatment to eliminate extracellular bacteria. At 1 h and 23 h post infection, the infected BMDMs were lysed, and serial dilutions were plated to determine the survival of intracellular bacteria by CFU assay. (A) The logarithm of intracellular bacteria count per well at 1h post infection. (B) The logarithm of intracellular bacteria count per well at 23h post infection. Results shown are the means from four independent experiments with duplicate infection wells. Error bars show standard deviations. *, P < 0.05 and ***, P < 0.001 compared to IP17, as determined by one-way ANOVA.

Figure 2.2: Comparison of different _Y. pseudotuberculosis_ strains for survival inside macrophages.

CFU assay were performed as described in Figure 2.1. Ratios of CFU at 23h/1h are shown, determined as [23h post infection CFU/1h post infection CFU]. Results shown are the means from three independent experiments with duplicate infection wells. Error bars show standard deviations. (A)***, $P < 0.001$ compared to IP17; (B) *, $P < 0.05$ and ***, $P < 0.001$ compared to IP6, as determined by one-way ANOVA.
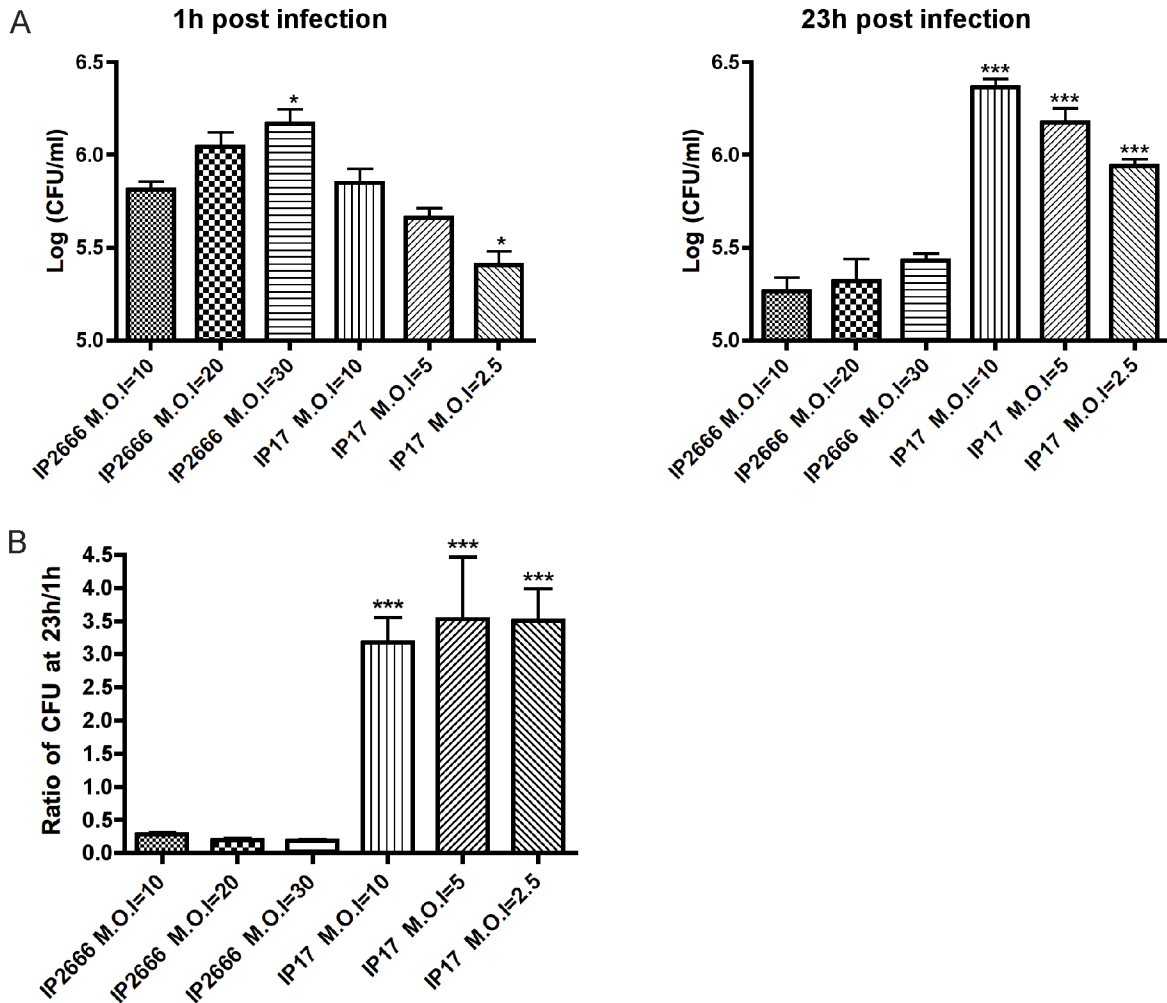
Figure 2.3: Survival of *Y. pseudotuberculosis* inside macrophages determined by CFU assay.

BMDMs were infected with the indicated strains as described in Figure 2.1, except that indicated MOIs were used. (A) The logarithm of intracellular bacteria count per well at 1h and 23h post infection. (B) Ratio of CFU at 23h/1h. Results shown are the means from three independent experiments with duplicate infection wells. Error bars show standard deviations. *, $P < 0.05$ and ***, $P < 0.001$ compared to IP2666 at an MOI of 10, as determined by one-way ANOVA.
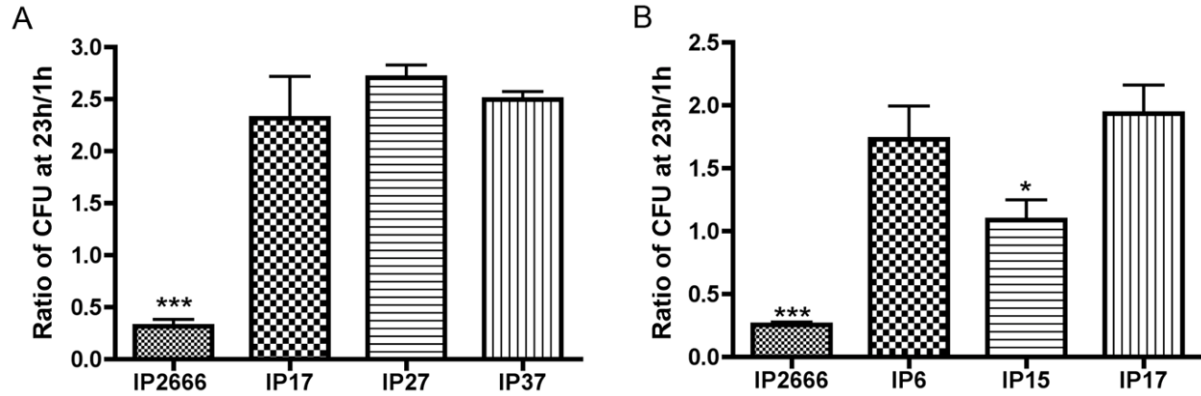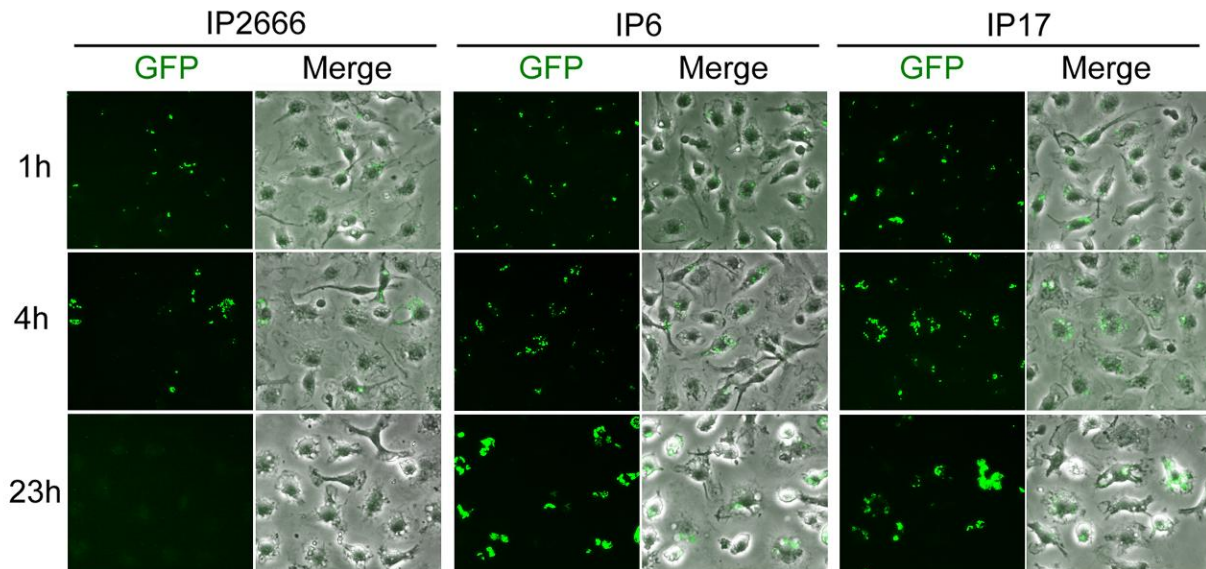
Figure 2.4: Comparison of different *Y. pseudotuberculosis* strains for survival inside macrophages as determined by fluorescence microcopy.

BMDMs were infected with the indicated GFP-encoding strains at an MOI of 10, as described in Figure 2.1. At 1h, 4h and 23h post infection, the infected BMDMs were fixed and analyzed by fluorescence microscopy. One hour before fixation, IPTG was added to induce de novo expression of GFP from viable intracellular bacteria. Shown are GFP or an overlay of GFP and phase contrast signal from representative images.
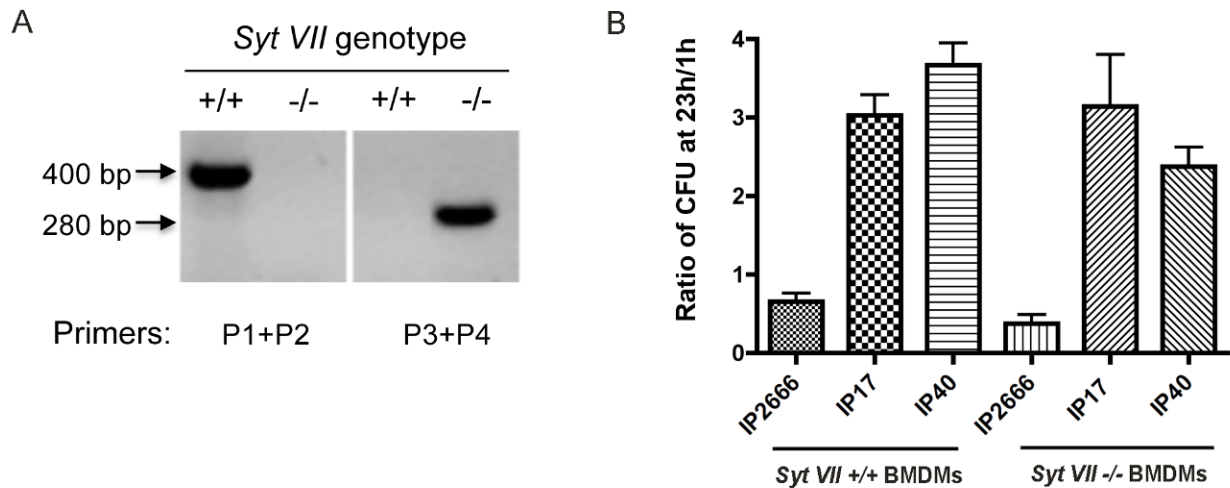
Figure 2.5: Survival of different *Y. pseudotuberculosis* strains in wild-type or *SytVII*^{-/-} macrophages.

(A) Verification of *SytVII*^{-/-} mice by tail genotyping. Shown are PCR results obtained with mouse-tail genomic DNA using indicated primers. Wild type = 400 bp; mutant = 280 bp. (B) Wild-type or *SytVII*^{-/-} BMDMs were infected with the indicated strains. Intracellular bacterial survival was measured by CFU assay, as described in Figure 2.1. Results shown are the means from three independent experiments with duplicate infection wells. Error bars show standard deviations. There is no significant difference in the survival of each strain in WT BMDMs as compared individually to that in *SytVII*^{-/-} BMDMs, as determined by one-way ANOVA.
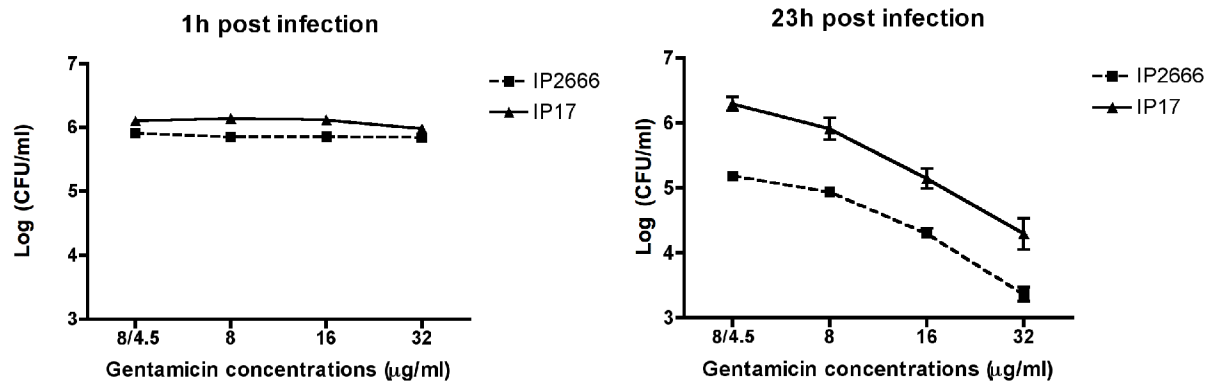
Figure 2.6: Survival of *Y. pseudotuberculosis* inside macrophages in the presence of different concentrations of gentamicin.

CFU assay were performed as described in Figure 2.1. After 20 min infection, infected cells were incubated in medium with 8 μg/ml, 16 μg/ml or 32 μg/ml gentamicin until the end of the experiment, except the first experimental group, which were incubated in medium with 8 *μ*g/ml gentamicin for 1 h and switched in medium with 4.5 μg/ml gentamicin until the end of the experiment. Shown are the logarithms of intracellular bacteria count per well at 1h and 23h post infection. IP2666 is shown in squares; IP17 is shown in triangles. Results shown are the means from three independent experiments with duplicate infection wells. Error bars show standard deviations.

Figure 2.7: Comparison of different *Y. pseudotuberculosis* strains for survival inside macrophages.

CFU assay were performed as described in Figure 2.1. Ratios of CFU at 23h/1h are shown for indicated strains. Results shown are the means from three independent experiments with duplicate infection wells. Error bars show standard deviations. ***, P < 0.001 and **, P < 0.01 compared to IP6, as determined by one-way ANOVA.
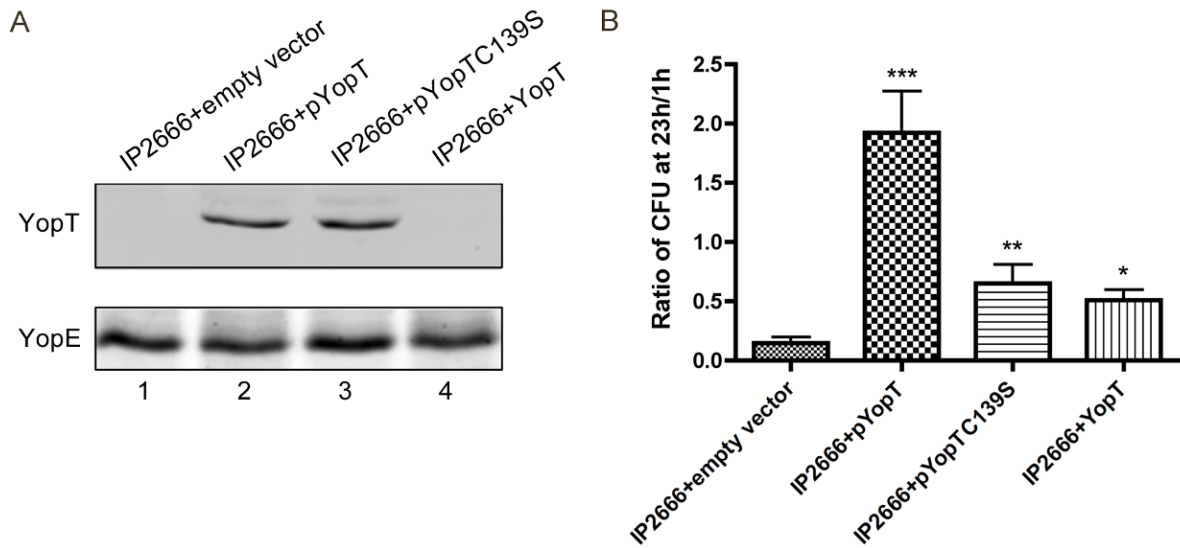
Figure 2.8: Measurement of YopT production and survival in macrophages by different *Y. pseudotuberculosis* strains.

(A) Amounts of YopT secreted by different strains as determined by immunoblotting analysis. Indicated strains were grown at 37 °C for 4 h under low Ca^{2+} conditions in a secretion assay. TCA-precipitated supernatants were analyzed using antibodies specific for YopT (upper panel). YopE levels as determined by staining with GelCode Blue Stain Reagent (bottom panel). (B) Intracellular bacterial survival was determined by CFU assay in infected macrophages, as described in Figure 2.1. Results shown are the means from four independent experiments with dup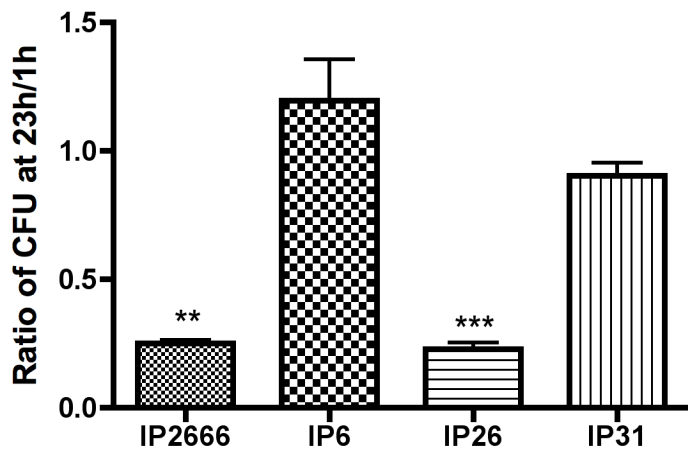licate infection wells. Error bars show standard deviations. ***, $P < 0.001$, **, $P < 0.01$ and *, $P < 0.05$ compared to IP2666+empty vector, as determined by one-way ANOVA.

49
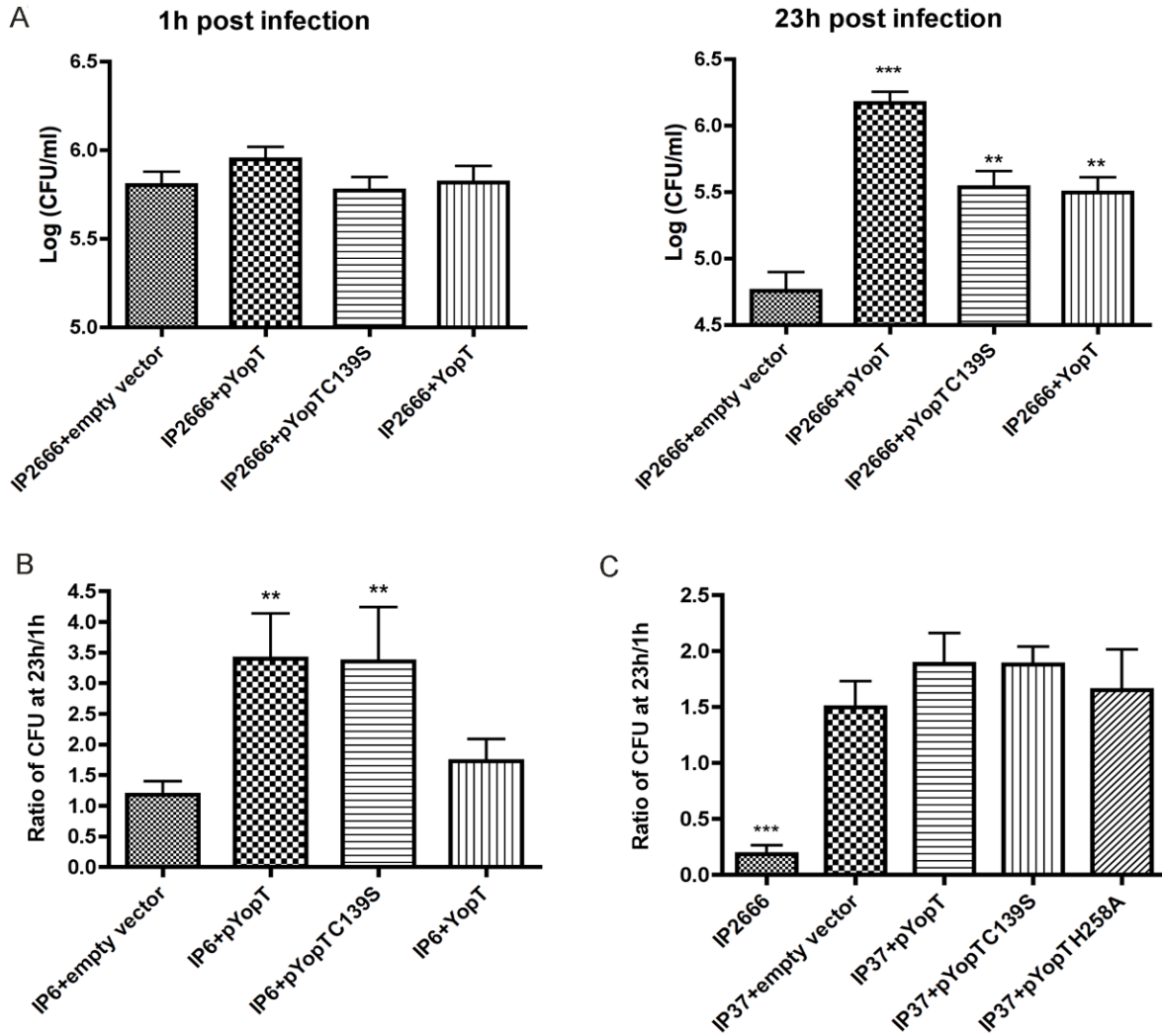
Figure 2.9: Survival of *Y. pseudotuberculosis* strains inside macrophages.

CFU assay were performed as described in Figure 2.1. (A) The logarithm of intracellular bacteria count per well at 1h post infection and 23h post infection. **, P < 0.01 and ***, P < 0.001 compared to IP2666+empty vector. (B) Ratio of CFU at 23h/1h. **, P < 0.01 compared to IP6+empty vector. (C) Ratio of CFU at 23h/1h. ***, P < 0.001 compared to IP37+empty vector. Results shown are the means from at least three independent experiments with duplicate infection wells. Error bars show standard deviations.
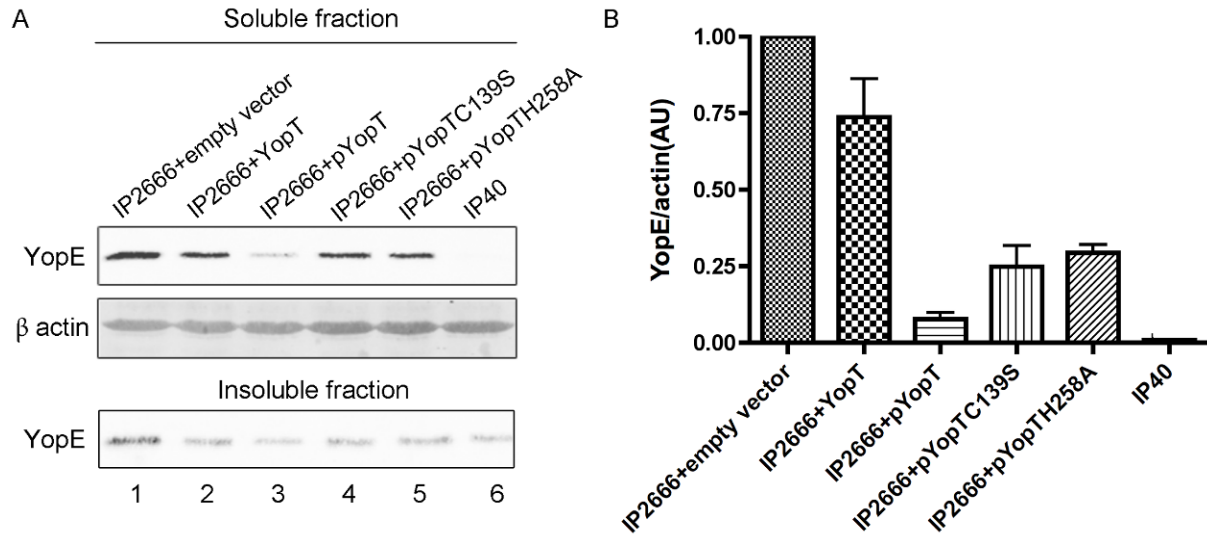
Figure 2.10: Measurement of YopE translocation in macrophages by different *Y. pseudotuberculosis* strains.

(A) YopE translocation levels in BMDMs infected by the indicated strains, determined by detergent extraction assay and immunoblotting analysis. BMDMs in 6 well plates were infected at an MOI of 30 for 2 h, then lysed using 1% Triton X-100 buffer. Cell lysates were centrifuged to obtain soluble and insoluble fractions, which were subjected to immunoblotting analysis using antibodies specific for YopE. β-actin levels from the soluble fraction are shown as loading controls. (B) The intensity of each band was calculated using Odyssey IR imaging system, and the YopE/β-actin ratios were normalized according to IP2666+empty vector. Results shown are the means from two independent experiments. Error bars show standard deviations.

Chapter 3: Investigate the role of YopE GAP activity in restricting *Yersinia* survival inside macrophages.

3.1 Summary

The effector YopE was shown in Chapter 2 to be a critical T3SS-dependent factor that restricted *Y. pseudotuberculosis* survival inside macrophages. This chapter aimed to investigate the role of YopE GAP activity in this process. Intra-macrophage survival of *Yersinia* producing YopE or YopE mutants was compared by CFU assay and fluorescence microscopy. Unlike wild-type YopE, YopER144A (catalytic-dead mutant) was impaired in restricting *Yersinia* intracellular survival, while YopE3N (defective in membrane localization) and YopER62K (less stable) presented decreased ability to trigger intracellular killing. Interestingly, *Clostridium difficile* Toxin B was able to mimic the effect of YopE and decreased *Yersinia* survival inside macrophages. These results demonstrate that sensing the manipulation of Rho GTPases by YopE GAP activity (or by other bacterial toxins like Toxin B) is critical for macrophages to restrict bacterial intracellular survival. In addition, using YopE variants with altered Rho GTPase specificities or specific Rho GTPase inhibitors, we obtained evidence that the target specificity of YopE impacts its ability to stimulate intracellular killing and that macrophages recognize inhibition of Rac but not Rho to stimulate a bactericidal response.

3.2 Introduction

In the previous chapter, we presented evidence that YopE is required for limiting survival of wild-type *Yersinia* in macrophages. YopE is a 219 amino acid, 23kDa effector containing a C terminal Rho GAP domain (YopE$_{GAP}$; residues 96 to 219) [110]. YopE binds to GTPases and

introduces an "arginine finger" into the GTPase catalytic site to promote GTP hydrolysis, which results in their deactivation. The residue Arg144 in the "arginine finger" is critical and required for the GAP activity of YopE [110]. YopE$_{GAP}$ shares structural similarity with SptP$_{GAP}$ from *Salmonella Typhimurium* and ExoS$_{GAP}$ from *Pseudomonas aeruginosa*. In mammalian cells, proper intracellular localization of YopE requires a hydrophobic leucine-rich motif within its membrane localization domain (MLD, residues 53 to 79) [84,114-116]. As found in different *Yersinia* strains, allelic variation of residues 62 and 75 influence the stability of YopE in host cells, in which lysine residues at these positions can mediate ubiquitination and degradation of YopE by the host cell proteasome pathway [117]. Both subcellular membrane localization and stability of YopE have been shown to be important for its GAP activity [115,117]. *In vitro,* YopE is equally active on Rac1, RhoA and Cdc42 [110], whereas it is preferably effective on Rac1 and RhoA, but not Cdc42, *in vivo* [118]. In this chapter, we aimed to determine if the GAP activity of YopE is essential for restricting *Yersinia* intracellular survival and identify the Rho GTPase target that is critical for the effect YopE in this process.

3.3 Materials and Methods

Bacterial strains and plasmids. The *Y. pseudotuberculosis* strains used in this study are listed in Table 2.1. Bacterial cultures were grown as described in Chapter 2. The plasmids pMMB67HE [105], pYopE [110], pYopER144A [110], pPEYopE [81] and p207mCherry [119] have been previously described.

A new series of plasmids expressing *yopE* mutants were created as described below. Plasmids encoding *yopEL109A*, *yopER62K* and *yopE3N* were generated as follows. DNA fragments encoding *yopEL109A*, *yopER62K* or *yopE3N* were obtained by PCR using primers

yopE-3 (5'-CGGATCCCATATGAAAATATCATCATTTATTTC-3') and yopE-EcoRI (5'-CGCGGAATTCCCATATCACATCAATGACAGTAATTT-3'). Recombinant plasmid DNA (pBAD33/YopEL109A, a gift from Joan Mecsas, Tufts University), or *Y. pseudotuberculosis* virulence plasmid DNA (from 32777 *yopER62K* or 32777 *yopE3N)* [120] was used as template for the PCR to obtain *yopEL109A*, *yopER62K* and *yopE3N*, respectively. The resulting DNA fragments were inserted into pETBlue2 vector using blunt end ligation. To create a plasmid encoding the *yopE-sptP fusion,* a DNA fragment containing the first 100 codons of *yopE* ($yopE_{1-100}$) was amplified from IP2666 virulence plasmid DNA with primers yopE-infusion-5 (5'-TAATAAATAGTCATATGAAAATATCATCATTTATTTCTACATCACTG-3') and yopE-infusion-3 (5'-AGGTTGCTTACTTTCCGTAGGACTTGGCATTTGTGC-3'). A DNA fragment containing codons 166-293 of *sptP* ($sptP_{166-293}$) was amplified with primers sptP-infusion-5 (5'-ATGCCAAGTCCTACGGAAAGTAAGCAACCTTTACTCAGTATCG-3') and sptP-infusion-3 (5'-CAGCCAAGCTGAATTTTAGCCGGCTTCTATTTTCTCAAGTTC-3') using chromosomal DNA from *Salmonella enterica* Typhimurium strain 14028 as template. A DNA fragment encoding the $yopE_{1-100}sptP_{166-263}$ fusion was made by overlapping PCR using the $yopE_{1-100}$ and $sptP_{166-293}$ fragments as templates and primers yopE-infusion-5 and sptP-infusion-3. The product was inserted into pETBlue2 by blunt end ligation. The sequences of the inserts in the plasmids described above were confirmed by DNA sequencing. DNA fragments encoding *yopEL109A*, *yopER62K, yopE3N* or $yopE_{1-100}sptP_{166-263}$ were obtained from the pETBlue2 vectors by digestion with NdeI and EcoRI, and ligated between the NdeI and EcoRI sites in pPEYopE, thereby replacing the wild-type *yopE* gene, and placing the mutant alleles under control of the native *yopE* promoter. The resulting plasmids pYopEL109A, pYopER62K,

pYopE3N and pYopE-SptP were introduced into *E. coli* S17-1 λpir by electroporation and subsequently transferred into IP6 (Table 2.1) by conjugation as described previously [121].

Cell culture. BMDMs were isolated and cultured from femurs of C57BL/6 wild-type mice (Jackson Laboratory) as previously described in Chapter 2. 24h before infection, macrophages were seeded into 24-well tissue culture plate at a density of 1.5×10^5 cells per well as previously mentioned.

Infection conditions. *Y. pseudotuberculosis* strains were cultured and prepared to infect BMDMs using the same conditions as previously described in Chapter 2. When indicated, 40 ng/ml Toxin B (Calbiochem), 100 μM NSC23766 (Calbiochem), or 10 μg/ml TAT-C3 was added at 0 h post infection and maintained throughout the experiment. TAT-C3 was purified and kindly provided by Dr. Gloria Viboud, Stony Brook University [82].

CFU assay, detergent extraction assay and immunoblotting. These assays were performed as described in Chapter 2.

Fluorescence microscopy. BMDMs were prepared, infected and fixed as described in Chapter 2. When needed, 0.5 mM IPTG was added at 2 h before fixation to induce de novo mCherry expression. Immunofluorescence staining was performed as described previously [101]. Briefly, the fixed cells were permeabilized with 0.1% Triton X-100 in PBS for 1 min, followed by blocking with 3% bovine serum albumin in PBS for 10 min. The cells were then incubated with a polyclonal rabbit anti-Yersinia antibody SB349 diluted 1:1000 for 30 min. After washing with PBS, the cells were incubated with FITC conjugated anti-rabbit antibody (Jackson Laboratories) diluted 1:250 for 40 min. The samples were further processed, examined and analyzed by

fluorescence microscopy as described in Chapter 2. Percentage of cells containing bacteria was quantified from at least three independent experiments.

3.4 Results

The GAP activity of YopE is critical for reduced survival of *Yersinia* inside macrophages.
To investigate if the GAP activity of YopE is essential to trigger intracellular killing, complementation experiments were carried out to compare the intracellular survival of *Yersinia* expressing YopE or YopER144A. A single substitution of arginine to alanine was introduced at residue 144 to generate a YopE catalytic-inactive mutant. Plasmid vectors producing YopE or YopER144A were introduced into IP6 (named IP6+pYopE or IP6+pYopER144A respectively, Table 2.1). As shown by SDS-PAGE and immunoblotting, the production level of YopE or YopER144A in trans was comparable to the native level in wild-type strains (Figure 3.1A). The intra-macrophage survival of IP6+pYopE and IP6+pYopER144A was then compared, with IP2666 or IP6 containing the empty vector shown in parallel as controls. In contrast to IP2666+empty vector or IP6+pYopE, IP6+pYopER144A exhibited significantly improved survival in macrophages, which is comparable to IP6+empty vector (Figure 3.1B). Unexpectedly, the empty vector (pMMB67HE) has a slight negative effect on bacterial intracellular survival (Figure 3.2), possibly caused by the metabolic burden introduced by the vector [122,123]. Nevertheless, these data further confirmed that YopE is the essential factor causing reduced survival of *Yersinia* in macrophages and proved that the GAP activity of YopE is indispensable for triggering intracellular killing.

Membrane localization, stability and target specificity of YopE are important for reduced survival of *Yersinia* in macrophages. Our results suggest that YopE GAP activity is required

for T3SS-dependent killing of *Y. pseudotuberculosis* inside macrophages. We hypothesize that the following three variables will impact the ability of YopE to stimulate intracellular killing: subcellular localization to membrane, stability and target specificity. To this end, plasmids producing YopE variants that were defective for membrane localization (YopE3N), less stable (YopER62K) or with altered target specificities (YopEL109A and YopE-SptP fusion) were introduced into IP6. Detergent extraction assay and immunoblotting were used to detect the amounts of YopE variants in infected macrophages. The *yopB* mutant (IP40, Table 2.1), defective in T3SS translocation, was shown in parallel as a negative control (Figure 3.3A). These strains (Table 2.1) were then used to infect macrophages to perform fluorescence microscopy or CFU assay.

The level of YopE3N in the soluble fraction was similar to wild-type YopE, indicating equal translocation of these proteins (Figure 3.3A, compare lane 3 to 1). The amount of YopER62K in the soluble fraction was lower in comparison to wild-type YopE, which is as expected due to its decreased stability (Figure 3.3A, compare lane 5 to 1). The presence of a slower migrating band for YopER62K corresponded with ubiquitination (Figure 3.3A, lane 5). IP6+YopE3N and IP6+YopER62K showed enhanced intra-macrophage survival compared to IP6+YopE at 24h post infection as revealed by fluorescence microscopy (Figure 3.3B), the results of which were quantified by showing percentage of macrophages containing fluorescent intracellular *Yersinia* (Figure 3.3C). CFU assay further confirmed that YopE3N and YopER62K displayed reduced ability to trigger intracellular killing as compared to wild-type YopE (Figure 3.4A). Given that subcellular membrane localization and stability of YopE are important for its GAP activity, these data provide additional proof that macrophages sense the inhibition of one or more Rho GTPases, which leads to increased killing of intracellular *Yersinia*.

To determine if target specificity of YopE impacts the intracellular killing response, YopE variants with altered target specificity were studied. YopEL109A has decreased activity towards RhoA (70% of wild-type level) and Rac2 (70% of wild-type level) [124]. YopE-SptP fusion protein, which has the secretion and translocation domains of YopE and the GAP domain of SptP, presents no GAP activity towards RhoA and lower activity towards Rac1 (83% of wild-type level) and Rac2 (34 of wild-type level) [124]. The amount of YopEL109A and YopE-SptP were similar to wild-type YopE in infected macrophages (Figure 3.3A, compare lane 1, 2 and 4). As expected, YopE-SptP displayed slower mobility due to its higher molecular weight (Figure 3.3A, lane 4). At 24h post infection, IP6+YopEL109A and IP6+YopE-SptP exhibited increased survival in macrophages comparing to IP6+YopE, as determined by fluorescence microcopy (Figure 3.5AB), which was consistent with the results from CFU assay (Figure 3.4B). These results suggest that the Rho GTPase specificity of YopE may impact its ability to promote *Yersinia* killing inside macrophages. However, it is difficult to declare how YopE inhibition of a specific Rho GTPase plays a central role in triggering intracellular killing, because the activity of YopEL109A and YopE-SptP towards Rho GTPases other than RhoA, Rac1 and Rac2 is not fully known.

Toxin B decreases Yesinia survival inside macrophages. To explore if macrophages sense inhibition of Rho GTPases by bacterial toxins as a common danger signal, the effect of *Clostridium difficile* Toxin B on *Yersinia* intracellular survival was studied. Toxin B inhibits a broad range of Rho GTPases by glucosylation, the targets of which include Rac1, RhoA/B/C, RhoG, Cdc42 and TC10 [125-127]. In macrophages treated with Toxin B, the survival of IP6, IP17 and IP40 was significantly decreased as shown by CFU assay (Figure 3.6AB) and fluorescence microscopy in conjunction with mCherry induction (Figure 3.6C). Toxin B had no

58

effect on *Yersinia* growth in tissue culture medium in the absence of macrophages; Toxin B did not show significant cytotoxicity to macrophages under our experimental conditions (data not shown). These results indicate that inactivation of Rho GTPases by Toxin B is detected by macrophages, triggering an intracellular killing response. Toxin B decreases *Yersinia* intra-macrophage survival in a way that mimics the effect of YopE. Hence, increased bacterial killing triggered by the Rho GTPase-inactivating toxins may be a conserved response to these bacterial toxins.

Rac inactivation, but not Rho inactivation, decreases *Yersinia* survival inside macrophages. To determine the Rho GTPase target of YopE important for inducing intracellular killing, the effect of specific Rho GTPase inhibitors on *Yersinia* intracellular survival were studied. With Rac1 inhibitor NSC23766 treatment, the survival of IP6 and IP40 was decreased in macrophages, as shown by CFU assay (Figure 3.7AB) and fluorescence microcopy with mCherry induction (Figure 3.7C). The Rac1 inhibitor displayed a reduced ability to trigger intracellular killing in comparison to Toxin B (compare Figure 3.7AB and Figure 3.6AB). Differently from the Rac1 inhibitor, the RhoA inhibitor TAT-C3 did not show any effect on *Yersinia* intra-macrophage survival (Figure 3.8BC). Dramatic morphological change was detected in TAT-C3 treated macrophages as early as 4h upon treatment, confirming the efficiency of this inhibitor towards RhoA (Figure 3.8A). These data revealed that macrophages constrain *Yersinia* intracellular survival in response to Rac inactivation, but not Rho inactivation.

3.5 Discussion

Our findings in this chapter indicate that primary naïve macrophages respond to modulation of Rho GTPases by *Yersinia* Yop effectors. We propose that the activity of YopE is

somehow sensed by macrophages as a "pattern of pathogenesis", which leads to killing of intracellular *Yersinia* as an ETIR. YopE is well known as a critical virulence factor for *Yersinia* pathogenesis, as a *Y. pseudotuberculosis yopE*⁻ mutant was unable to spread systemically following oral infection in the mouse model [27]. Interestingly, on the other hand, here we show that the GAP activity of YopE is sensed by macrophages as a danger signal, triggering killing of intracellular bacteria (Figure 3.1). Zhang *et al.* investigated a *Y. pseudotuberculosis* strain (32777), different from the strain used here (IP2666), and reported that a 32777 mutant expressing catalytically inactive YopJ, YopT, YopE and YopH exhibited a similar phenotype like wild-type 32777, showing reduced intracellular survival in comparison to a *pYV* mutant [89]. We speculate that 32777 has additional T3SS-dependent effector that could stimulate bacterial killing, like other unknown Rho GTPase-inactivating effector(s), which remains to be identified.

We provided evidence that Toxin B reduces *Yersinia* survival in macrophages possibly due to its activity towards Rho GTPases (Figure 3.6). To date, at least 20 Rho GTPase proteins belonging to 8 subfamilies have been described in mammals [128,129]. One intriguing question to ask here is, among these Rho GTPases, the status of which specific Rho GTPase(s) is closely monitored by the innate immune system in a surveillance pathway? Importantly, we have shown that the target preference of YopE impacts its ability to trigger bacterial killing (Figure 3.5). Our results showed that Rac inactivation, but not Rho inactivation, stimulates killing of intracellular *Yersinia* (Figure 10). However, the Rac inhibitor has lower ability to trigger intracellular killing comparing to Toxin B or YopE, indicating that disturbance of additional Rho GTPases contributes to the bactericidal effect. Other Rho GTPase candidates may include, but are not limited to, Rac2 and RhoG, which have been shown to be YopE targets found in macrophages

60

[124,129-131]. More studies are required to determine the role of other Rho GTPases

macrophage surveillance pathways in response to pathogenic infection [129].

Rho GTPases are important molecular switches that regulate a variety of cellular

functions, ranging from cytoskeleton dynamics, gene transcription, vesicular trafficking to cell

growth and apoptosis. Because of the importance of Rho GTPases, host cells tightly regulate the

activation and inactivation of Rho GTPases through multiple mechanisms, including the

canonical regulators (GAPs, GEFs and GDIs) and direct post-translational modifications (such as

phosphorylation and ubiquitination). The manipulation of Rho GTPases by YopE or Toxin B

could influence multiple Rho GTPases-mediated pathways leading to many different

consequences to trigger intracellular killing. Possible down-stream pathways that could mediate

a YopE-triggered killing response include disruption of actin cytoskeleton [10], inflammasome

activation [132], modulation of vesicular trafficking or an autophagy pathway [91,92], which

remain to be explored.
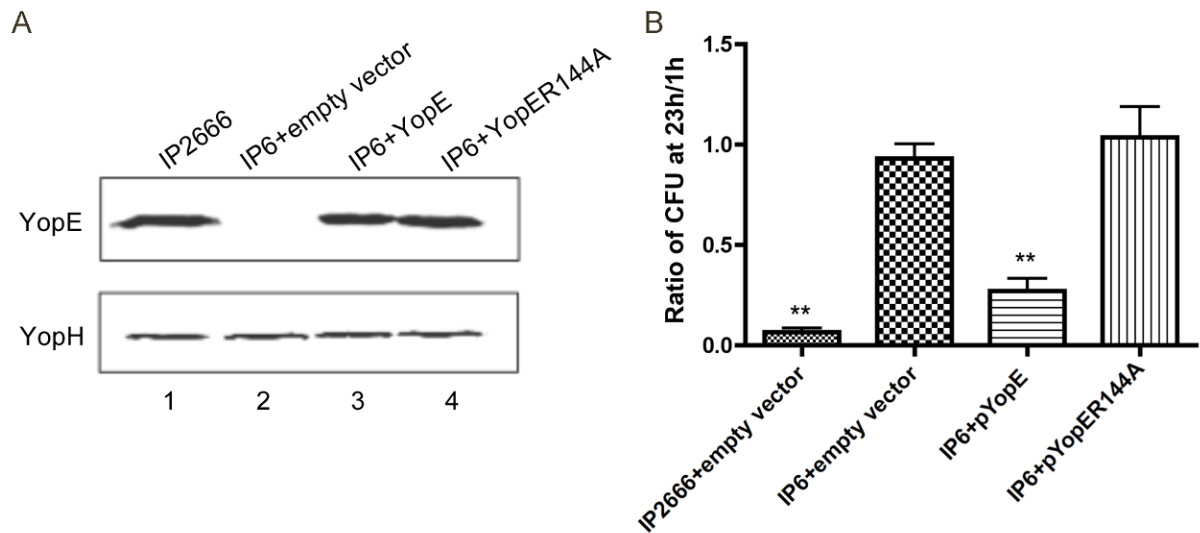
3.6 Figures

Figure 3.1: Measurement of YopE production and survival in macrophages by different *Y. pseudotuberculosis* strains.

(A) Static expression levels of YopE in the indicated strains as determined by immunoblotting analysis. Indicated bacteria strains were grown at 37 ℃ in the presence of 2.5mM CaCl$_2$ for 2h. Bacterial pellets were collected and analyzed by immunoblotting using antibodies specific for YopE. YopH levels are shown as loading controls. (B) Survival of intracellular bacteria was determined by CFU assay in infected macrophages, as described in Figure 2.1. Results shown are the means from three independent experiments with duplicate infection wells. Error bars show standard deviations. **, P < 0.01 compared to IP6+empty vector, as determined by one-way ANOVA.

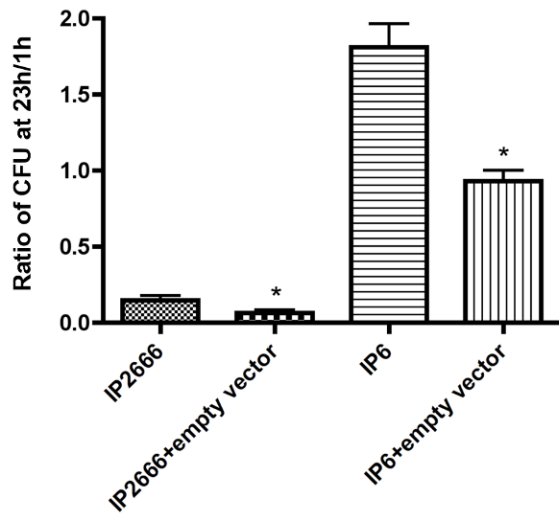**Figure 3.2: Survival of *Y. pseudotuberculosis* strains with or without empty vector inside macrophages.**

CFU assay were performed as described in Figure 2.1. Results shown are the means from three independent experiments with duplicate infection wells. Error bars show standard deviations. *, $P < 0.05$, comparing each strain with to without empty vector individually, as determined by one-way ANOVA.
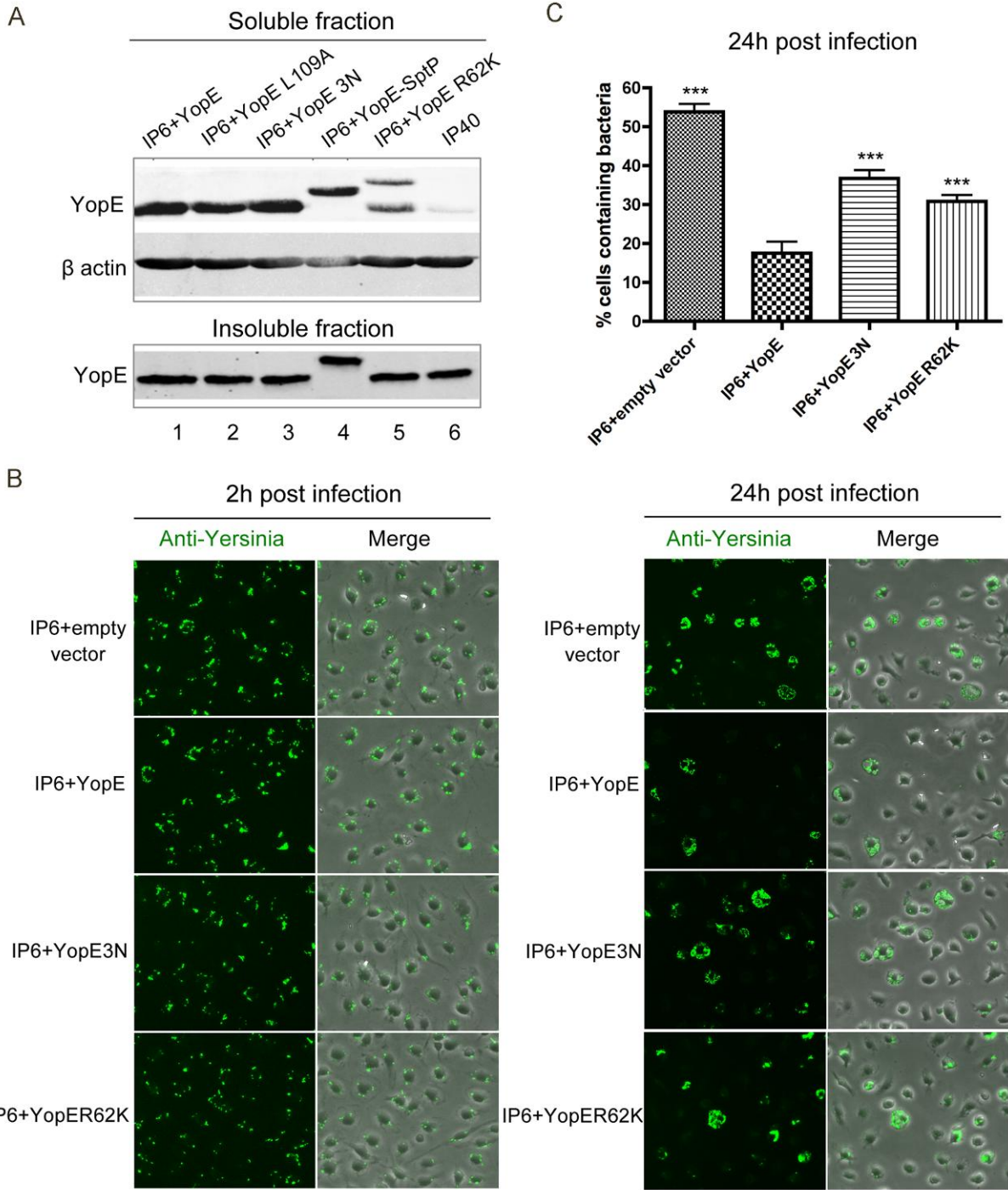
Figure 3.3: Measurement of YopE translocation and survival in macrophages by different *Y. pseudotuberculosis* strains.

(A) YopE translocation levels in BMDMs infected by the indicated strains, determined by detergent extraction assay and immunoblotting analysis. BMDMs in 6 well plates were infected at an MOI of 30 for 2 h. Cell lysates were centrifuged to obtain soluble and insoluble fractions, which were subjected to immunoblotting analysis using antibodies specific for YopE. β-actin

levels from the soluble fraction are shown as loading controls. (B) BMDMs were infected with the indicated strains at an MOI of 10, as described in Figure 2.1. At 2h and 24h post infection, infected cells were fixed, permeabilized and labeled with a rabbit anti-*Yersinia* antibody (green). Shown is bacteria or an overlay of bacteria and phase contrast signal from representative images obtained by fluorescence microscopy. (C) Percentage of macrophages containing fluorescent *Yersinia* at 24h post infection, quantified from three independent microscopic experiments as described in (B). Error bars show standard deviations. ***, P < 0.001 compared to IP6+YopE, determined by one-way ANOVA.

Figure 3.4: Survival of *Y. pseudotuberculosis* strains inside macrophages.

CFU assay were performed as described in Figure 2.1. Shown is the logarithm of intracellular bacteria count per well at 1h post infection and 23h post infection comparing IP6+empty vector, IP6+YopE, IP6+YopE3N and IP6+YopER62K (A) or IP6+empty vector, IP6+YopE, IP6+YopEL109A and IP6+YopE-SptP (B). Results are the means from three independent experiments with duplicate infection wells. Error bars show standard deviations. *, $P < 0.05$; **, $P < 0.01$ and ***, $P < 0.001$ compared to IP6+YopE, as determined by one-way ANOVA.
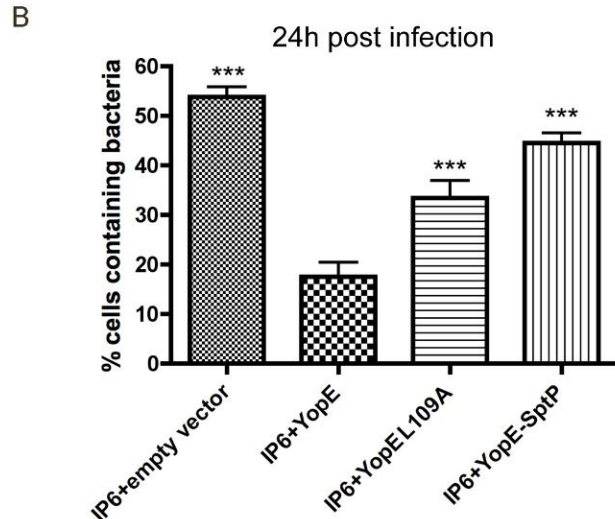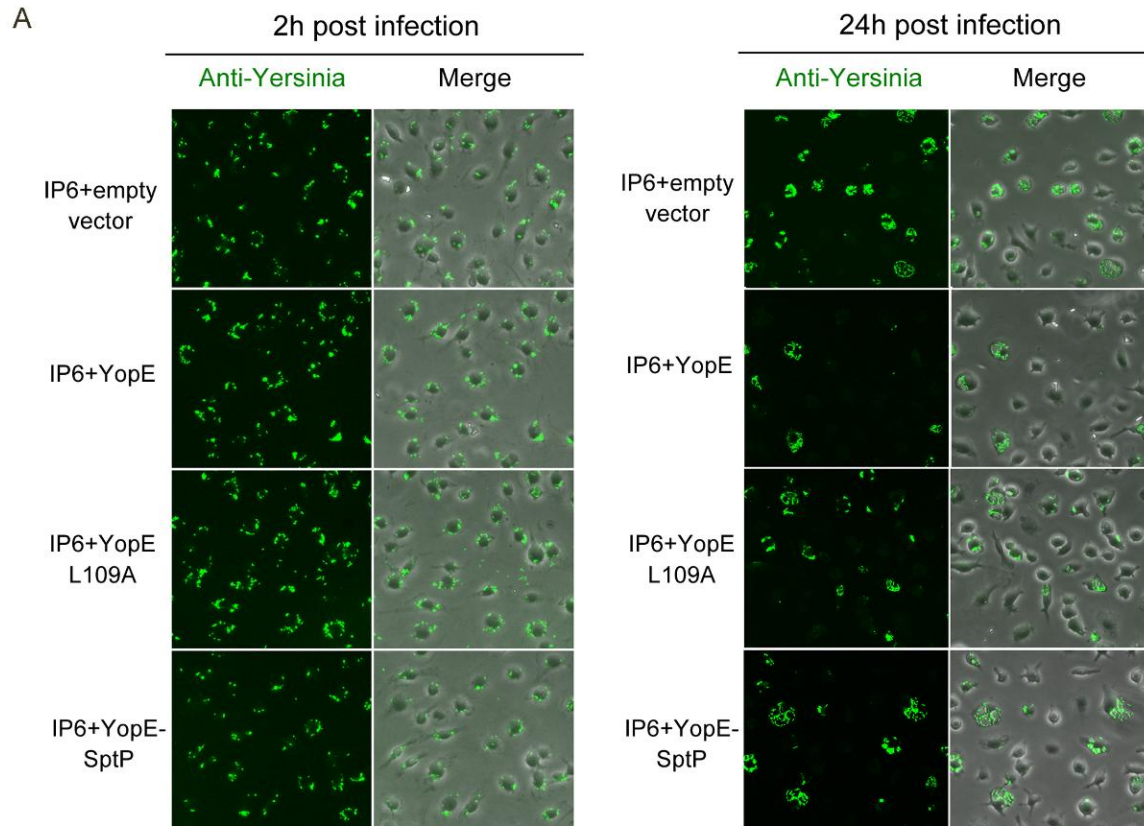
Figure 3.5: Survival of different *Y. pseudotuberculosis* strains in macrophages as determined by fluorescence microscopy.

(A) BMDMs were infected with indicated strains as described in Figure 2.1. At 2h and 24h post infection, infected cells were fixed, permeabilized and labeled with a rabbit anti-*Yersinia* antibody (green). Shown is bacteria or an overlay of bacteria and phase contrast signal from representative images. (B) Percentage of macrophages containing fluorescent *Yersinia* at 24h post infection, quantified from three independent microscopy experiments as described in (A).

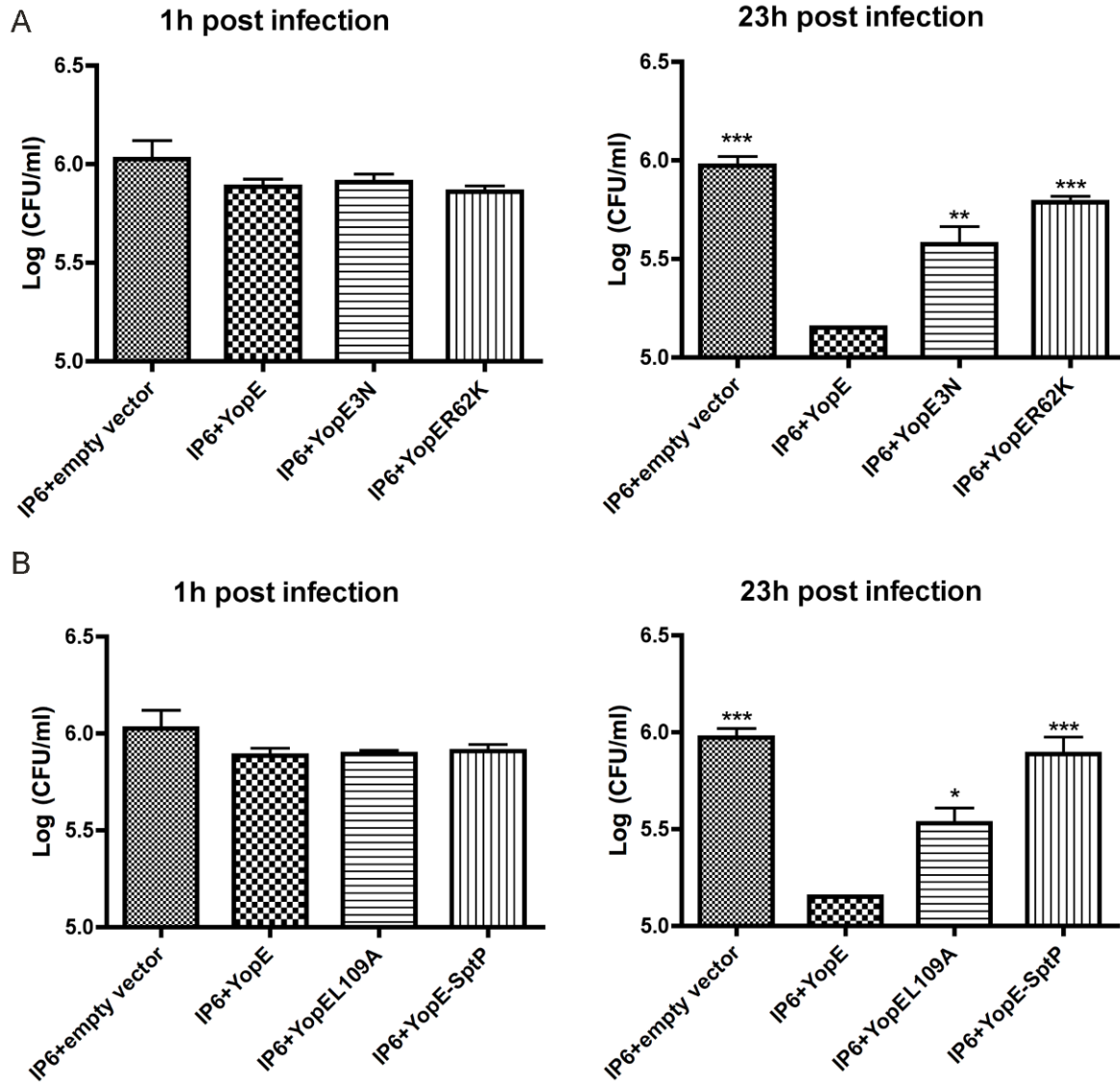Error bars show standard deviations. ***, P < 0.001 compared to IP6+YopE, determined by one-way ANOVA.

Figure 3.6: Survival of different *Y. pseudotuberculosis* strains inside macrophages, in the presence or absence of Toxin B.

BMDMs were infected with the indicated strains as described in Figure 2.1. When indicated, 40 ng/ml Toxin B was present throughout the experiment. (A-B) Intracellular bacterial survival was determined by CFU assay, as described in Figure 2.1. Results shown are the means from four

independent experiments with duplicate infection wells. Error bars show standard deviations. ***, P < 0.001 and *, P < 0.05 comparing each strain with to without Toxin B treatment individually, as determined by one-way ANOVA. (C) Intracellular survival of the indicated mCherry encoding strains was determined by fluorescence microscopy as described in Figure 2.4. Two hours before fixation, IPTG was added to induce de novo expression of mCherry. The upper panel shows mCherry or an overlay of mCherry and phase contrast signal at 24h post infection, from representative images. The lower panels show percentage of mCherry positive macrophages quantified from three independent experiments. Error bars show standard deviations. **, P < 0.01 and ***, P < 0.001 determined by t-test.
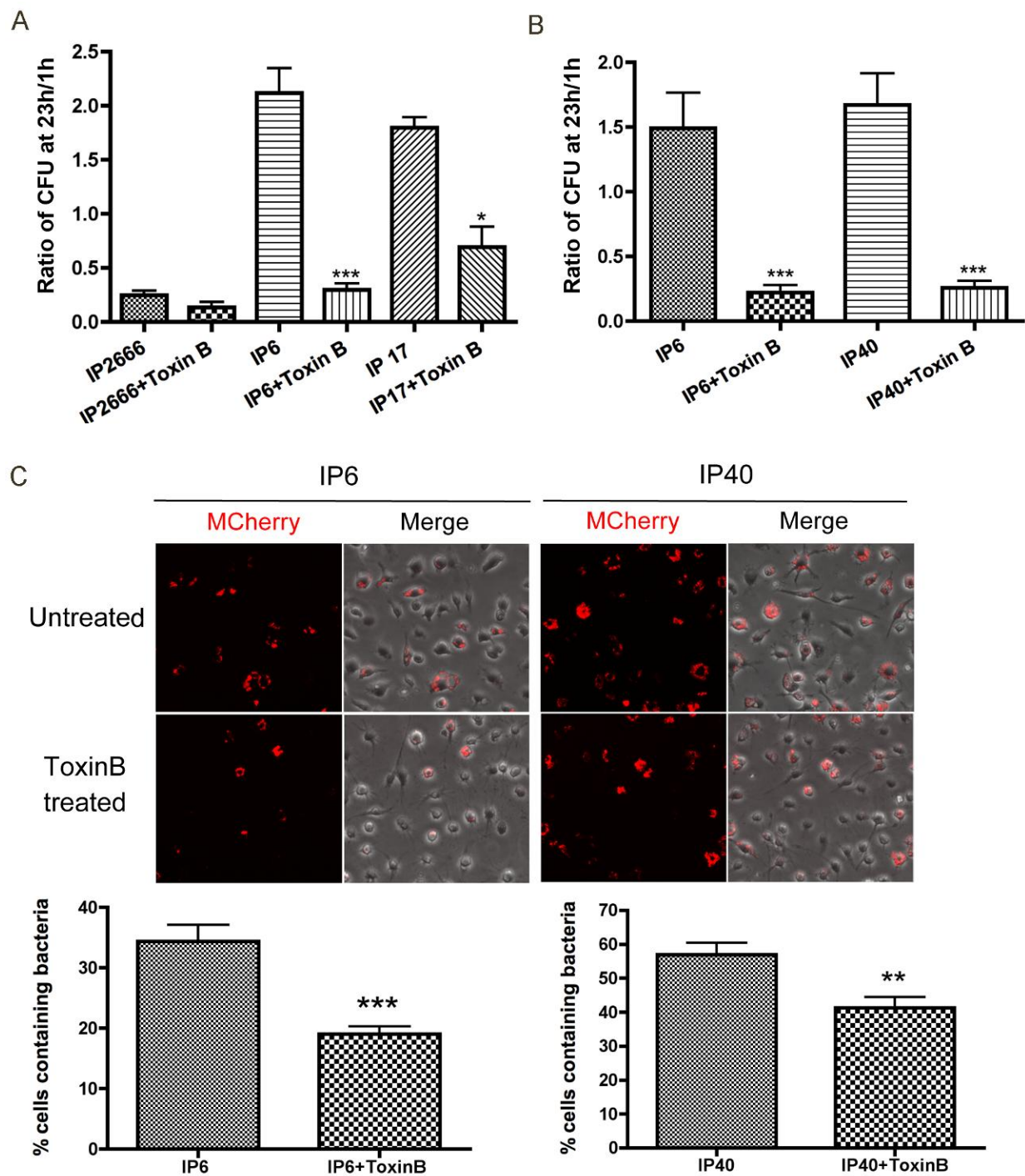
Figure 3.7: Survival of different *Y. pseudotuberculosis* strains inside macrophages, in the presence or absence of Rac inhibitor NSC23766.

BMDMs were infected with the indicated strains as described in Figure 2.1. When indicated, 100 μM NSC23766 was present throughout the experiment. (A-B) Intracellular bacterial survival was determined by CFU assay, as described in Figure 2.1. Results shown are the means from three independent experiments with duplicate infection wells. Error bars show standard deviations. ***, $P < 0.001$, comparing each strain with to without Rac inhibitor treatment individually, as determined by one-way ANOVA. (C) Intracellular survival of mCherry-encoding IP6 was determined by fluorescence microscopy, as described in Figure 3.6C. The left panel shows mCherry or an overlay of mCherry and phase contrast signal at 24h post infection from representative images. The right panel shows percentage of mCherry positive macrophages quantified from three independent experiments. Error bars show standard deviations. ***, $P < 0.001$ determined by t-test.

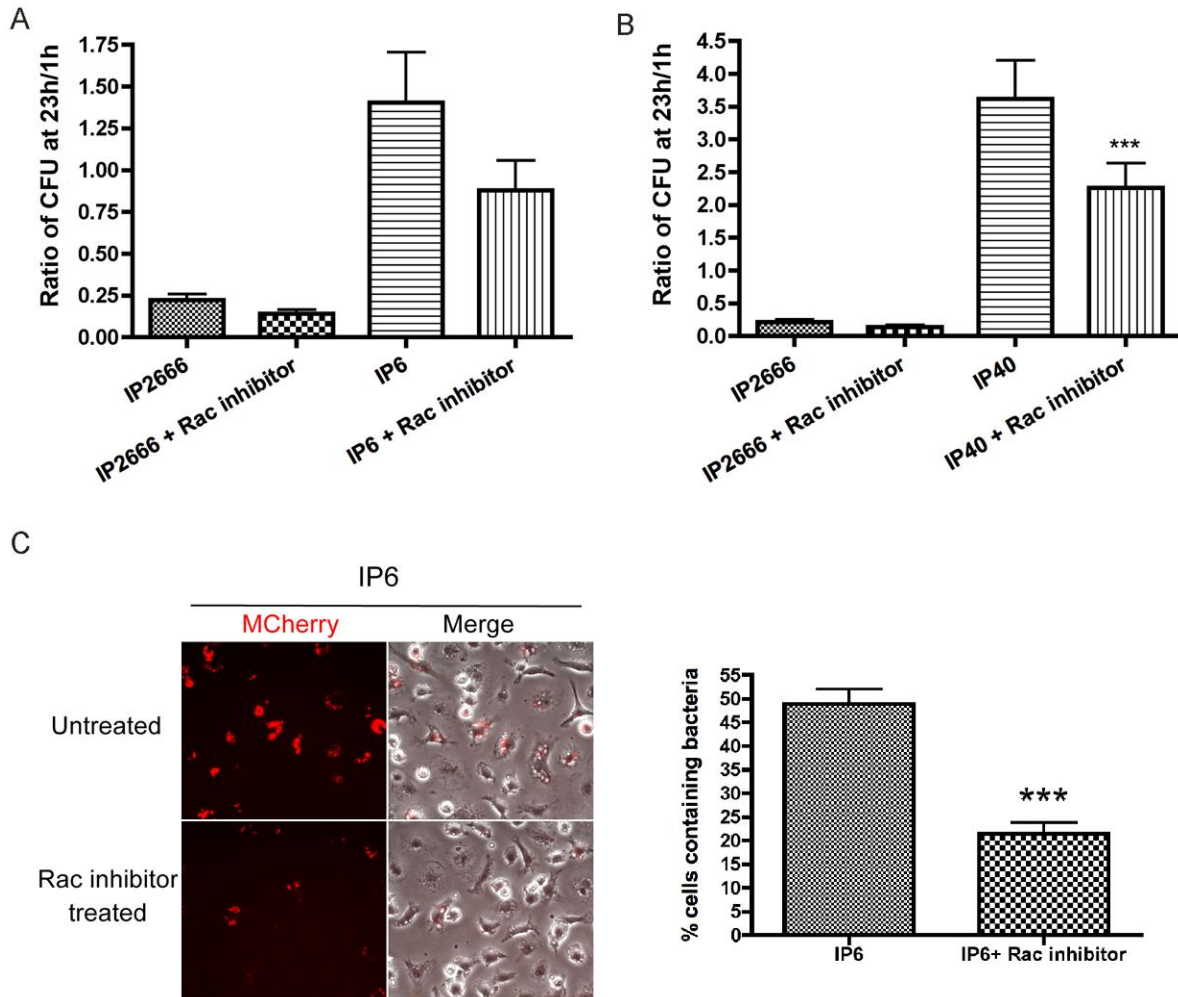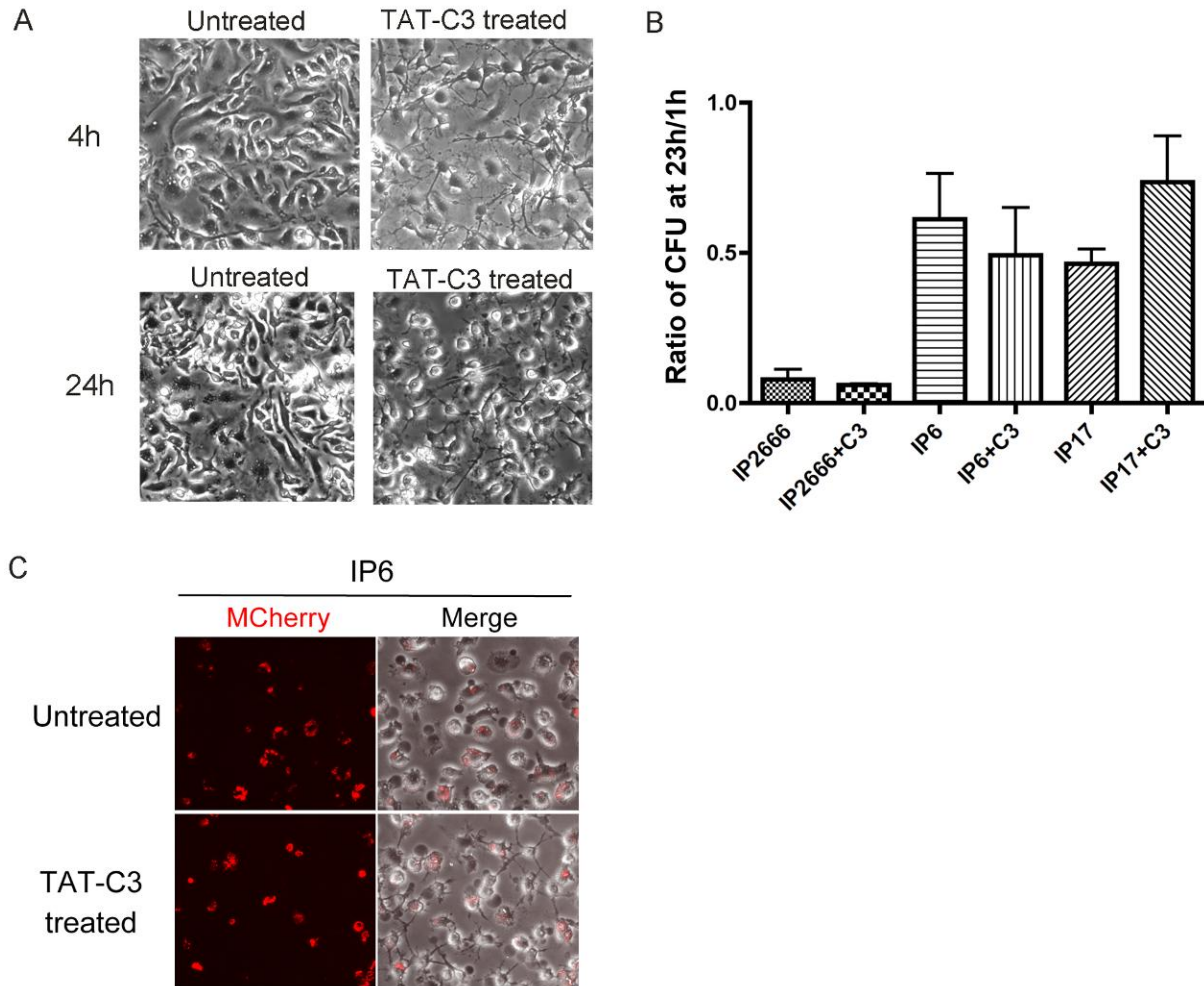**Figure 3.8: Survival of *Y. pseudotuberculosis* strains inside macrophages, in the presence or absence of TAT-C3.**

(A) Morphological changes of BMDMs upon TAT-C3 treatment were determined by phase contrast microscopy. Shown are BMDMs treated with 10 µg/ml TAT-C3 for 4h or 24h. BMDMs with no treatment are also shown as controls. (B) Intracellular bacterial survival was determined by CFU assay, as described in Figure 2.1. When indicated, 10 µg/ml TAT-C3 was present throughout the experiment. Results shown are the means from three independent experiments with duplicate infection wells. There is no significant difference in the survival of each strain with TAT-C3 treatment as compared individually to that without treatment. (C) Intracellular survival of mCherry encoding IP6 was determined by fluorescence microcopy, as described in Figure 3.6. When indicated, 10 µg/ml TAT-C3 was present throughout the experiment. Shown is mCherry or an overlay of mCherry and phase contrast signal at 24h post infection.

Chapter 4: Characterize the mechanism of YopE-triggered killing of *Yersinia* inside macrophages.

4.1 Summary

Previous work (Chapters 2 and 3) demonstrated that macrophages respond to the GAP activity of YopE and restrict survival of intracellular *Yersinia* as a protective response. In this chapter, we sought to further explore the mechanism of YopE-triggered killing of *Yersinia* inside macrophages. On the upstream level, we considered whether YopE activity requires a second pro-inflammatory signal to stimulate killing of intracellular *Yersinia*. Our results suggest that the YopB/D translocon is not required for Toxin B-triggered intracellular killing of *Yersinia*, and LPS-TLR signaling is dispensable for YopE-stimulated intracellular killing; however, the role of YadA/Invasin-β1 integrin signaling in this process is ambiguous. On the downstream level, we aimed to elucidate what signaling pathway mediates YopE-induced intracellular killing. We studied if macrophages respond actively to the disturbance of the actin cytoskeleton. The actin polymerization activator Jasplakinolide had no effect on *Yersinia* intra-macrophage survival, yet, unexpectedly, the actin polymerization inhibitor Cytochalsin D slightly increased *Yersinia* intracellular survival, the mechanism of which is enigmatic. Our work also revealed that Capase1/11 or NOD1 signaling pathways are not involved in YopE-elicited killing response. Additionally, the autophagy inducer Rapamycin decreases intracellular survival of *Yersinia*, indicating a role of autophagy in suppressing *Yersinia* survival in macrophages. However, YopE-induced killing does not specifically require the autophagy pathway. Interestingly, translocated YopE induces higher levels of NO from infected macrophages, although NO production does not seem to mediate YopE-triggered killing.

4.2 Introduction

In the previous chapter, we established the important role of YopE GAP activity in stimulating intra-macrophage killing of *Yersinia*. We proposed that the consequences of YopE activity were detected by macrophages as a pattern of pathogenesis leading to an ETIR. Previous studies suggested "a two-signal model" for the activation of ETIR, which requires a MAMP and a pattern of pathogenesis [133]. For example, five effectors delivered by *Legionella pneumophila* type IV secretion system act to inhibit host protein synthesis [15]. The activities of these effectors, in concert with TLR signaling, results in prolonged activation of NF-κB as an ETIR [15]. It is believed that the two-signal requirement allows host cells to evaluate the virulence potential of a pathogen and adjust immune response appropriately to avoid self-damaging inflammation. Thus, further studies are needed to determine if a second signal generated by a MAMP facilitates YopE-triggered killing effect.

Rho GTPases serve as molecular switches that regulate various cellular functions. The activity of YopE towards multiple Rho GTPases might result in many different consequences to stimulate intracellular bacterial killing. One possibility is that YopE GAP activity disrupts the actin cytoskeleton to alarm host cells. It was suggested host cells monitor the status of the actin cytoskeleton to detect pathogen activity, which could be mediated by inflammasome activation or NLR activation [10]. Alternatively, since Rho GTPases are involved in regulation of vesicular trafficking, it is possible that YopE activity somehow influences the fate of *Yersinia*-containing vesicles, for example by promoting lysosome-phagosome fusion or impacting the autophagy pathway. Additionally, several recent studies have revealed that the activities of certain bacterial effectors can stimulate transcriptional changes in host cells, resulting in ETIRs [14-18]. We

investigated if YopE promotes an altered host response that can occur at the transcriptional level in regards to NO production.

4.3 Materials and Methods

Bacterial strains and plasmids. The *Y. pseudotuberculosis* strains used in this study are listed in Table 2.1. Bacterial cultures were grown as described in Chapter 2. The strains *yadA⁻*, *inv⁻* and *yadA⁻inv⁻* were generously provided by Dr. Joan Mecsas, Tufts University [41].

Cell culture. BMDMs were isolated and cultured from femurs of C57BL/6 wild-type mice (Jackson Laboratory), *Nod1 $^{-/-}$* C57BL/6 mice (a generous gift from Dr. Andreas Baumler, University of California at Davis), *iNOS $^{-/-}$* C57BL/6 mice, *Caspase1/11 $^{-/-}$* C57BL/6 mice (kind gifts from Dr. Adrianus van der Velden, Stony Brook University), *Atg5 $^{flox/flox}$* (namely *Atg5 $^{+/+}$*) or *Atg5 $^{flox/flox}$ –Lyz-Cre* (namely *Atg5 $^{-/-}$*) C57BL/6 mice (a kind gift from Dr. Robert Watson, University of California at San Francisco), as previously described in Chapter 2. Immortalized C57BL/6 BMDMs or *MyD88 $^{-/-}$/Trif $^{-/-}$* BMDMs (kindly provided by Dr. Jonathan Kagan, Harvard University) were grown routinely in DMEM supplemented with 10% feta bovine serum (Hyclone) and 2 mM glutamate. 24h before infection, macrophages were seeded into 24-well tissue culture plate at a density of 1.5×10^5 cells per well as previously mentioned in Chapter 2.

Infection conditions. *Y. pseudotuberculosis* strains were cultured and prepared to infect BMDMs or immortalized BMDMs using the same conditions as previously described in Chapter 2. To obtain opsonized bacteria, bacterial samples were additionally incubated in HBSS supplemented with 10% mouse serum at 37 ℃ for 20 min before adding into macrophages. When indicated, 100 μM iNOS inhibitor 1400W (Sigma), 0.02 μM Jasplakinolide (Molecular Probes), 0.2 μM Cytochalasin D (Sigma), 10 μg/ml Rapamycin (LC laboratories) or

75

corresponding Dimethyl Sulfoxide (DMSO, Fisher Scientific) was added at 0 h post infection and maintained throughout the experiment.

CFU assay, detergent extraction assay, and immunoblotting. These assays were performed as mentioned in Chapter 2.

GRIESS assay. NO levels generated by infected macrophages were determined by measuring the accumulation of nitrite (NO_2^-) using the Griess assay as described previously [134]. Control macrophages were treated with *E.coli* LPS (100 μg/μl, Sigma) and IFN γ (0.1 units/μl, ROCHE) throughout the experiment. At 23 h post infection, conditioned medium were collected and centrifuged (14000 rpm, 10 min, RT). 100 μl of the supernatant was mixed with 100 μl Griess reagent (0.5% sulfanilamide and 0.05% N-(1-naphthyl)ethylenediamide in 2.5% acetic acid) and incubated for 10 min at room temperature. The samples were then measured at $OD_{550\,nm}$. The concentration of NO_2^- was calculated by using a standard curve prepared with sodium nitrite.

Fluorescence microscopy. Fluorescence microscopy assays using GFP or mCherry encoding bacteria were performed as previously described in Chapter 2. Specifically for lysotracker assays, bacteria killed by fixation for 30 min with 2.5% paraformaldehyde (PFA) were used as positive controls. LysoTracker Red (Invitrogen) was added at a concentration of 50 nM 30 min prior to the fixation of samples to track acidic compartments. At 2 h or 3 h post infection, infected BMDMs were fixed, permeabilized and stained using anti-*Yersinia* antibody as described in Chapter 3. Co-distribution of LysoTracker and *Yersinia* were examined and analyzed by confocal microscopy with a 100×oil immersion objective. At least three randomly selected fields of each slide were examined, with each field at least 50 bacteria counted. Percentage of lysotracker positive bacteria was quantified from two independent experiments.

76

4.4 Results

LPS-TLR signaling is not required for YopE-triggered killing of *Yersinia* inside macrophages. TLRs are important mediators generating signaling responses by sensing MAMPs in *Yersinia* infected macrophages. TLR recognition of *Yersinia* LPS initiates proinflammatory signaling pathways such as MAPK and NF-κB pathways, which requires MyD88 and TRIF as essential adaptor proteins. To investigate if LPS-TLR signaling is required as a second signal for YopE-induced intracellular killing, immortalized MyD88/TRIF KO BMDMs were compared to wild-type BMDMs for their ability to restrict survival of IP2666 or IP6 (*yopE*⁻) by CFU assay (Figure 4.1AB). No significant difference was observed for IP2666 survival inside wild-type or MyD88/TRIF KO macrophages, suggesting that TLR signaling is dispensable for YopE triggered killing of *Yersinia* inside macrophages (Figure 4.1AB).

The role of YadA/invasin-integrin signaling is inconclusive in YopE-triggered killing of *Yersinia* inside macrophages. Enteropathogenic *Yersinia* expresses adhesin molecules, including YadA and invasin, to mediate bacterial attachment and entry into host cells. Invasin directly binds to β1-integrins with high affinity, while YadA binds to diverse extracellular matrix proteins, such as collagen and fibronectin, which in turn bind to β1-integrins [25]. Binding to β1-integrins by YadA or invasin stimulates multiple signaling cascades involving activation of Src kinases, tyrosine phosphorylation of focal adhesion proteins, activation of Rac1 and PI3K, and stimulation of MAPK, NF-κB signaling pathways [25,135-137]. To determine if β1-integrin signaling stimulated by invasin or YadA is critical for YopE-triggered killing, the intracellular survival of IP2666, *yadA*⁻, *inv*⁻ and *yadA*⁻*inv*⁻ (Table 2.1) were studied by CFU assay. At 23h post infection, all four strains displayed similar intracellular bacterial count; however, the initial

uptake levels of *yadA⁻* or *yadA⁻inv⁻* were much lower in comparison to IP2666 or *inv⁻* (Figure 4.2). This is not surprising since YadA/invasin are critical for enteropathogenic *Yersinia* binding to host cells and YadA is the major adhesin molecule expressed in the IP2666 strain [138]. To achieve equal internalization by macrophages, complement opsonized bacteria were prepared by incubating the bacteria with mouse serum before infection. The intracellular survival of these opsonized bacteria was examined by fluorescence microscopy with mCherry induction (Figure 4.3). With comparable uptake levels at 2h post infection, *yadA⁻* and *yadA⁻inv⁻* showed improved intra-macrophages survival in comparison to IP2666 and *inv⁻* at 24h post infection (Figure 4.3). However, the absence of YadA greatly decreased the amount of translocated YopE in *Yersinia* infected macrophages (about 50% of wild-type level), as revealed by detergent extraction assay (Figure 4.4). Thus, it is difficult to determine if YadA/invasin-integrin interaction provides an essential second signal for the YopE-induced killing response, since the translocation level of YopE is reduced when *yadA*/*invasin* genes are deleted. Therefore, the role of YadA/invasin and β1-integrin signaling remains ambiguous in YopE-triggered killing of *Yersinia* inside macrophages.

Jasplakinolide has no effect on *Yersinia* intracellular survival, while Cytochalasin D promotes *Yersinia* intracellular survival by unknown mechanisms. As a common strategy, many bacterial pathogens target host cell actin cytoskeleton to favor bacterial pathogenesis. It has been proposed that host cells sense actin cytoskeleton disruption as a surveillance mechanism to detect pathogen invasion [10]. To explore if disruption of actin cytoskeleton mediates YopE-induced killing, actin polymerization activator (Jasplakinolide) and actin polymerization inhibitor (Cytochalasin D) were assessed for their effect on *Yersinia* intra-macrophage survival. The survival of IP2666, IP6 (*yopE⁻*) or IP40 (*yopB⁻*) was examined in

BMDMs treated with Jasplakinolide or Cytochalasin D by fluorescence microscopy with GFP induction. Treatment with low concentrations of these compounds, 0.02 μM Jasplakinolide or 0.2 μM Cytochalasin D, was used to ensure efficient disruption of actin without causing cytotoxicity (Figure 4.5A). Survival of bacteria in DMSO treated macrophages was determined in parallel as a control. Jasplakinolide showed no influence on *Yersinia* intracellular survival (Figure 4.5BC). Unexpectedly, survival of IP2666, IP6 and IP40 was slightly elevated in Cytochalasin D treated macrophages (Figure 4.5BC). Hence, disturbance of actin cytoskeleton by Jasplakinolide does not impact *Yesinia* intracellular survival, while actin polymerization inhibitor Cytochalasin D increases *Yersinia* intracellular survival by unknown mechanisms.

NOD1 signaling is not involved in YopE-mediated killing of *Yersinia* inside macrophages. Vance et al. proposed that disruption of host cytoskeleton by pathogens might stimulate NLR responses, as both NOD1 and NOD2 were located at actin rich regions near plasma membrane [10]. Recently, Keestra *et al.* gained evidence that activation of Rac1 and Cdc42 by SopE from *Salmonella enterica* serovar Typhimurium is sensed through NOD1 receptor, eliciting NF-κB activation in the host cells as a protective response [18]. To study whether YopE-dependent intracellular killing signals through NOD1 receptor, *Nod1*$^{-/-}$ BMDMs were compared to wild-type BMDMs for their ability to inhibit survival of intracellular IP2666 or IP6 (*yopE*$^-$) by CFU assay (Figure 4.6). No significant difference was observed for IP2666 survival in wild-type or *Nod1*$^{-/-}$ BMDMs (Figure 4.6), indicating that NOD1 signaling does not contribute to YopE-mediated killing of *Yersinia* inside macrophages.

Caspase1/11 signaling is not involved in YopE-mediated killing of *Yersinia* inside macrophages. It was proposed that host cells may respond to cytoskeleton disruption through inflammasome activation, since inflammasome components such as pyrin and ASC have been

shown to locate at regions of active actin polymerization [10]. To study the role of inflammasome activation in YopE-dependent killing of *Yersinia*, survival of IP2666 or IP6 was compared in Caspase1$^{-/-}$/11$^{-/-}$ (Caspase1/11 KO) or wild-type BMDMs by fluorescence microscopy with GFP induction (Figure 4.7). IP2666 displayed similar intracellular survival level in wild-type or Caspase1/11 KO macrophages (Figure 4.7), suggesting that Caspase1/11 do not mediate YopE-induced killing response.

Presence of YopE induces higher levels of nitric oxide from *Yersinia* infected macrophages, yet NO production is dispensable for YopE-triggered intracellular killing. Production of reactive nitrogen species (RNS) is a critical defensive mechanism by which macrophages control intracellular bacteria [1]. RNS production requires de novo synthesis of the inducible nitric oxide synthase (iNOS), which is regulated at the transcriptional level. RNS exert a highly toxic effect on intracellular bacteria, impairing bacterial metabolism and eventually inhibiting bacterial replication [1]. To study if YopE stimulates an altered host response that is associated with RNS, the production of NO from macrophages infected with IP2666, IP6, IP17 or IP40 was compared. Specifically, the concentration of nitrite (NO_2^-), an indicator of NO, was measured by Griess assay. At 23h post infection, comparing to IP6-, IP17- or IP40-infected macrophages, IP2666-infected macrophages produced significantly higher levels of NO (Figure 4.8). LPS- and IFN γ-treated macrophages were used as a positive control, while uninfected macrophages were used as a negative control (Figure 4.8).

To further determine if NO production facilitates YopE-triggered intracellular killing, the effect of iNOS inhibitor 1400W on *Yersinia* intracellular survival was evaluated by fluorescence microscopy and CFU assay. 1400W efficiently inhibited NO production by IP2666 or IP6 infected macrophages (below detectable level, data not shown). No significant difference was

detected for IP2666 survival inside untreated or 1400W treated macrophages (Figure 4.9). Additionally, survival of IP2666 or IP6 was compared in wild-type or $iNOS^{-/-}$ BMDMs by fluorescence microscopy in conjunction with GFP induction (Figure 4.10). Similar survival level of IP2666 was found in wild-type and $iNOS^{-/-}$ BMDMs (Figure 4.10). These results revealed that YopE stimulates NO production in *Yersinia* infected macrophages, however NO production does not contribute to YopE-mediated intracellular killing. The fact that higher levels of NO were produced from wild-type *Yersinia* infected macrophages indicates that macrophages respond actively to *Yersinia* infection.

Rapamycin treatment decreases *Yersinia* survival inside macrophages. Given the role of Rho GTPases in regulating vesicular trafficking, we explored if YopE activity impacts the fate of *Yersinia* containing vesicles, like promoting lysosome-phagosome fusion or affecting the autophagy pathway.

Phagosome acidification is of great importance to the bactericidal activity of macrophages. To see if YopE activity stimulates phagosome acidification to increase intracellular killing, the acidification levels of *Yersinia* containing vesicles (YCVs) were measured using LysoTracker and fluorescence microscopy (Figure 4.11). In infected macrophages, IP2666 and IP6 displayed similar levels of colocalization with LysoTracker at 2h or 3h post infection (Figure 4.11), suggesting that YopE activity does not promote YCVs acidification to cause intracellular killing. Acidification of phagosomes containing IP6 fixed with PFA prior to infection of macrophages was shown in parallel as a positive control (Figure 4.11).

To explore the role of autophagy on *Yersinia* intra-macrophage survival, autophagy inducer Rapamycin was used to treat macrophages. Survival of IP2666 or IP6 was compared in DMSO or Rapamycin treated BMDMs by CFU assay and fluorescence microscopy with

mCherry induction (Figure 4.12). Rapamycin treatment presented no effect on IP2666 intracellular survival (Figure 4.12). Interestingly, the intracellular survival of IP6 was decreased in Rapamycin treated macrophages, comparing to control macrophages. To further elucidate the role of autophagy in YopE-induced intracellular killing, *Yersinia* survival was compared in $Atg5^{+/+}$ or $Atg5^{-/-}$ BMDMs by CFU assay (Figure 4.13AB). ATG5 is an essential E3 ubiquitin ligase required for autophagosomes elongation, therefore $Atg5^{-/-}$ BMDMs are defective in the autophagy pathway. No significant difference was observed for IP2666 survival inside $Atg5^{+/+}$ or $Atg5^{-/-}$ BMDMs (Figure 4.13AB), illustrating that autophagy pathway does not mediate YopE-dependent intracellular killing. The survival of IP6 and IP40 was slightly increased in $Atg5^{-/-}$ BMDMs in comparison to $Atg5^{+/+}$ BMDMs (Figure 4.13AB), suggesting that autophagy pathway somehow impairs *Yersinia* intracellular survival, which is consistent with the results from the Rapamycin experiment (Figure 4.12). For some reason, *Yersinia* infection induced higher levels of cell rounding in these floxed BMDMs, but the extent was equal among IP2666, IP6 and IP40 infected macrophages (Figure 4.13C). These results revealed that the autophagy pathway negatively influences *Yersinia* intracellular survival, however specifically it is not involved in YopE-triggered intracellular killing response.

4.5 Discussion

The overall host cell innate immune response to a T3SS-containing bacterial pathogen is unique and multifactorial. MAMPs, the T3SS translocon channel, and the activities of bacterial effectors are likely recognized as combined pathogenic signals by the host cell. The two-signal model, requiring a MAMP and a pattern of pathogenesis, was proposed as an innate immune strategy to evaluate the virulence potential of a pathogen and adjust immune response appropriately to avoid self-damaging inflammation [133]. Our data suggest that the YopBD

translocon is not essential for Toxin B- or Rac inhibitor-triggered bacterial killing in macrophages (Figure 3.6 and 3.7). Also, LPS-TLRs pathway does not contribute to YopE-triggered killing effect (Figure 4.1). Thus, whether YopE-triggered intracellular killing requires a MAMP-PRR signal remains to be determined. Alternatively, some studies in the literature support the idea that patterns of pathogenesis are sufficient to induce defense responses independently of classical MAMPs [14,139,140]. Boyer et *al.* demonstrated that *Escherichia coli* CNF1 elicited a vigorous ETIR in flies via activation of Rac2 and the IMD kinase pathway, which was observed even in the absence of PRR ligation [14]. Thus, it is possible that unbalanced disruption of Rho GTPases by YopE is adequate to stimulate a protective immune response, resulting in restriction of *Yersinia* survival in macrophages.

Our results showed that treatment of macrophages with Jasplakinolide had no effect on *Yersinia* intracellular survival (Figure 4.5). Activation of actin polymerization by Jasplakinolide cannot rescue wild-type *Yersinia* survival inside macrophages, which may indicate that sensing of YopE activity is not related to host cytoskeleton disruption. However, it should be noted that the treatment timing and the specificity of Jasplakinolide could influence the results. Cytochalasin D treatment improved *Yersinia* survival inside macrophages (Figure 4.5). Cytochalasin D could give a negative effect on Yop translocation, since actin polymerization has been shown to facilitate Yop delivery in epithelial cells [80]. However, this does not explain how Cytochalasin D improves intracellular survival of IP40, which is defective in Yop translocation.

Interesting, a recent study by Shao and colleagues showed that Rho-inactivating toxins such as *Clostridium difficile* Toxin B and *Clostridium botulinum* C3 trigger Pyrin inflammasome activation in BMDMs [132]. They further demonstrated that *Burkholderia cenocepacia* induced inactivation of Rho GTPase stimulates Pyrin inflammasome activation as an immune defense,

which limits bacterial intra-macrophage growth and regulates lung inflammation in infected mice [132]. In this case, inhibition of RhoA but not Rac1 triggers Pyrin inflammasome activation. Here our results showed that inhibition of Rac1 but not RhoA elicits intra-macrophage *Yersinia* killing; however, YopE-triggered intracellular killing does not require Caspase1/11 mediated inflammasome activation. These results suggest that macrophages might sense inactivation of specific Rho GTPases through different pathways to fight against pathogen invasion.

The role of autophagy in *Yersinia* intracellular survival is controversial [91,92]. Using bacteria prepared at 28 ℃ without pre-induction of T3SS, Moreau et al. demonstrated that autophagosomes supported *Y. pseudotuberculosis* replication in macrophages, while inhibition of autophagy resulted in bacterial killing [92]. On the other hand, Deuretzbaher et *al.* showed that β1-integrin-mediated *Y. enterocolitica* internalization by macrophages was coupled to autophagy activation, which seemed to be deleterious for bacterial intracellular survival [91]. In this study, T3SS was pre-induced by culturing *Yersinia* at 37 ℃ before infection. Under our experimental conditions, autophagy seems to impair the survival of *Y. pseudotuberculosis* inside naïve macrophages. Autophagy may play a species-specific role in survival of *Yersinia* in macrophages. The growth condition of *Yersinia* and the state of macrophages before infection should also be taken into consideration. How T3SS influences the fate of *Yersinia* containing vesicles and modulates the autophagy pathway in this process requires more investigation.
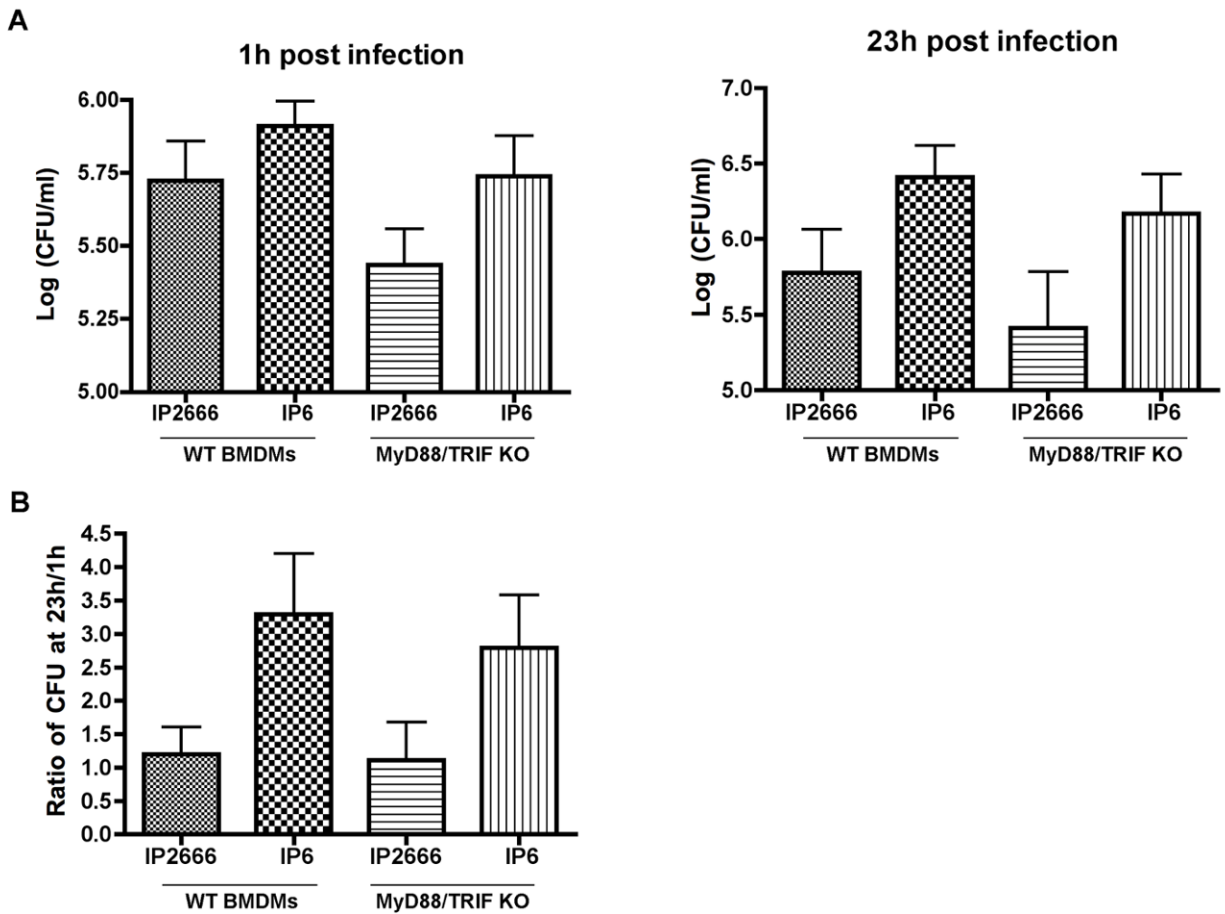
4.6 Figures

A

B

Figure 4.1: Survival of different *Y. pseudotuberculosis* strains in wild-type or MyD88/TRIF KO macrophages.

Wild-type or MyD88/TRIF KO BMDMs were infected with indicated strains. Intracellular bacterial survival was measured by CFU assay, as described in Figure 2.1. (A) The logarithm of intracellular bacteria count per well at 1h post infection and 23h post infection. (B) Ratio of CFU at 23h/1h. Results shown are the means from two independent experiments with duplicate infection wells. Error bars show standard deviations.
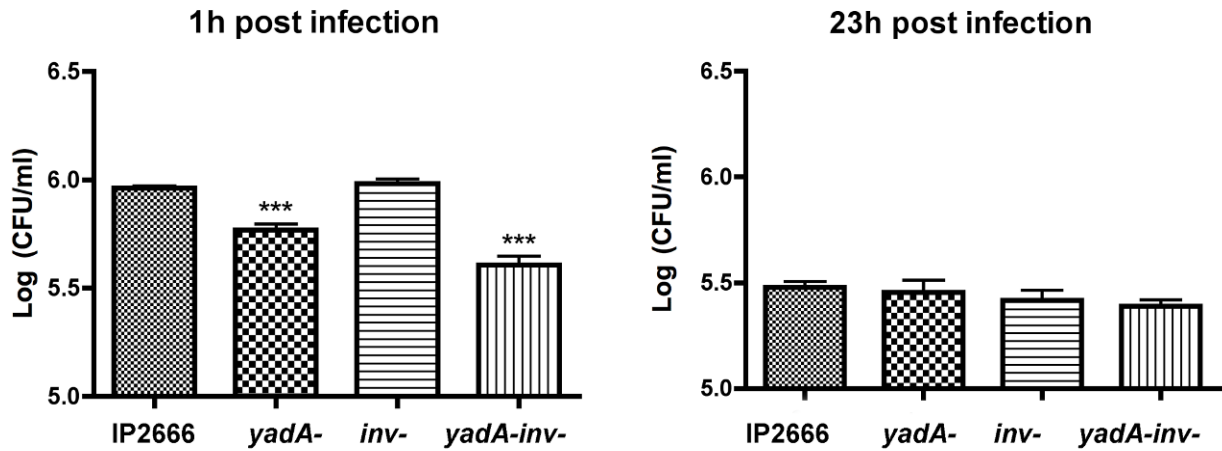
Figure 4.2: Survival of different *Y. pseudotuberculosis* strains in macrophages determined by CFU assay.

BMDMs were infected with indicated strains as described in Figure 2.1. The logarithm of intracellular bacteria counts per well at 1h post infection and 23h post infection is shown. Results shown are the means from three independent experiments with duplicate infection wells. Error bars show standard deviations. ***, $P < 0.001$ compared to IP2666, as determined by one-way ANOVA.
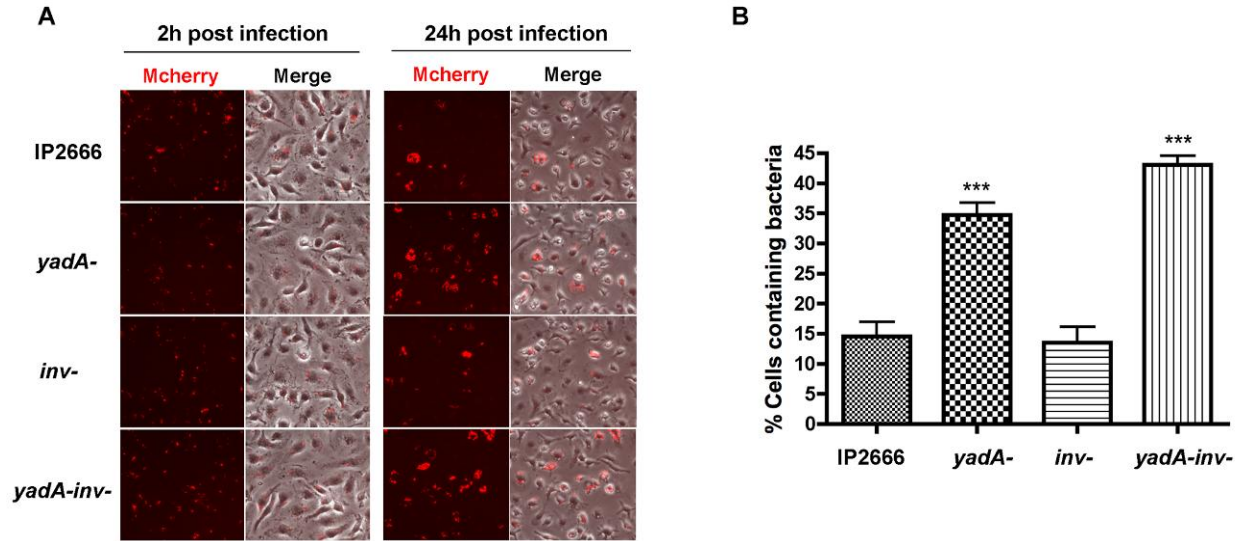
Figure 4.3: Survival of different *Y. pseudotuberculosis* strains in macrophages determined by fluorescence microscopy.

BMDMs were infected by indicated mCherry encoding strains as described in Figure 2.1, except that complement opsonized bacterial samples were used. Fluorescence microscopy with mCherry induction was performed as described in Figure 3.6C. (A) MCherry or an overlay of mCherry and phase contrast signal at 24h post infection from representative images. (B) Percentage of mCherry positive macrophages quantified from two independent experiments with duplicate infection wells as described in (A). Error bars show standard deviations. ***, $P < 0.001$ compared to IP2666 as determined by one-way ANOVA.
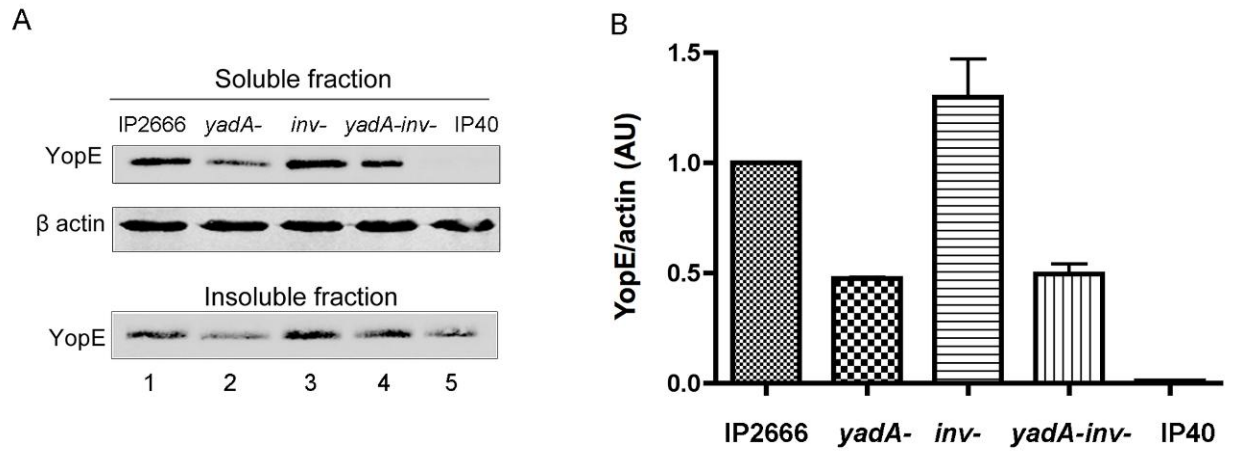
Figure 4.4: Measurement of YopE translocation in macrophages by different *Y. pseudotuberculosis* strains.

(A) YopE translocation levels in BMDMs infected by the indicated strains, determined by detergent extraction assay and immunoblotting analysis as described in Figure 2.10. β-actin levels from the soluble fraction are shown as loading controls. (B) The intensity of each band was calculated using Odyssey IR imaging system, and the YopE/β-actin ratios were normalized according to IP2666. Results shown are the means from two independent experiments. Error bars show standard deviations.
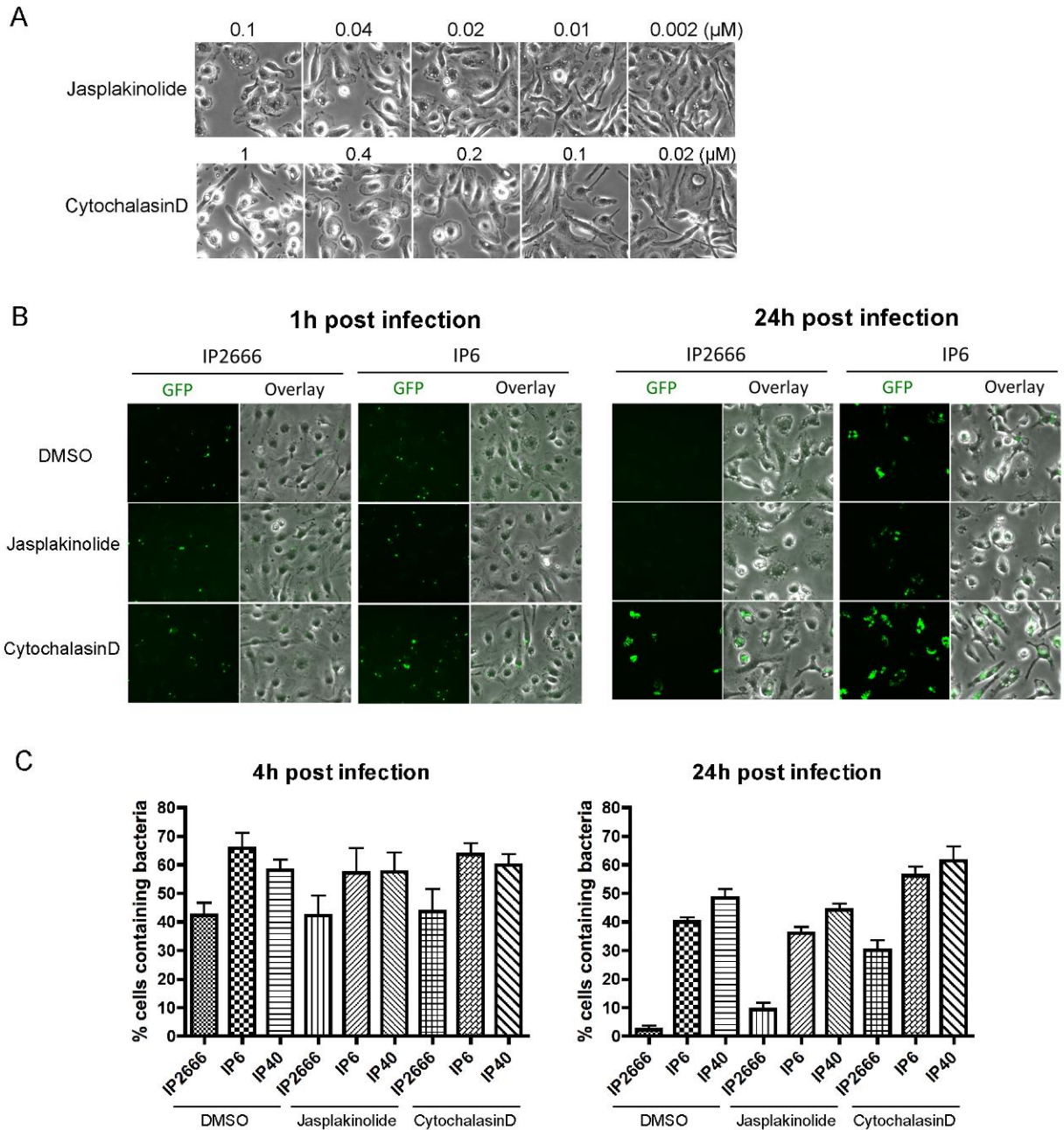
Figure 4.5: Survival of *Y. pseudotuberculosis* strains inside macrophages, in the presence of DMSO, Jasplakinolide or Cytochalasin D.

(A) Morphological changes of BMDMs upon Jasplakinolide or Cytochalasin D treatment were determined by phase contrast microscopy. Shown are BMDMs treated with indicated concentrations of Jasplakinolide or Cytochalasin for 24h. (B) BMDMs were infected with indicated GFP encoding strains as described in Figure 2.1. Intracellular bacterial survival was determined by fluorescence microscopy with GFP induction, as described in Figure 2.4. When indicated, 0.02 μM Jasplakinolide or 0.2 μM Cytochalasin D was present throughout the experiment. (C) Percentage of GFP positive macrophages at 4h and 24h post infection,

quantified from two independent experiments with duplicate infection wells as described in (B). Error bars show standard deviations.
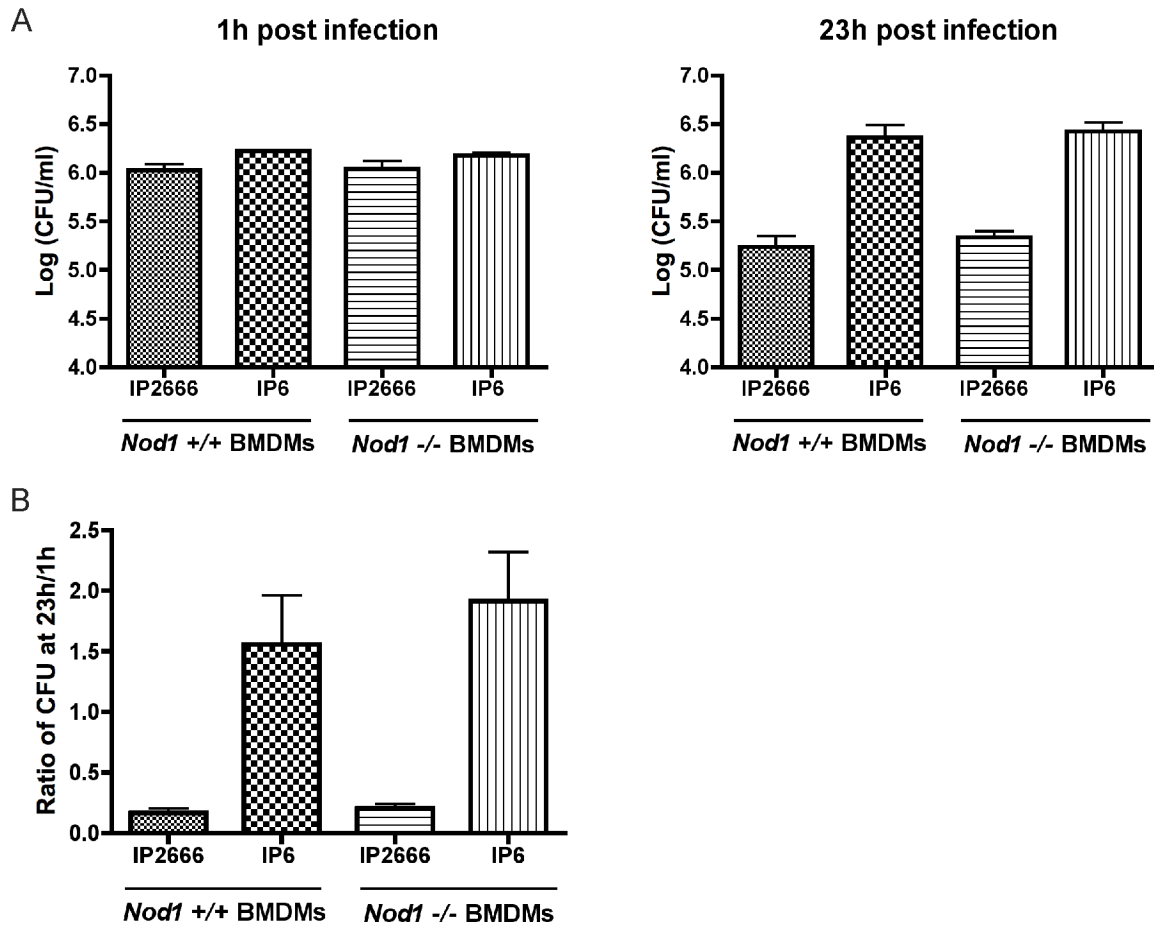
Figure 4.6: Survival of different *Y. pseudotuberculosis* strains in wild-type or *Nod1* [-/-] macrophages.

Wild-type or *Nod1* [-/-] BMDMs were infected with indicated strains and intracellular bacterial survival was measured by CFU assay, as described in Figure 2.1. (A) The logarithm of intracellular bacteria count per well at 1h post infection and 23h post infection. (B) Ratio of CFU at 23h/1h. Results shown are the means from three independent experiments with duplicate infection wells. Error bars show standard deviations. There is no significant difference in the survival of each strain in WT BMDMs as compared individually to that in *Nod1* [-/-] BMDMs.
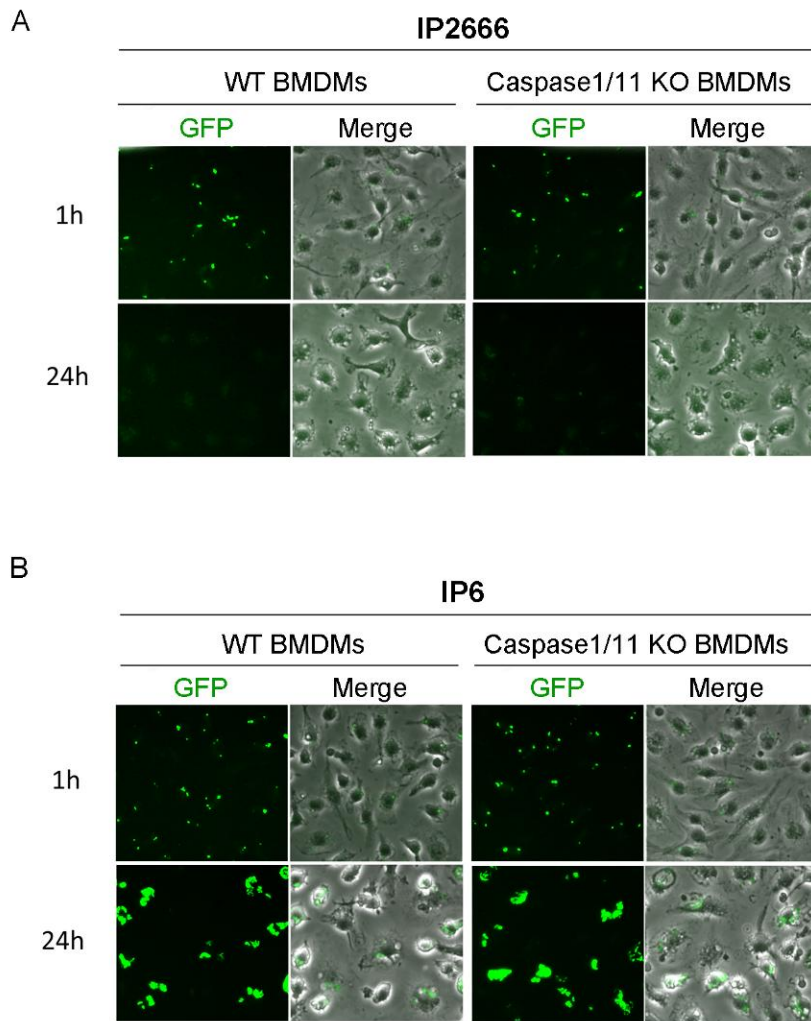
Figure 4.7: Survival of different *Y. pseudotuberculosis* strains in wild-type or Capase1/11 KO macrophages.

 (A-B) BMDMs were infected with indicated GFP encoding strains as described in Figure 2.1. Intracellular bacterial survival was determined by fluorescence microscopy with GFP induction, as described in Figure 2.4. Shown is GFP or an overlay of GFP and phase contrast signal at 1h or 24h post infection of representative images from one experiment.
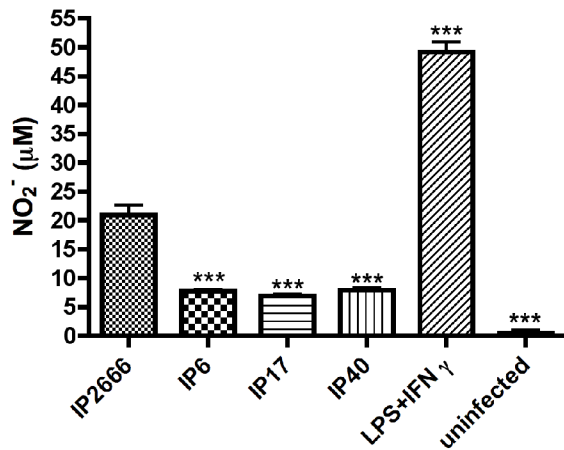
Figure 4.8: Measurement of NO production by macrophages infected with different *Y. pseudotuberculosis* strains.

BMDMs were infected with the indicated strains as described in Figure 2.1. At 23h post infection, medium from the infected macrophages were collected and subjected to Griess assay to determine nitrite (NO_2^-) concentrations. Lipopolysaccharide (LPS)- and IFN γ- treated macrophages are shown as a positive control. Results shown are the means from three independent experiments with duplicate infection wells. Error bars show standard deviations. ***, P < 0.001, comparing to IP2666 infected macrophages, as determined by one-way ANOVA.

Figure 4.9: Survival of *Y. pseudotuberculosis* strains inside macrophages, in the presence or absence of 1400W.

BMDMs were infected with the indicated strains as described in Figure 2.1. When indicated, 100 μM 1400W was present throughout the experiment. (A) Intracellular bacterial survival was determined by fluorescence microscopy with GFP induction, as described in Figure 2.4. Shown is GFP or an overlay of GFP and phase contrast signal at 24h post infection of representative images from one experiment. (B) Intracellular bacterial survival was measured by CFU assay, as described in Figure 2.1. Shown is the logarithm of intracellular bacteria count per well at 1h post infection or 23h post infection from one experiment.
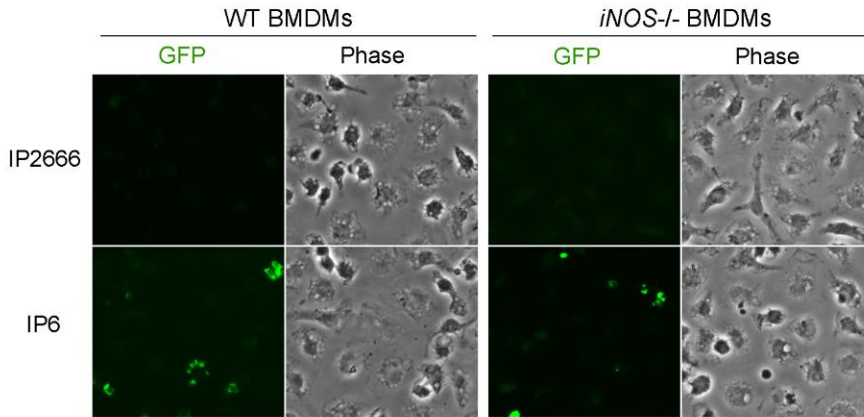
**Figure 4.10: Survival of different *Y. pseudotuberculosis* strains in wild-type or *iNOS⁻/⁻*
macrophages.**

BMDMs were infected with indicated GFP encoding strains as described in Figure 2.1.
Intracellular bacterial survival was determined by fluorescence microscopy with GFP induction,
as described in Figure 2.4. Shown is GFP or an overlay of GFP and phase contrast signal at 24h
post infection from representative images in one experiment.
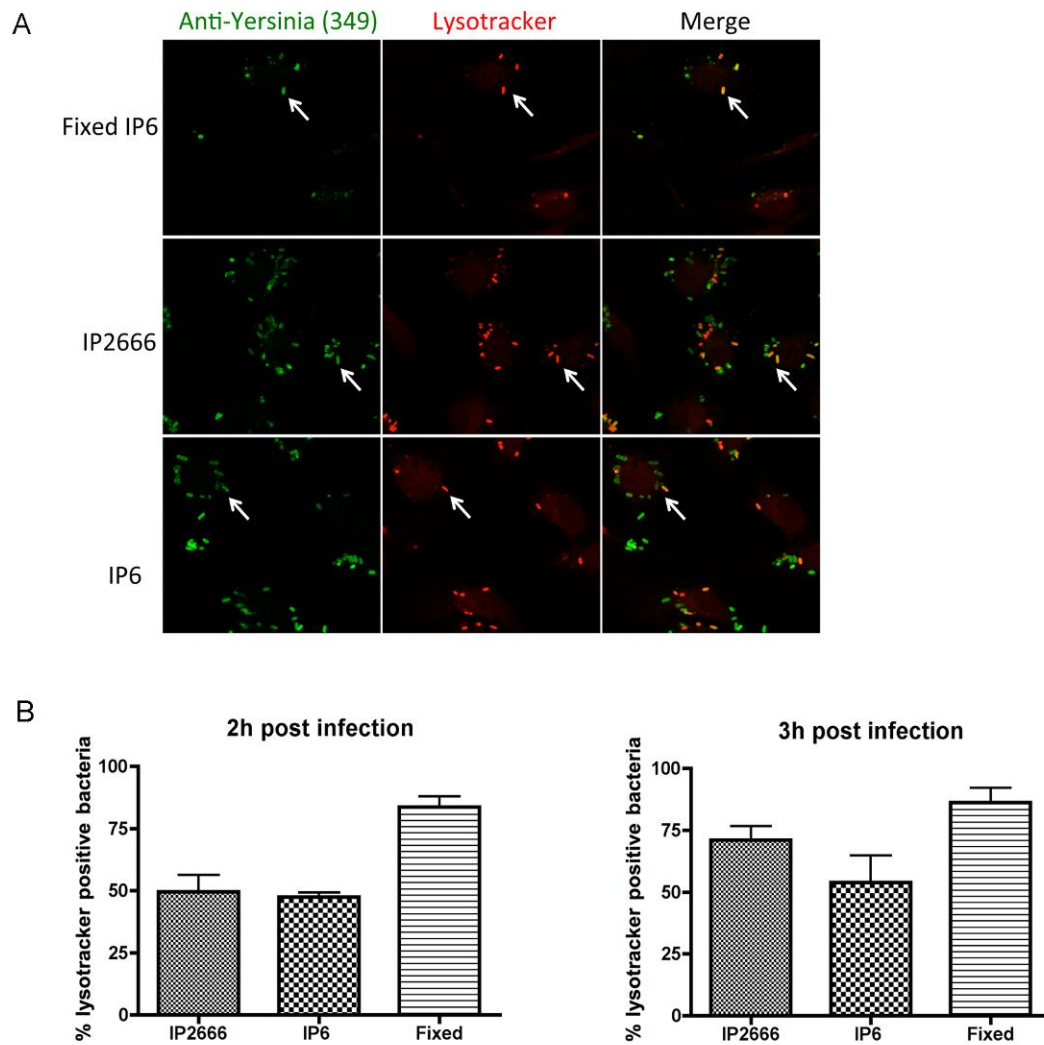
Figure 4.11: Colocalization of different *Y. pseudotuberculosis* strains with acidic compartments inside macrophages as determined by lysotracker assays.

BMDMs were infected with indicated strains at an MOI of 10 as mentioned in Figure 2.1. PFA fixed IP6 was added into macrophages in parallel as a positive control. At 2 h or 3 h post infection, infected BMDMs were fixed, permeabilized and stained using anti-*Yersinia* antibody as described in Figure 3.3B. 30 min prior to the fixation of the samples, LysoTracker Red was added to track acidic compartments. (A) Shown is bacteria or lysotracker or an overlay of bacteria and lysotracker signal at 2h post infection from representative images obtained by confocal microscopy. (B) Percentage of lysotracker positive *Yersinia* at 2h or 3h post infection, quantified from two independent microscopic experiments as described in (B).
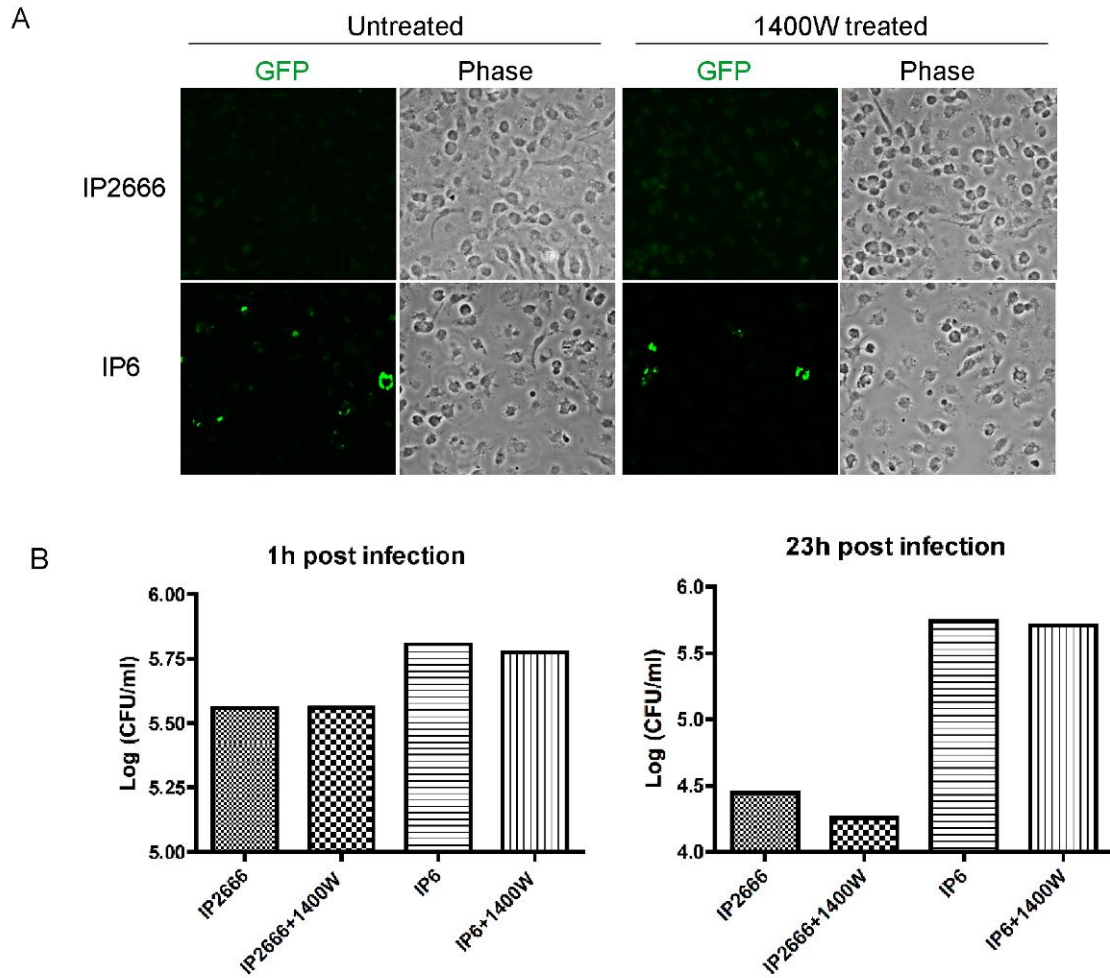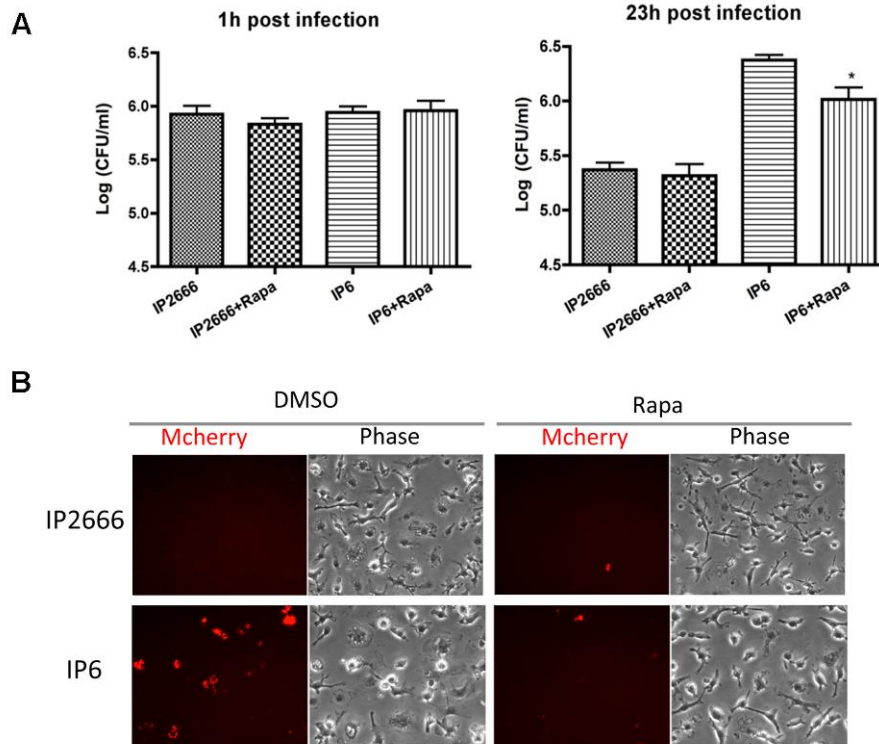
Figure 4.12: Survival of *Y. pseudotuberculosis* strains inside macrophages, in the presence or absence of Rapamycin.

BMDMs were infected with the indicated strains as described in Figure 2.1. When indicated, 10 μg/ml Rapamycin or DMSO was present throughout the experiment. (A) Intracellular bacterial survival was measured by CFU assay, as described in Figure 2.1. Shown is the logarithm of intracellular bacteria count per well at 1h post infection or 23h post infection from at least three independent experiments with duplicate infection wells. Error bars show standard deviations. *, $P < 0.5$, compare survival of each strain in presence of DMSO or Rapamycin, as determined by one-way ANOVA. (B) Intracellular bacterial survival was determined by fluorescence microscopy with mCherry induction, as described in Figure 3.6C. Shown is mCherry signal or phase contrast at 24h post infection of representative images.
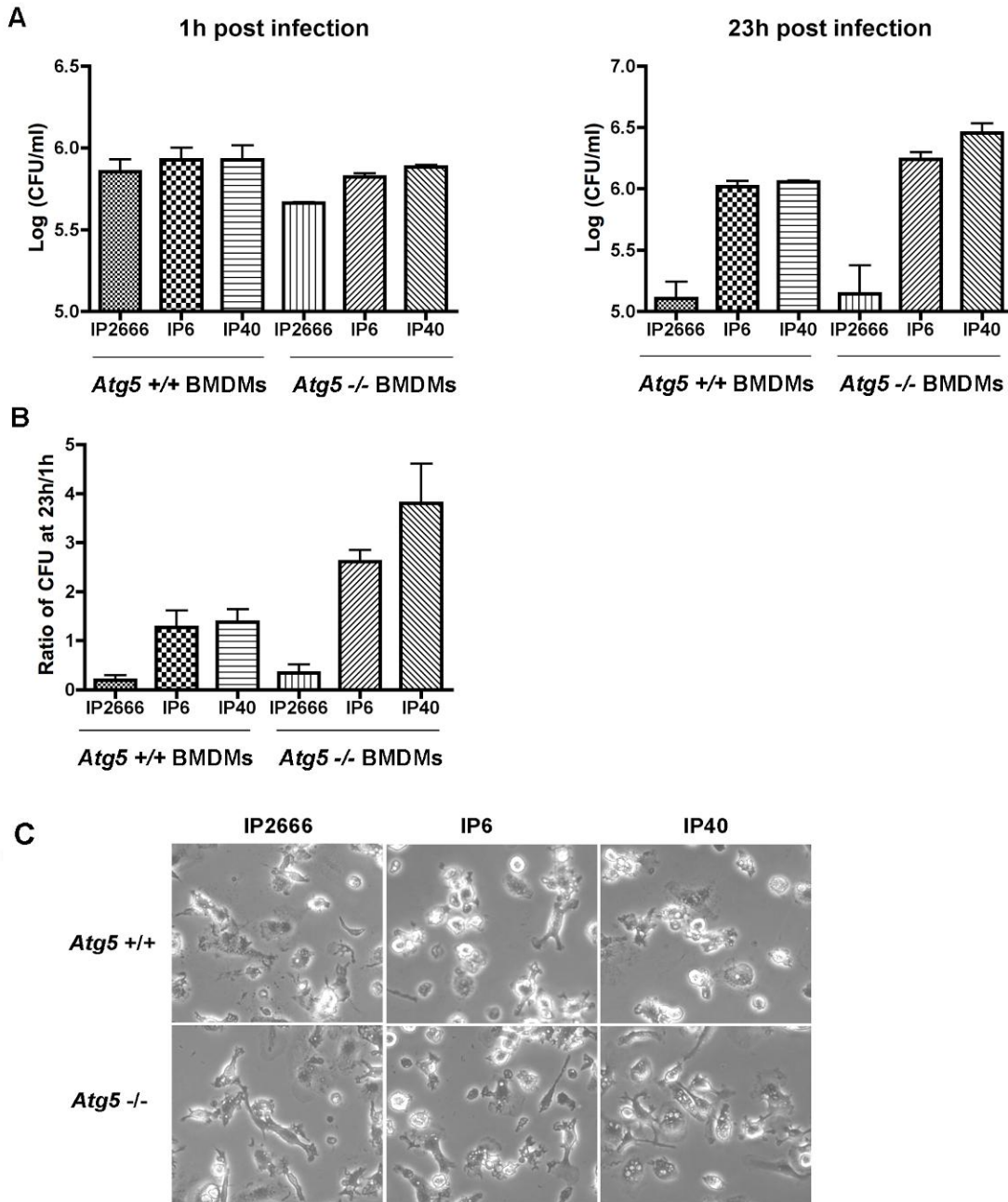
Figure 4.13: Survival of different _Y. pseudotuberculosis_ strains in _Atg5_^{+/+} or _Atg5_ ^{-/-} macrophages.

Atg5^{+/+} or _Atg5_ ^{-/-} BMDMs were infected with indicated strains and intracellular bacterial survival was measured by CFU assay, as described in Figure 2.1. (A) The logarithm of intracellular bacteria count per well at 1h post infection and 23h post infection. (B) Ratio of CFU at 23h/1h. Results shown are the means from two independent experiments with duplicate infection wells. Error bars show standard deviations. (C) Phase contrast images of indicated strains infected _Atg5_^{+/+} or _Atg5_ ^{-/-} BMDMs at 23h post infection.

Chapter 5: Conclusion Remarks and Future Directions

The aim of this dissertation project was to identify effectors that restrict *Yersinia* intracellular survival and study the mechanism of effector-triggered killing of *Yersinia* inside macrophages.

Initially, the intra-macrophage survival of *Y. pseudotuberculosis* wild-type strain (IP2666) and several *yop* deletion mutants was compared by colony forming unit assays and fluorescence microscopy (Chapter 2). YopE was identified as a critical factor limiting the survival of *Yersinia* inside macrophages. YopH cooperates with YopE to cause this effect. We speculate that YopH inhibits signals that activate Rho GTPases, thus stimulating increased killing of intracellular *Yersinia*. It would be interesting to compare *Yersinia* strains expressing wild-type YopH and catalytically inactive YopH for intra-macrophage survival. Our data also suggest that overexpressed YopT counteracts YopE-triggered killing effect by decreasing the translocation level of YopE and possibly by competing for the same pool of Rho GTPases targets (Chapter 2). Overexpressed YopT is known to act on Rac1 and promote Rac1 translocation into the nucleus in *Yersinia*-infected epithelial cells [108]. The combination action of YopE and YopT may allow fine-tuned manipulation of host Rho GTPases by *Yersinia* T3SS. Interestingly, YopT-induced Rac1 pool maintains in the active conformation inside nucleus, which could bind nuclear factors and regulate host cell transcription program [108,141-143]. It would be interesting to investigate the effect of Rac1 translocated into the nucleus in response to YopT activity in macrophages and how this influences *Yersinia* intracellular survival and pathogenesis.

Comparison of wild-type and *Synaptotagmin VII* $^{-/-}$ (*SytVII*) macrophages revealed that SytVII-mediated phagolysosome fusion does not contribute to YopE-induced killing of *Yersinia*

in macrophages (Chapter 2). It is possible that *Yersinia* T3SS elicits at least two independent killing pathways once recognized by macrophages: the YopE-induced pathway sensed through bacterial manipulation of Rho GTPases and the SytVII-mediated Ca^{2+}-dependent phagosome-lysosome fusion pathway. Bergsbaken *et al.* recently reported that *Y. pseudotuberculosis* T3SS triggers Ca^{2+}- and caspase-1-dependent lysosome exocytosis in LPS-pretreated macrophages [90]. Under our experimental conditions, the SytVII-mediated killing pathway was not observed in naïve macrophages. It would be valuable to study whether SytVII is essential for lysosome exocytosis in LPS-pretreated macrophages, the impact of this pathway on *Yersinia* intracellular survival and pathogenesis, and how other Yops may potentially regulate this pathway.

As control experiments, we showed that the decreased intracellular survival of the wild-type strain is not due to increased gentamicin uptake or *Yersinia*-induced macrophage cell death, which might lead to exposure of the intracellular bacteria to gentamicin. Another concern might be that wild-type bacteria escape from macrophages, which would also expose them to gentamicin. For this purpose, time-lapse microscopy could be used to track the movement of GFP$^+$ intracellular *Yersinia*.

YopE mimics eukaryotic GTPase activating proteins (GAPs) and inactivates Rho GTPases in host cells. To investigate the role of YopE GAP activity in this process, intra-macrophage survival of *Yersinia* producing YopE or YopE mutants was compared (Chapter 3). Unlike wild-type YopE, YopER144A (catalytic-dead mutant) was impaired in restricting *Yersinia* intracellular survival, while YopE3N (defective in membrane localization) and YopER62K (less stable) presented decreased ability to trigger intracellular killing. Interestingly, *Clostridium difficile* Toxin B was able to mimic the effect of YopE and decreased *Yersinia* survival inside macrophages. These results suggest that macrophages sense the manipulation of

Rho GTPases by YopE GAP activity (or by other bacterial toxins like Toxin B) to limit bacterial intracellular survival (Chapter 3). To further validate that macrophages actively limit *Yersinia* intracellular survival by promoting a killing effect, it would be valuable to track the appearance of dead intracellular bacteria over time. Electron microscopy could be used to detect degraded intracellular bacteria or fluorescence microscopy (with anti-*Yersinia* staining in conjunction with de novo induction of GFP) could be used to measure the percentage of dead intracellular bacteria over time.

YopE$_{GAP}$ shares structural similarity with SptP$_{GAP}$ from *Salmonella Typhimurium* and ExoS$_{GAP}$ from *Pseudomonas aeruginosa*. To achieve a broader view on other bacterial pathogens, it would be interesting to study if similar GAP effector-triggered killing happens in *Salmonella Typhimurium-* or *Pseudomonas aeruginosa*-infected macrophages. A simple experiment to start with might be to compare the survival of *Salmonella Typhimurium sipB* mutant in Toxin B treated or untreated macrophages.

Using a Rac inhibitor NSC23766 and a Rho inhibitor TAT-C3, we show that macrophages restrict *Yersinia* intracellular survival in response to Rac1 inhibition, but not Rho inhibition (Chapter 3). However, Rac inhibitor only partially promotes killing of *Yersinia* in comparison to Toxin B or YopE, indicating that disturbance of additional Rho GTPases contributes to the intracellular killing response. Recently, Xu H *et al.* showed that Rho-inactivating toxins such as *Clostridium difficile* Toxin B and *Clostridium botulinum* C3 trigger Pyrin inflammasome activation in BMDMs. Modification of Rho but not Rac/Cdc42 induces Pyrin inflammasome activation as an immune defense, which limits *Burkholderia cenocepacia* intra-macrophages growth. Thus, bacterial manipulation of different Rho GTPases may generate distinct host cell responses through different pathways. In the future, specific Rho GTPase

inhibitors (if available) or RNA interference of specific Rho GTPases by retrovirus transfection could be used, to investigate how manipulation of other Rho GTPases impacts *Yersinia* survival in macrophages.

To further explore the mechanism of YopE-triggered killing of *Yersinia* inside macrophages, on the upstream level, we considered whether YopE activity requires a second pro-inflammatory signal to generate the killing response. Our results suggest that the YopB/D translocon is not required for Toxin B-triggered intracellular killing of *Yersinia*, and LPS-TLR signaling is dispensable for YopE-stimulated intracellular killing (Chapter 4). On the downstream level, we sought to elucidate what signaling pathway mediates YopE-induced intracellular killing. We studied if macrophages respond actively to the disturbance of actin cytoskeleton: actin polymerization activator Jasplakinolide had no effect on *Yersinia* intra-macrophage survival; yet, unexpectedly, actin polymerization inhibitor Cytochalsin D slightly increased *Yersinia* intracellular survival, the mechanism of which is enigmatic. Our work also indicates that Capase1/11 signaling pathway, NOD1 signaling pathway or the autophagy pathway is not involved in YopE-elicited killing response. Interestingly, presence of YopE induces higher levels of nitric oxide (NO) from *Yersinia* infected macrophages. However, NO production does not seem to mediate YopE-triggered killing (Chapter 4). The specific down-stream pathway that mediates YopE-triggered killing still requires more investigation. One possibility is that YopE may cause accumulation of inactivated GDP-bound Rho GTPases on phagosome, which could be modified by ubiquitination to stimulate signaling pathways. Activation of Rac1 by cytotoxic necrotizing factor 1 (CNF1) from *Escherichia coli* induces Rac1 poly- and mono-ubiquitination, the biological function of the latter remains unclear [144]. In line with this, GDP-bound RhoA is targeted by the ubiquitin E3 ligase Cullin-3 for poly-

ubiquitination and degradation [145]. Thus, it is tempting to speculate that YopE-inactivated GDP-bound Rho GTPases could be mono-ubiquitinated and serve as signaling components; or they could be poly-ubiquitinated to mediate xenophagic degradation of bacteria-containing vesicles [146]. It would be interesting to check if intracellular *Yersinia* or YCVs display higher levels of ubiquitination in the presence of YopE. In this case, an autophagy blocker could be used in order to observe accumulated ubiquitination without missing a transient effect. Additionally, to study if YopE triggers macrophage activation on a global level, microarray analysis could be used to identify genes up-regulated or down-regulated by YopE activity, which could provide helpful clues of the down-stream mechanism in this process.

In summary, our results demonstrate that macrophages recognize pathogenic *Y. pseudotuberculosis* through T3SS functions and elicit intracellular killing response to counteract infection. Our work suggest that primary macrophages sense manipulation of Rho GTPases by bacterial toxins as a surveillance mechanism, revealing new insights into innate immune recognition of pathogenic infection.

References

1. Flannagan RS, Cosio G, Grinstein S (2009) Antimicrobial mechanisms of phagocytes and bacterial evasion strategies. Nat Rev Microbiol 7: 355-366.

2. Pluddemann A, Mukhopadhyay S, Gordon S (2011) Innate immunity to intracellular pathogens: macrophage receptors and responses to microbial entry. Immunol Rev 240: 11-24.

3. Medzhitov R (2007) Recognition of microorganisms and activation of the immune response. Nature 449: 819-826.

4. Kawai T, Akira S (2006) TLR signaling. Cell Death Differ 13: 816-825.

5. Broz P, Monack DM (2013) Newly described pattern recognition receptors team up against intracellular pathogens. Nat Rev Immunol 13: 551-565.

6. Strober W, Murray PJ, Kitani A, Watanabe T (2006) Signalling pathways and molecular interactions of NOD1 and NOD2. Nat Rev Immunol 6: 9-20.

7. Lamkanfi M, Dixit VM (2012) Inflammasomes and Their Roles in Health and Disease. Annual Review of Cell and Developmental Biology, Vol 28 28: 137-161.

8. Horvath GL, Schrum JE, De Nardo CM, Latz E (2011) Intracellular sensing of microbes and danger signals by the inflammasomes. Immunol Rev 243: 119-135.

9. Rathinam VA, Vanaja SK, Fitzgerald KA (2012) Regulation of inflammasome signaling. Nat Immunol 13: 333-342.

10. Vance RE, Isberg RR, Portnoy DA (2009) Patterns of pathogenesis: discrimination of pathogenic and nonpathogenic microbes by the innate immune system. Cell Host Microbe 6: 10-21.

11. Stuart LM, Paquette N, Boyer L (2013) Effector-triggered versus pattern-triggered immunity: how animals sense pathogens. Nat Rev Immunol 13: 199-206.

12. Blander JM, Sander LE (2012) Beyond pattern recognition: five immune checkpoints for scaling the microbial threat. Nat Rev Immunol 12: 215-225.

13. Sander LE, Davis MJ, Boekschoten MV, Amsen D, Dascher CC, et al. (2011) Detection of prokaryotic mRNA signifies microbial viability and promotes immunity. Nature 474: 385-389.

14. Boyer L, Magoc L, Dejardin S, Cappillino M, Paquette N, et al. (2011) Pathogen-derived effectors trigger protective immunity via activation of the Rac2 enzyme and the IMD or Rip kinase signaling pathway. Immunity 35: 536-549.

15. Fontana MF, Banga S, Barry KC, Shen X, Tan Y, et al. (2011) Secreted bacterial effectors that inhibit host protein synthesis are critical for induction of the innate immune response to virulent Legionella pneumophila. PLoS Pathog 7: e1001289.

16. Fontana MF, Shin S, Vance RE (2012) Activation of host mitogen-activated protein kinases by secreted Legionella pneumophila effectors that inhibit host protein translation. Infect Immun 80: 3570-3575.

17. Dunbar TL, Yan Z, Balla KM, Smelkinson MG, Troemel ER (2012) C. elegans detects pathogen-induced translational inhibition to activate immune signaling. Cell Host Microbe 11: 375-386.

18. Keestra AM, Winter MG, Auburger JJ, Frassle SP, Xavier MN, et al. (2013) Manipulation of small Rho GTPases is a pathogen-induced process detected by NOD1. Nature 496: 233-237.

19. Bliska JB, Wang X, Viboud GI, Brodsky IE (2013) Modulation of innate immune responses by Yersinia type III secretion system translocators and effectors. Cell Microbiol 15: 1622-1631.

20. Chisholm ST, Coaker G, Day B, Staskawicz BJ (2006) Host-microbe interactions: shaping the evolution of the plant immune response. Cell 124: 803-814.

21. Wren BW (2003) The yersiniae--a model genus to study the rapid evolution of bacterial pathogens. Nat Rev Microbiol 1: 55-64.

22. Perry RD, Fetherston JD (1997) Yersinia pestis--etiologic agent of plague. Clin Microbiol Rev 10: 35-66.

23. Skurnik M, Peippo A, Ervela E (2000) Characterization of the O-antigen gene clusters of Yersinia pseudotuberculosis and the cryptic O-antigen gene cluster of Yersinia pestis shows that the plague bacillus is most closely related to and has evolved from Y. pseudotuberculosis serotype O:1b. Mol Microbiol 37: 316-330.

24. Sansonetti PJ, Phalipon A (1999) M cells as ports of entry for enteroinvasive pathogens: Mechanisms of interaction, consequences for the disease process. Seminars in Immunology 11: 193-203.

25. Isberg RR, Barnes P (2001) Subversion of integrins by enteropathogenic Yersinia. J Cell Sci 114: 21-28.

26. Pujol C, Bliska JB (2005) Turning Yersinia pathogenesis outside in: subversion of macrophage function by intracellular yersiniae. Clin Immunol 114: 216-226.

27. Viboud GI, Bliska JB (2005) Yersinia outer proteins: role in modulation of host cell signaling responses and pathogenesis. Annu Rev Microbiol 59: 69-89.

28. Cornelis GR (2006) The type III secretion injectisome. Nat Rev Microbiol 4: 811-825.

29. Buttner D (2012) Protein export according to schedule: architecture, assembly, and regulation of type III secretion systems from plant- and animal-pathogenic bacteria. Microbiol Mol Biol Rev 76: 262-310.

30. Cornelis GR (2002) The Yersinia Ysc-Yop 'type III' weaponry. Nat Rev Mol Cell Biol 3: 742-752.

31. Galan JE, Collmer A (1999) Type III secretion machines: bacterial devices for protein delivery into host cells. Science 284: 1322-1328.

32. Cornelis GR, Van Gijsegem F (2000) Assembly and function of type III secretory systems. Annu Rev Microbiol 54: 735-774.

33. Mota LJ, Cornelis GR (2005) The bacterial injection kit: type III secretion systems. Ann Med 37: 234-249.

34. Raymond B, Young JC, Pallett M, Endres RG, Clements A, et al. (2013) Subversion of trafficking, apoptosis, and innate immunity by type III secretion system effectors. Trends Microbiol 21: 430-441.

35. Straley SC, Plano GV, Skrzypek E, Haddix PL, Fields KA (1993) Regulation by Ca2+ in the Yersinia low-Ca2+ response. Mol Microbiol 8: 1005-1010.

36. Michiels T, Wattiau P, Brasseur R, Ruysschaert JM, Cornelis G (1990) Secretion of Yop Proteins by Yersiniae. Infect Immun 58: 2840-2849.

37. Cornelis GR (2010) The type III secretion injectisome, a complex nanomachine for intracellular 'toxin' delivery. Biol Chem 391: 745-751.

38. Mueller CA, Broz P, Cornelis GR (2008) The type III secretion system tip complex and translocon. Mol Microbiol 68: 1085-1095.

39. Dewoody RS, Merritt PM, Marketon MM (2013) Regulation of the Yersinia type III secretion system: traffic control. Front Cell Infect Microbiol 3: 4.

40. Brodsky IE, Palm NW, Sadanand S, Ryndak MB, Sutterwala FS, et al. (2010) A Yersinia Effector Protein Promotes Virulence by Preventing Inflammasome Recognition of the Type III Secretion System. Cell Host Microbe 7: 376-387.

41. Durand EA, Maldonado-Arocho FJ, Castillo C, Walsh RL, Mecsas J (2010) The presence of professional phagocytes dictates the number of host cells targeted for Yop translocation during infection. Cell Microbiol 12: 1064-1082.

42. Koberle M, Klein-Gunther A, Schutz M, Fritz M, Berchtold S, et al. (2009) Yersinia enterocolitica targets cells of the innate and adaptive immune system by injection of Yops in a mouse infection model. PLoS Pathog 5: e1000551.

43. Marketon MM, DePaolo RW, DeBord KL, Jabri B, Schneewind O (2005) Plague bacteria target immune cells during infection. Science 309: 1739-1741.

44. Rolan HG, Durand EA, Mecsas J (2013) Identifying Yersinia YopH-targeted signal transduction pathways that impair neutrophil responses during in vivo murine infection. Cell Host Microbe 14: 306-317.

45. Trosky JE, Liverman AD, Orth K (2008) Yersinia outer proteins: Yops. Cell Microbiol 10: 557-565.

46. Von Pawel-Rammingen U, Telepnev MV, Schmidt G, Aktories K, Wolf-Watz H, et al. (2000) GAP activity of the Yersinia YopE cytotoxin specifically targets the Rho pathway: a mechanism for disruption of actin microfilament structure. Mol Microbiol 36: 737-748.

47. Schmidt G (2011) Yersinia enterocolitica outer protein T (YopT). Eur J Cell Biol 90: 955-958.

48. Groves E, Rittinger K, Amstutz M, Berry S, Holden DW, et al. (2010) Sequestering of Rac by the Yersinia effector YopO blocks Fcgamma receptor-mediated phagocytosis. J Biol Chem 285: 4087-4098.

49. Persson C, Nordfelth R, Andersson K, Forsberg A, Wolf-Watz H, et al. (1999) Localization of the Yersinia PTPase to focal complexes is an important virulence mechanism. Mol Microbiol 33: 828-838.

50. Hallett MB, Lloyds D (1997) The molecular and ionic signaling of neutrophils. Austin. Tex.

New York: Landes Bioscience ;

North American distributor, Chapman & Hall. 212 p. p.

51. Cornelius C, Quenee L, Anderson D, Schneewind O (2007) Protective immunity against plague. Adv Exp Med Biol 603: 415-424.

52. Brubaker RR (2003) Interleukin-10 and inhibition of innate immunity to Yersiniae: roles of Yops and LcrV (V antigen). Infect Immun 71: 3673-3681.

53. Broz P, Mueller CA, Muller SA, Philippsen A, Sorg I, et al. (2007) Function and molecular architecture of the Yersinia injectisome tip complex. Mol Microbiol 65: 1311-1320.

54. Bergsbaken T, Cookson BT (2007) Macrophage activation redirects yersinia-infected host cell death from apoptosis to caspase-1-dependent pyroptosis. PLoS Pathog 3: e161.

55. Zheng Y, Lilo S, Mena P, Bliska JB (2012) YopJ-induced caspase-1 activation in Yersinia-infected macrophages: independent of apoptosis, linked to necrosis, dispensable for innate host defense. PLoS One 7: e36019.

56. Erfurth SE, Grobner S, Kramer U, Gunst DS, Soldanova I, et al. (2004) Yersinia enterocolitica induces apoptosis and inhibits surface molecule expression and cytokine production in murine dendritic cells. Infect Immun 72: 7045-7054.

57. Monack DM, Mecsas J, Ghori N, Falkow S (1997) Yersinia signals macrophages to undergo apoptosis and YopJ is necessary for this cell death. Proc Natl Acad Sci U S A 94: 10385-10390.

58. Zhang Y, Ting AT, Marcu KB, Bliska JB (2005) Inhibition of MAPK and NF-kappa B pathways is necessary for rapid apoptosis in macrophages infected with Yersinia. J Immunol 174: 7939-7949.

59. Philip NH, Brodsky IE (2012) Cell death programs in Yersinia immunity and pathogenesis. Front Cell Infect Microbiol 2: 149.

60. Mittal R, Peak-Chew SY, McMahon HT (2006) Acetylation of MEK2 and I kappa B kinase (IKK) activation loop residues by YopJ inhibits signaling. Proc Natl Acad Sci U S A 103: 18574-18579.

61. Mukherjee S, Keitany G, Li Y, Wang Y, Ball HL, et al. (2006) Yersinia YopJ acetylates and inhibits kinase activation by blocking phosphorylation. Science 312: 1211-1214.

62. Meinzer U, Barreau F, Esmiol-Welterlin S, Jung C, Villard C, et al. (2012) Yersinia pseudotuberculosis effector YopJ subverts the Nod2/RICK/TAK1 pathway and activates caspase-1 to induce intestinal barrier dysfunction. Cell Host Microbe 11: 337-351.

63. Orth K (2002) Function of the Yersinia effector YopJ. Curr Opin Microbiol 5: 38-43.

64. Zheng Y, Lilo S, Brodsky IE, Zhang Y, Medzhitov R, et al. (2011) A Yersinia effector with enhanced inhibitory activity on the NF-kappaB pathway activates the NLRP3/ASC/caspase-1 inflammasome in macrophages. PLoS Pathog 7: e1002026.

65. Lilo S, Zheng Y, Bliska JB (2008) Caspase-1 activation in macrophages infected with Yersinia pestis KIM requires the type III secretion system effector YopJ. Infect Immun 76: 3911-3923.

66. Philip NH, Dillon CP, Snyder AG, Fitzgerald P, Wynosky-Dolfi MA, et al. (2014) Caspase-8 mediates caspase-1 processing and innate immune defense in response to bacterial blockade of NF-kappaB and MAPK signaling. Proc Natl Acad Sci U S A 111: 7385-7390.

67. Weng D, Marty-Roix R, Ganesan S, Proulx MK, Vladimer GI, et al. (2014) Caspase-8 and RIP kinases regulate bacteria-induced innate immune responses and cell death. Proc Natl Acad Sci U S A 111: 7391-7396.

68. Brodsky IE, Medzhitov R (2008) Reduced secretion of YopJ by Yersinia limits in vivo cell death but enhances bacterial virulence. PLoS Pathog 4: e1000067.

69. Monack DM, Mecsas J, Bouley D, Falkow S (1998) Yersinia-induced apoptosis in vivo aids in the establishment of a systemic infection of mice. J Exp Med 188: 2127-2137.

70. Zauberman A, Tidhar A, Levy Y, Bar-Haim E, Halperin G, et al. (2009) Yersinia pestis endowed with increased cytotoxicity is avirulent in a bubonic plague model and induces rapid protection against pneumonic plague. PLoS One 4: e5938.

71. Kwuan L, Adams W, Auerbuch V (2013) Impact of host membrane pore formation by the Yersinia pseudotuberculosis type III secretion system on the macrophage innate immune response. Infect Immun 81: 905-914.

72. Holmstrom A, Pettersson J, Rosqvist R, Hakansson S, Tafazoli F, et al. (1997) YopK of *Yersinia pseudotuberculosis* controls translocation of Yop effectors across the eukaryotic cell membrane. Mol Microbiol 24: 73-91.

73. Evdokimov AG, Anderson DE, Routzahn KM, Waugh DS (2001) Unusual molecular architecture of the Yersinia pestis cytotoxin YopM: a leucine-rich repeat protein with the shortest repeating unit. J Mol Biol 312: 807-821.

74. McDonald C, Vacratsis PO, Bliska JB, Dixon JE (2003) The Yersinia virulence factor YopM forms a novel protein complex with two cellular kinases. J Biol Chem 278: 18514-18523.

75. Hentschke M, Berneking L, Belmar Campos C, Buck F, Ruckdeschel K, et al. (2010) Yersinia virulence factor YopM induces sustained RSK activation by interfering with dephosphorylation. PLoS One 5: e13165.

76. Straley SC (2012) YopM and plague. Adv Exp Med Biol 954: 247-252.

77. McPhee JB, Mena P, Zhang Y, Bliska JB (2012) Interleukin-10 induction is an important virulence function of the Yersinia pseudotuberculosis type III effector YopM. Infect Immun 80: 2519-2527.

78. LaRock CN, Cookson BT (2012) The Yersinia virulence effector YopM binds caspase-1 to arrest inflammasome assembly and processing. Cell Host Microbe 12: 799-805.

79. Chung LK, Philip NH, Schmidt VA, Koller A, Strowig T, et al. (2014) IQGAP1 Is Important for Activation of Caspase-1 in Macrophages and Is Targeted by Yersinia pestis Type III Effector YopM. MBio 5.

80. Viboud GI, Bliska JB (2001) A bacterial type III secretion system inhibits actin polymerization to prevent pore formation in host cell membranes. EMBO J 20: 5373-5382.

81. Viboud GI, Mejia E, Bliska JB (2006) Comparison of YopE and YopT activities in counteracting host signalling responses to Yersinia pseudotuberculosis infection. Cell Microbiol 8: 1504-1515.

82. Mejia E, Bliska JB, Viboud GI (2008) Yersinia controls type III effector delivery into host cells by modulating Rho activity. PLoS Pathog 4: e3.

83. Zhang Y, Bliska JB (2003) Role of Toll-like receptor signaling in the apoptotic response of macrophages to *Yersinia* infection. Infect Immun 71: 1513-1519.

84. Auerbuch V, Golenbock DT, Isberg RR (2009) Innate immune recognition of Yersinia pseudotuberculosis type III secretion. PLoS Pathog 5: e1000686.

85. Kayagaki N, Warming S, Lamkanfi M, Vande Walle L, Louie S, et al. (2011) Non-canonical inflammasome activation targets caspase-11. Nature 479: 117-121.

86. Broz P, Monack DM (2013) Noncanonical inflammasomes: caspase-11 activation and effector mechanisms. PLoS Pathog 9: e1003144.

87. Casson CN, Copenhaver AM, Zwack EE, Nguyen HT, Strowig T, et al. (2013) Caspase-11 activation in response to bacterial secretion systems that access the host cytosol. PLoS Pathog 9: e1003400.

88. Roy D, Liston DR, Idone VJ, Di A, Nelson DJ, et al. (2004) A process for controlling intracellular bacterial infections induced by membrane injury. Science 304: 1515-1518.

89. Zhang Y, Murtha J, Roberts MA, Siegel RM, Bliska JB (2008) Type III secretion decreases bacterial and host survival following phagocytosis of Yersinia pseudotuberculosis by macrophages. Infect Immun 76: 4299-4310.

90. Bergsbaken T, Fink SL, den Hartigh AB, Loomis WP, Cookson BT (2011) Coordinated host responses during pyroptosis: caspase-1-dependent lysosome exocytosis and inflammatory cytokine maturation. J Immunol 187: 2748-2754.

91. Deuretzbacher A, Czymmeck N, Reimer R, Trulzsch K, Gaus K, et al. (2009) Beta1 integrin-dependent engulfment of Yersinia enterocolitica by macrophages is coupled to the activation of autophagy and suppressed by type III protein secretion. J Immunol 183: 5847-5860.

92. Moreau K, Lacas-Gervais S, Fujita N, Sebbane F, Yoshimori T, et al. (2010) Autophagosomes can support Yersinia pseudotuberculosis replication in macrophages. Cell Microbiol 12: 1108-1123.

93. Grosdent N, Maridonneau-Parini I, Sory MP, Cornelis GR (2002) Role of Yops and adhesins in resistance of Yersinia enterocolitica to phagocytosis. Infect Immun 70: 4165-4176.

94. Rosqvist R, Bolin I, Wolf-Watz H (1988) Inhibition of phagocytosis in Yersinia pseudotuberculosis: a virulence plasmid-encoded ability involving the Yop2b protein. Infect Immun 56: 2139-2143.

95. Rosqvist R, Forsberg A, Rimpilainen M, Bergman T, Wolf-Watz H (1990) The cytotoxic protein YopE of Yersinia obstructs the primary host defence. Mol Microbiol 4: 657-667.

96. Finegold MJ (1969) Pneumonic plague in monkeys. An electron microscopic study. Am J Pathol 54: 167-185.

97. Fujimura Y, Kihara T, Mine H (1992) Membranous cells as a portal of Yersinia pseudotuberculosis entry into rabbit ileum. J Clin Electron Microsc 25: 35-45.

98. Une T (1977) Studies on the pathogenicity of Yersinia enterocolitica. I. Experimental infection in rabbits. Microbiol Immunol 21: 341-363.

99. Straley SC, Harmon PA (1984) Yersinia pestis grows within phagolysosomes in mouse peritoneal macrophages. Infect Immun 45: 655-659.

100. Straley SC, Harmon PA (1984) Growth in mouse peritoneal macrophages of Yersinia pestis lacking established virulence determinants. Infect Immun 45: 649-654.

101. Pujol C, Bliska JB (2003) The ability to replicate in macrophages is conserved between Yersinia pestis and Yersinia pseudotuberculosis. Infect Immun 71: 5892-5899.

102. Grabenstein JP, Marceau M, Pujol C, Simonet M, Bliska JB (2004) The response regulator PhoP of Yersinia pseudotuberculosis is important for replication in macrophages and for virulence. Infect Immun 72: 4973-4984.

103. Oyston PC, Dorrell N, Williams K, Li SR, Green M, et al. (2000) The response regulator PhoP is important for survival under conditions of macrophage-induced stress and virulence in Yersinia pestis. Infect Immun 68: 3419-3425.

104. Grabenstein JP, Fukuto HS, Palmer LE, Bliska JB (2006) Characterization of phagosome trafficking and identification of PhoP-regulated genes important for survival of Yersinia pestis in macrophages. Infect Immun 74: 3727-3741.

105. Furste JP, Pansegrau W, Frank R, Blocker H, Scholz P, et al. (1986) Molecular cloning of the plasmid RP4 primase region in a multi-host-range tacP expression vector. Gene 48: 119-131.

106. Celada A, Gray PW, Rinderknecht E, Schreiber RD (1984) Evidence for a gamma-interferon receptor that regulates macrophage tumoricidal activity. J Exp Med 160: 55-74.

107. Ryndak MB, Chung H, London E, Bliska JB (2005) Role of predicted transmembrane domains for type III translocation, pore formation, and signaling by the Yersinia pseudotuberculosis YopB protein. Infect Immun 73: 2433-2443.

108. Wong KW, Isberg RR (2005) Yersinia pseudotuberculosis spatially controls activation and misregulation of host cell Rac1. PLoS Pathog 1: e16.

109. Simonet M, Falkow S (1992) Invasin expression in Yersinia pseudotuberculosis. Infect Immun 60: 4414-4417.

110. Black DS, Bliska JB (2000) The RhoGAP activity of the Yersinia pseudotuberculosis cytotoxin YopE is required for antiphagocytic function and virulence. Mol Microbiol 37: 515-527.

111. Black DS, Bliska JB (1997) Identification of p130Cas as a substrate of Yersinia YopH (Yop51), a bacterial protein tyrosine phosphatase that translocates into mammalian cells and targets focal adhesions. EMBO J 16: 2730-2744.

112. Palmer LE, Pancetti AR, Greenberg S, Bliska JB (1999) YopJ of Yersinia spp. is sufficient to cause downregulation of multiple mitogen-activated protein kinases in eukaryotic cells. Infect Immun 67: 708-716.

113. Zhang Y, Romanov G, Bliska JB (2011) Type III secretion system-dependent translocation of ectopically expressed Yop effectors into macrophages by intracellular Yersinia pseudotuberculosis. Infect Immun 79: 4322-4331.

114. Krall R, Zhang Y, Barbieri JT (2004) Intracellular membrane localization of pseudomonas ExoS and Yersinia YopE in mammalian cells. J Biol Chem 279: 2747-2753.

115. Isaksson EL, Aili M, Fahlgren A, Carlsson SE, Rosqvist R, et al. (2009) The membrane localization domain is required for intracellular localization and autoregulation of YopE in Yersinia pseudotuberculosis. Infect Immun 77: 4740-4749.

116. Zhang Y, Barbieri JT (2005) A leucine-rich motif targets Pseudomonas aeruginosa ExoS within mammalian cells. Infect Immun 73: 7938-7945.

117. Gaus K, Hentschke M, Czymmeck N, Novikova L, Trulzsch K, et al. (2011) Destabilization of YopE by the ubiquitin-proteasome pathway fine-tunes Yop delivery into host cells and facilitates systemic spread of Yersinia enterocolitica in host lymphoid tissue. Infect Immun 79: 1166-1175.

118. Andor A, Trulzsch K, Essler M, Roggenkamp A, Wiedemann A, et al. (2001) YopE of Yersinia, a GAP for Rho GTPases, selectively modulates Rac-dependent actin structures in endothelial cells. Cell Microbiol 3: 301-310.

119. Pujol C, Klein KA, Romanov GA, Palmer LE, Cirota C, et al. (2009) Yersinia pestis can reside in autophagosomes and avoid xenophagy in murine macrophages by preventing vacuole acidification. Infect Immun 77: 2251-2261.

120. Zhang Y, Mena P, Romanov G, Bliska JB (2014) Effector CD8+ T Cells Are Generated in Response to an Immunodominant Epitope in Type III Effector YopE during Primary Yersinia pseudotuberculosis Infection. Infect Immun 82: 3033-3044.

121. Bliska JB, Black DS (1995) Inhibition of the Fc receptor-mediated oxidative burst in macrophages by the Yersinia pseudotuberculosis tyrosine phosphatase. Infect Immun 63: 681-685.

122. Bentley WE, Mirjalili N, Andersen DC, Davis RH, Kompala DS (1990) Plasmid-encoded protein: the principal factor in the "metabolic burden" associated with recombinant bacteria. Biotechnol Bioeng 35: 668-681.

123. Meyer R (2009) Replication and conjugative mobilization of broad host-range IncQ plasmids. Plasmid 62: 57-70.

124. Songsungthong W, Higgins MC, Rolan HG, Murphy JL, Mecsas J (2010) ROS-inhibitory activity of YopE is required for full virulence of Yersinia in mice. Cell Microbiol 12: 988-1001.

125. Wilkins TD, Lyerly DM (1996) Clostridium difficile toxins attack Rho. Trends Microbiol 4: 49-51.

126. Genth H, Dreger SC, Huelsenbeck J, Just I (2008) Clostridium difficile toxins: more than mere inhibitors of Rho proteins. Int J Biochem Cell Biol 40: 592-597.

127. Belyi Y, Aktories K (2010) Bacterial toxin and effector glycosyltransferases. Biochim Biophys Acta 1800: 134-143.

128. Heasman SJ, Ridley AJ (2008) Mammalian Rho GTPases: new insights into their functions from in vivo studies. Nat Rev Mol Cell Biol 9: 690-701.

129. Wennerberg K, Der CJ (2004) Rho-family GTPases: it's not only Rac and Rho (and I like it). J Cell Sci 117: 1301-1312.

130. Mohammadi S, Isberg RR (2009) Yersinia pseudotuberculosis virulence determinants invasin, YopE, and YopT modulate RhoG activity and localization. Infect Immun 77: 4771-4782.

131. Roppenser B, Roder A, Hentschke M, Ruckdeschel K, Aepfelbacher M (2009) Yersinia enterocolitica differentially modulates RhoG activity in host cells. J Cell Sci 122: 696-705.

132. Xu H, Yang J, Gao W, Li L, Li P, et al. (2014) Innate immune sensing of bacterial modifications of Rho GTPases by the Pyrin inflammasome. Nature.

133. Fontana MF, Vance RE (2011) Two signal models in innate immunity. Immunol Rev 243: 26-39.

134. Pujol C, Grabenstein JP, Perry RD, Bliska JB (2005) Replication of Yersinia pestis in interferon gamma-activated macrophages requires ripA, a gene encoded in the pigmentation locus. Proc Natl Acad Sci U S A 102: 12909-12914.

135. Wong KW, Isberg RR (2005) Emerging views on integrin signaling via Rac1 during invasin-promoted bacterial uptake. Curr Opin Microbiol 8: 4-9.

136. Owen KA, Thomas KS, Bouton AH (2007) The differential expression of Yersinia pseudotuberculosis adhesins determines the requirement for FAK and/or Pyk2 during bacterial phagocytosis by macrophages. Cell Microbiol 9: 596-609.

137. Grassl GA, Bohn E, Muller Y, Buhler OT, Autenrieth IB (2003) Interaction of Yersinia enterocolitica with epithelial cells: invasin beyond invasion. Int J Med Microbiol 293: 41-54.

138. Maldonado-Arocho FJ, Green C, Fisher ML, Paczosa MK, Mecsas J (2013) Adhesins and host serum factors drive Yop translocation by yersinia into professional phagocytes during animal infection. PLoS Pathog 9: e1003415.

139. Shin S, Case CL, Archer KA, Nogueira CV, Kobayashi KS, et al. (2008) Type IV secretion-dependent activation of host MAP kinases induces an increased proinflammatory cytokine response to Legionella pneumophila. PLoS Pathog 4: e1000220.

140. Bruno VM, Hannemann S, Lara-Tejero M, Flavell RA, Kleinstein SH, et al. (2009) Salmonella Typhimurium type III secretion effectors stimulate innate immune responses in cultured epithelial cells. PLoS Pathog 5: e1000538.

141. Lanning CC, Ruiz-Velasco R, Williams CL (2003) Novel mechanism of the co-regulation of nuclear transport of SmgGDS and Rac1. J Biol Chem 278: 12495-12506.

142. Yin J, Haney L, Walk S, Zhou S, Ravichandran KS, et al. (2004) Nuclear localization of the DOCK180/ELMO complex. Arch Biochem Biophys 429: 23-29.

143. Simon AR, Vikis HG, Stewart S, Fanburg BL, Cochran BH, et al. (2000) Regulation of STAT3 by direct binding to the Rac1 GTPase. Science 290: 144-147.

144. Nethe M, Anthony EC, Fernandez-Borja M, Dee R, Geerts D, et al. (2010) Focal-adhesion targeting links caveolin-1 to a Rac1-degradation pathway. J Cell Sci 123: 1948-1958.

145. Chen Y, Yang Z, Meng M, Zhao Y, Dong N, et al. (2009) Cullin mediates degradation of RhoA through evolutionarily conserved BTB adaptors to control actin cytoskeleton structure and cell movement. Mol Cell 35: 841-855.

146. Manzanillo PS, Ayres JS, Watson RO, Collins AC, Souza G, et al. (2013) The ubiquitin ligase parkin mediates resistance to intracellular pathogens. Nature 501: 512-516.